Hepatic remodeling, serum biomarkers and prevention of fibrosis progression in liver disease

Vedrana Reichenbach Marinkovic

UNIVERSITAT DE BARCELONA

HEPATIC REMODELING, SERUM BIOMARKERS AND PREVENTION OF FIBROSIS PROGRESSION IN LIVER DISEASE

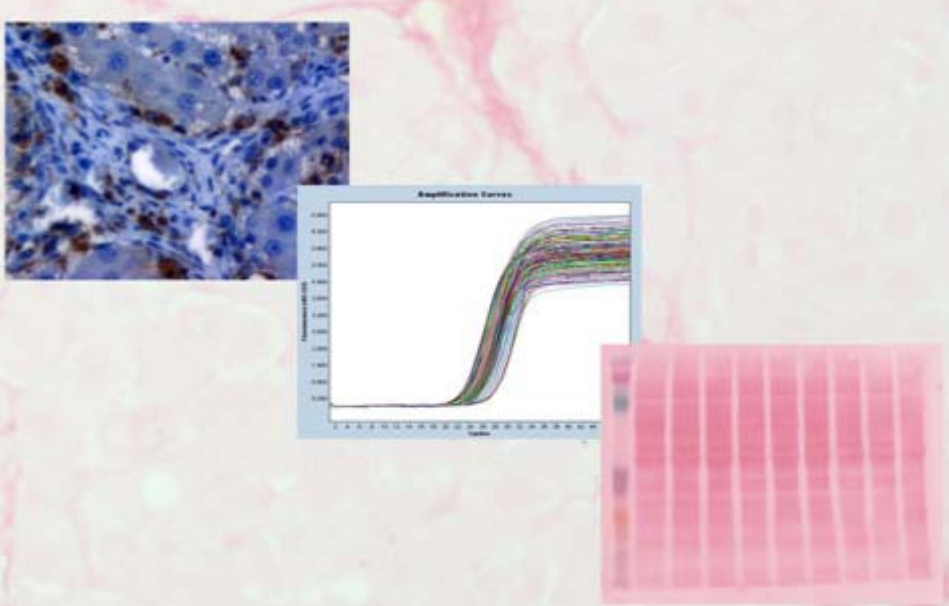

VEDRANA REICHENBACH

2012

HEPATIC REMODELING, SERUM BIOMARKERS AND PREVENTION OF FIBROSIS PROGRESSION IN LIVER DISEASE

Memoria presentada por

VEDRANA REICHENBACH MARINKOVIC

Para optar al título de Doctora en Biología
por la Universidad de Barcelona

Trabajo realizado bajo la dirección del **Dr.Wladimiro Jiménez Povedano**

Servicio de Bioquímica y Genética Molecular

Departamento de Ciencias Fisiológicas I

Hospital Clínic/Facultad de Medicina

Universidad de Barcelona

Tesis inscrita en el programa de Doctorado de Medicina

Departamento de Ciencias Fisiológicas I

Facultad de Medicina de la Universidad de Barcelona

A mis padres y a Albert

INDEX

FIGURES AND TABLES INDEX

INTRODUCTION

1. Hepatic fibrosis and cirrhosis.

Definition and characteristics

Hepatic cirrhosis is an end-stage consequence of chronic damage to the liver in coordination with the accumulation of extracellular matrix (ECM) proteins, which leads to fibrogenesis and ultimately to hepatic function alteration. The outcome of severe cirrhosis is the development of major complications such as portal hypertension, ascites, variceal bleeding, renal and liver failure, liver cancer and ultimately death (Anthony et al., 1977; Bataller and Brenner, 2005).

According to a study performed by the *Ministerio de Sanidad y Consumo (see refs)*, in our country, hepatic cirrhosis has an 11/100.000 inhabitants death rate every year. Worldwide, around 27.000 people die from this disease in the developed countries (Anderson et al., 2003).

Liver diseases have different etiologies depending on the source of the damage, the main causes are chronic hepatitis B and C infection (HBV, HCV), followed by alcoholic liver disease, non-alcoholic fatty liver disease (NAFLD) and cholestasis.

The early diagnosis of the liver disease is complicated, as approximately a 40 % of the patients remain asymptomatic for 15-20 years before major complications appear. Asymptomatic patients are in a state known as compensated fibrosis. The cease of the source of hepatic damage can lead to fibrosis regression, although it depends on the underlying cause of the disease and its severity. When a patient develops any of the major complications the status of the disease changes from compensated to decompensated cirrhosis. In this situation, there is a bad prognosis associated with short survival and the only effective therapy is liver transplantation. In several clinical settings, cirrhotic patients can develop acute episodes that lead to an alarming fast development from fibrosis to cirrhosis in a short period of time. It's the case of acute alcoholic hepatitis, subfulminant hepatitis and fibrosing cholestasis in HCV reinfection after liver transplantation. The development of cirrhosis is also a major risk factor for developing hepatocellular carcinoma.

Aside from the etiology of the disease, damage to the liver can be classified as acute or chronic. The acute damage triggers inflammatory stimuli but ECM accumulation is limited, while the chronic damage is characterized by a sustained inflammatory response with the consequence of continuous pro-inflammatory

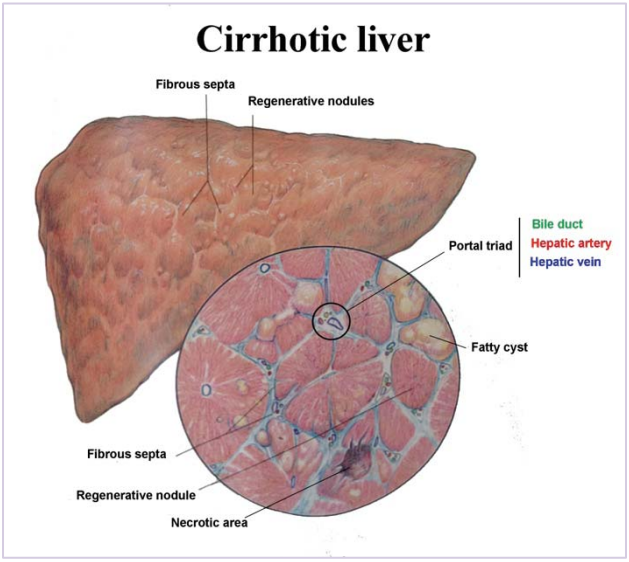

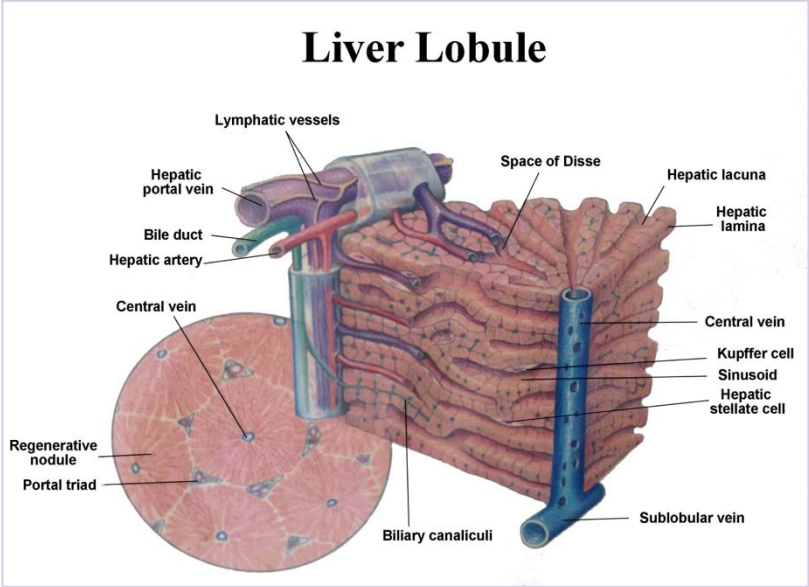

Figure 1. Cirrhotic liver architecture. Detail of the liver lobule. Image modified from Wolters Kluwer Health, 2007 (poster).

cytokine and chemokine release and important ECM accumulation. This chronic damage leads to the disruption of the liver architecture forming a fibrous scar and the subsequent formation of regenerative nodules that characterize cirrhosis (Figure 1).

Liver fibrosis is a wound-healing process that responds to a wide variety of stimuli. Excessive ECM proteins deposition of proteoglycans, glycoproteins and specially collagens accumulate in the liver tissue. Hepatic stellate cells (HSC) are the

main cellular type involved in the fibrogenic process, they undergo activation, transdifferentiate into myofibroblastic–like cells, proliferate and release proinflammatory and profibrogenic factors that perpetuate fibrosis (Marra, 1999). Activated HSC migrate and accumulate replacing slowly the parenchyma with fibrotic tissue. Other cell types also take part in the fibrogenesis process. Hepatocytes are targeted by most hepatotoxic agents and trigger the release of reactive oxygen species (ROS) and the recruitment of macrophages to the injured site. Apoptosis of hepatocytes also stimulate profibrogenic actions of myofibroblasts and Kupffer cells are the major source of TGFβ. Fibrogenesis is a vicious circle where liver and inflammatory cells stimulate each other leading slowly to the progression of the liver disease (Henderson and Iredale, 2007).

Treatments for liver diseases are directed against the agent that cause the damage and palliate the consequent complications. For viral hepatitis, the treatment is based on a combination of pegilated-interferon (a lymphocyte stimulator) and ribavirin (an antiviral agent). Liver diseases have in common water retention, for this reason, doctors encourage patients to reduce sodium intake within the diet and to take diuretics. Also, alcohol consumption is not recommended for any patient suffering a liver disease. TIPS (transjugular intrahepatic portosystemic shunt) has proven successful in patients with portal hypertension and hepatorenal syndrome. Patients that develop ascites are treated with profilaxis with antibiotics to prevent infection with spontaneous bacterial peritonitis (SBP). Paracentesis is also used to drain abdominal liquid in cases of severe ascites, and also diuretics. Nowadays, ascites formation has become less common in cirrhotic patients thanks to the advances in early diagnosis tools. Nevertheless, the only option for advanced cirrhosis up to date is liver transplantation with a 75% of survival rate after 5 years. Unfortunately, patients suffering from HCV recidivism develop chronic hepatitis again few years later. Spain is the leading country in liver transplantations with a 6% of intervention of the total worldwide count. However, the organ availability is not always possible, for this reason there is a strong need for research for new effective therapeutics targets.

Intrahepatic alterations and its complications

Inflammation, fibrosis and angiogenesis

The first response of the liver to damage regardless its source is inflammation. Liver cells release inflammatory mediators that stimulate recruitment of more inflammatory cells such as TGFβ, TNFα, IL1, IL6, IL8 or MCP1, genes involved in cell proliferation and fibrogenesis such as PDGF or VEGF with angiogenic properties. Liver cells also release reactive oxygen species (ROS) and cytokines that induce parenchymal cell apoptosis (Pinzani and Marra, 2001). Sustained inflammatory stimuli perpetuate fibrosis and lead to cirrhosis and its complications. Another key component in a chronic damaged liver is the renin-angiotensin system (RAS). Angiotensin II (AII) is the main effector of this system, as it is responsible for many profibrogenic effects on HSCs and together with endothelin 1 (ET1) are the most important vasoconstrictors implicated in cirrhosis. Pharmacologic treatment or gene therapy targeting RAS components have proved to attenuate experimental fibrosis (Moreno and Bataller, 2008). It has also been demonstrated that angiogenesis plays an important part in cirrhosis. Angiogenesis in the liver is a compensatory reaction to the lack of oxygen to the cells present where the inflammation is occurring. Many studies have proved that there is an increase in vascular formation in the liver as well as the splanchnic area (Tugues et al., 2007).

All these intrahepatic alterations lead to major physiological complications that characterize liver diseases. The most common alterations that occur in liver cirrhosis are portal hypertension, ascites formation, renal failure, variceal bleeding and hepatic encephalopathy. Thanks to the animal models, the study of most of these complications has been possible. The CCl_4 inhalation animal model in rats (Jiménez et al., 1992) allowed studying portal hypertension and ascites in our laboratory.

Hemodynamics deregulation

Portal pressure is a clinical syndrome characterized by a pathological increase in portal venous pressure above normal values of 5 mmHg. This phenomenon induces the formation of an extensive network of portosystemic collaterals that divert the blood flow to the systemic circulation bypassing the liver (Bosch et al., 1992). This process is

called portosystemic shunting. The portal pressure gradient (PPG) is the difference between the portal pressure (PP) and the inferior vena cava pressure (IVC):

$$PPG = PP - IVC$$

and is determined by the product of portal blood flow and the vascular resistance that opposes that flow. This hemodynamic principle is explained by Ohm's law equation:

$$PPG = Q \times R$$

where Q is the total portal venous blood flow, and R is the sum of the vascular resistance that exerts the portal venous system, the collateral veins and the liver.

The PPG is considered clinically significant when the hepatic venous gradient (HVG) surpasses 10-12 mmHg. This syndrome is responsible for other major complications such as variceal bleeding, ascites and hepatorenal syndrome among others. Patients with advanced cirrhosis have chronic portal hypertension, and with values above 12 mmHg there is a high risk of variceal bleeding. The hemodynamic balance is maintained by vasoconstrictor substances like ET1, AII, noradrenalin and ADH (antidiuretic hormone) and vasodilators such as nitric oxide (NO). Hepatic damage prompts an increase of vasoconstrictors and a decrease of NO, mainly due to the decrease of regulators of the signaling pathway of eNOS (endothelial NO synthase) such as Akt (Morales-Ruiz et al., 2003).

Edema and ascites

Ascites is the most common complication of cirrhosis and is associated with increased risks of infections, renal failure and poor quality of life in general. Ascites appears due to increased intrahepatic resistance to portal blood flow and gradually causes portal hypertension, collateral vein formation and shunting of the blood to the systemic circulation (Ginès et al., 2004) The production of local vasodilators such as NO increases when portal hypertension develops, leading to splanchnic vasodilation. In advanced cirrhosis, due to the pronounced splanchnic arterial vasodilation, the arterial blood volume decreases considerably and as a consequence there is a marked fall of the arterial pressure. As a consequence, vasoconstrictor and antinatriuretic factors are in charge of maintaining the arterial pressure, which causes sodium and fluid

retention. The intestinal capillary pressure and permeability are also altered, and fluid accumulation in the abdominal cavity also takes place. As the disease progresses, renal excretion is impaired and there is also renal vasoconstriction leading to more complications such as dilutional hyponatremia and hepatorenal syndrome. The presence of ascites is associated with poor long-term survival, therefore it is important to identify if the patient has infections such as SBP or impaired renal or circulatory functions. Patients with those complications are given priority for liver transplantation. In recent years, the management of ascites has improved considerably. Patients receive guidelines to palliate the symptoms, such as reduction of the sodium intake through a low sodium diet, diuretics intake (although sometimes the patients do not respond) or restrict the fluid intake in cases of dilutional hyponatremia. Patients with a large volume of ascites require paracentesis (a fast and effective method) together with the administration of diuretics as a maintenance therapy. The removal of a large volume of ascites (more than 5 liters) can produce a derangement in the circulatory function, therefore, the administration of a plasma expander such as albumin is needed.

Fibrosis degree assessment

During the past decade, research has been focused on the development of new techniques to provide better and more accurate diagnosis of the liver disease. There is

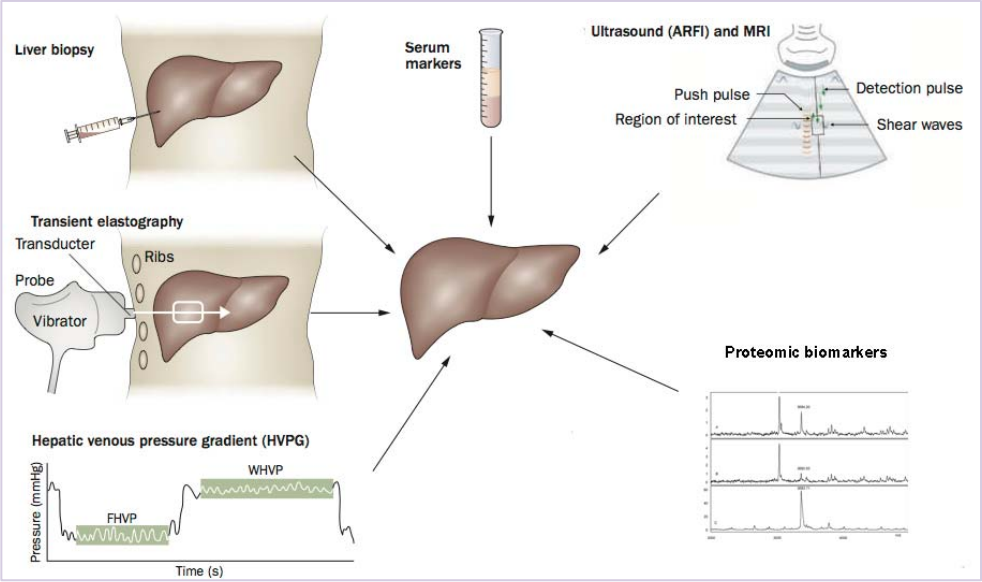

Figure 2. Fibrosis degree assessment. Modified figure from Friedman, 2010.

a great interest in providing early diagnosis to patients in order to start possible treatments as early as possible. Usual proceedings include invasive methods such as liver biopsy, or non-invasive methods such as blood sampling and measurement of typical liver damage parameters like alanine aminotransferase (ALT), aspartate aminotansferase (AST), platelet count or prothrombine time. In the last years, imaging techniques have been largely improved and included in the inspection routines. Last but not least, basic research on liver diseases has been focused on finding new non-invasive molecular markers of liver fibrosis and cirrhosis. Figure 2 illustrates the different possibilities for fibrosis degree assessment.

Liver Biopsy

Liver biopsy (LB) is considered the gold standard method for the diagnosis of liver fibrosis. Histological examination is used to identify the underlying cause of the liver disease and it is also is important in order to classify the biopsies into different staging groups. In 1981, Knodell at al. described a semiquantitative staging method based on four features: periportal necrosis with or without bridging necrosis, parenchymal injury, portal inflammation and fibrosis. The combination of all four provides the total histology activity index (HAI) ranging from 0-22. The first three consider the necroinflammatory grade of the disease, while the fourth considers the staging of fibrosis. Liver fibrosis is classified as 0 = absent, 1-2 = mild, 3-4 = moderate and 5-6 =severe/cirrhosis. The Metavir score is specifically used for evaluating chronic hepatitis C. It includes two separate scores, one measures the necroinflammatory activity (A) and the second the fibrosis stage (F). The score values range from 0-4, being 0 no inflammation or no fibrosis and 4 the most severe grade of inflammation or cirrhosis (Baranova et al., 2011). Other important and widely used scores are MELD and Child-Pugh. However, they are more focused on assessing the required treatment, severity and prognosis of the end-stage liver disease more than assessing the fibrosis stage. MELD score uses patient's values of total bilirubin, serum creatinine and the prothrombin time and Child-Pugh includes all mentioned together with ascitis and hepatic encephalopathy (Farnsworth et al., 2004). Forns score, like Child-Pugh, also combines clinical, hematologic and biochemical variables. In this case the age of the patient, γ-glutamyl transpeptidase (GGT) values, platelet count and cholesterol are

considered (Forns et al., 2002). The authors described the score as accurate to discriminate patients with hepatitis C without significant liver fibrosis in order to avoid LB. Figure 3 shows a graphic representation of cirrhosis progression and a typical classification of the different stages depending on the Metavir score.

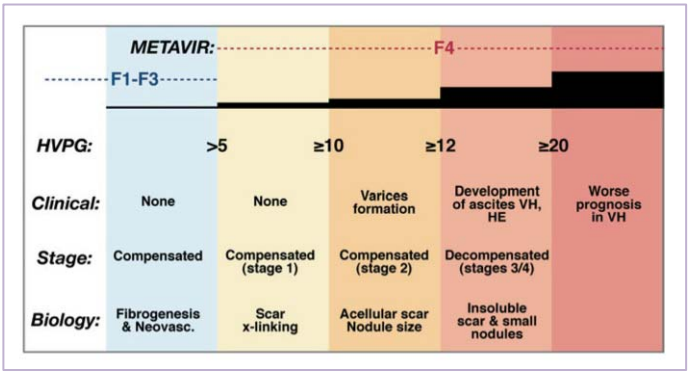

Figure 3.Cirrhosis progression. Original figure from Friedman, 2008.

However, LB carries important disadvantages, the most evident is that it is an invasive method and as any other surgery carries risks, about 0,3-0,5% of the patients present some complications while a 40% at least feels slight pain or discomfort (Bataller and Brenner, 2005). Follow-up studies for fibrosis progression relying on LB are risky and the cost is high, and there is also the possibility of a sampling error during the biopsy. LB is not an objective method, there exists an intra-inter observer error during histology assessment (Bedossa, 1994). Fibrosis is the most important factor in prognosis of the progression of the liver disease, but LB cannot predict the progression, and that is considered as the greatest limitation of this method. However, in almost all cases HCV patients must undergo LB before the initiation of the antiviral treatment and often as a follow up to evaluate the results of the therapy (Perrillo, 1997). Despite being still considered for some patients, the aim of researchers and clinicians is to find a non-invasive method capable of predicting fibrosis progression, study its regression or the response to antiviral treatments. Other methods such as hepatic venous gradient pressure (HVPG) have outperformed LB at identifying patients with HCV recurrence (Perrillo, 1997).

Ultrasound and imaging-based techniques

Non-invasive evaluation of liver fibrosis has been in the spotlight for many years. Back in 2003, Sandrin et al. described a new method based on one-dimensional (1-D)

transient elastography (TE) to measure liver stiffness or elasticity using ultrasound (5 MHz) and low frequency elastic waves (50 Hz). The propagation speed is directly related to elasticity, the stiffer the liver, the more severe the hepatic fibrosis. The device used is known as Fibroscan. The result is expressed in kilopascals (kPa) and is obtained after 10 pulse-echo acquisitions that measure the speed of the waves. This method is non-invasive, painless, rapid, objective and less costly than the biopsy. It has proved to be successful in a wide range of chronic liver disorders, including chronic hepatitis C, patients with ascites, biliary fibrosis, NAFLD and NASH (Corpechot et al., 2006; Yoneda et al., 2008; Hirooka et al., 2011). However, it also presents some limitations. It has been proved to be unreliable in 25% of obese patients due to abdominal fat (Friedrich-Rust et al., 2010). To overcome this limitation, a different type of probe was developed, the Fibroscan XL probe.

Magnetic resonance elastography (MRE) is also a novel method used to measure liver stiffness. In addition, it also measures spleen stiffness, which has been observed to be more closely correlated with portal pressure. A negative remark is that it is more expensive and time consuming and it is only used as an additional tool (Berzigotti et al., 2011).

The next commented methods are not used to assess tissue stiffness but other parameters involved in the liver disease, the ultrasonography (US), abdominal computed tomographic scan (CT-scan) and magnetic resonance (MRI). US-Doppler is used to assess causes of portal hypertension different than cirrhosis, such as portal or hepatic vein thrombosis, it is also very sensitive in diagnosing ascites and is useful as a non-invasive method for follow-up of TIPS. CT-scan and MRI allow an accurate visualization of the liver parenchyma and the portal venous system (Berzigotti et al., 2011).

Serum markers

There was an urgent need to develop surrogate markers of liver fibrosis other than LB to assess the extent of fibrosis, or alternatively use serum markers in combination with a single biopsy to follow up the progression of the disease. The aim of serum fibrosis markers is to differentiate efficiently between different stages of fibrosis: mild, moderate, severe and cirrhosis. Serological markers can be classified as

direct or class I and indirect or class II. Indirect biomarkers include several blood parameters measured by simple laboratory tests such as AST, AST/ALT ratio, platelet count, prothrombine time, cholesterol, gamma globulin, GGT or bilirubin. All those parameters have been reported to be significant predictors of fibrosis/cirrhosis but in a lesser extent of fibrogenesis/fibrolysis. Indirect markers measure liver fibrosis by multi-parameter combinations or scores selected by statistical models and mathematical algorithms. An example of an indirect fibrosis biomarker score is APRI (aspartate transaminase to platelet ratio index) (Wai et al., 2003). Progression of liver fibrosis may reduce AST clearance, resulting in an increased serum levels, on the contrary, platelet count is inversely proportional to the progression of the disease due to portal hypertension worsening. APRI was influenced by sex as males have higher values of AST than women (Toniutto et al., 2007). Another example is Fibrotest, which combines 5 blood test components (α2-macroglobulin, haptoglobin, apolipoprotein A1, GGT and total bilirubin). In this case, AST, which has been proved to have poor sensitivity for fibrosis assessment, is not included (Imbert-Bismut et al., 2001). In a recent study, Fibrotest has been validated to be as efficient as a LB when assessing fibrosis transition rates and its risk factors (Ponyard et al., 2012). There are more than 20 described scores based on indirect fibrosis markers used for the diagnosis of the liver disease, however not all have been deeply studied or validated for all etiologies.

Some variables can be altered after liver transplantation due to other causes not related to fibrosis, in those cases direct markers are more indicated to identify patients with rapid fibrosis progression (Punpapong et al., 2008). Direct biomarkers mainly include secretion products of activated HSCs, portal myofibroblasts, matrix components such as collagen fragments and split products, ECM–related enzymes or mediators of ECM turnover. The fibrogenesis process triggers the release of these components to the bloodstream. ECM components can be classified into collagens (type I and III are the most predominant in the liver, and with a lesser amount type IV and V), non-collagenous glycoproteins (fibronectin, laminin and elastin are the most abundant), proteoglycans (heparan, dermatan and chondroitin sulfates) and the polysaccharide hyluronan or hyaluronic acid (HA).

HA is widely distributed in the extracellular matrix. In the liver, it is synthesized and secreted by fat-storing cells (HSCs) and degraded by sinusoidal endothelial cells

(Gressner and Bachem, 1990). There were several studies in the mid 80's and 90's that described HA as a good serum marker of fibrosis progression for different types of liver disease such as alcoholic cirrhosis, primary biliary cirrhosis, viral hepatitis and non-alcoholic fatty liver disease (Frébourg et al., 1986; Guéchot et al., 1995, 1995b; Suzuki et al., 2005).

Markers linked to the matrix components derived from the procollagen and collagen have also been studied as possible biomarkers of fibrosis, such as the aminoterminal propeptide of type III procollagen (PIIINP) or the procollagen type I carboxy terminal peptide (PICP). PIIINP is the N-terminal cleavage product of procollagen III into collagen III and one of the major components of the connective tissue. PIIINP levels are higher during fibrogenesis followed by an increase in its serum levels (Guéchot et al., 1996). PICP did not prove to be a good liver fibrosis marker, as it was only elevated in 50% of the patients with advanced chronic hepatitis C and was normal in patients with mild fibrosis (Jarcuska et al., 2010; Baranova et al. 2011).

Some limitations of these direct serum markers have appeared, both HA and PIIINP are poorly correlated with liver inflammation and necrosis and they are not disease specific, because increase of those products have also been reported in rheumatoid arthritis, pancreatitis or lung fibrosis among others (Gressner et al., 2007).

Glycoprotein YKL-40 (chondrex, molecular mass 40 Kda) is a growth factor for fibroblasts and endothelial cells, which has been found to be strongly expressed in liver tissue. Several studies have detected elevated concentrations of this glicoprotein in the serum of patients with different etiologies and have showed a direct correlation with the rate of progression of fibrosis (Kamal et al., 2006; Tran et al. 2000). YKL40 serum levels paralleled those of TGFβ in this same study. The combination of YKL-40 and HA was able to predict short to medium term risk of hepatic fibrosis progression following liver transplantation in patients with HCV (Punpapong et al., 2008).

TGFβ is a key profibrogenic cytokine involved in tissue growth, differentiation, ECM production and immune response. There are many studies that analyze TGFβ1 as a possible biomarker as it is found in high levels in serum and the concentrations are correlated with the hepatic dysfunction such as AST and ALT levels (Flisiak et al., 2000).

Matrix metalloproteinases (MMPs) and their inhibitors, tissue inhibitors of matrix metalloproteinases (TIMPs) regulate collagen formation and degradation. These

proteases have also been found to be significant when assessing fibrosis as their expression correlates with hepatic collagen turnover (Walsh et al., 1999; Boeker et al., 2002; Leroy et al. 2004).

Scores combining direct markers have also emerged in the last few years. ELF score (Enhanced Liver Fibrosis), developed by Rosenberg at al., have demonstrated that the combination of three direct biomarkers (PIIINP, HA and TIMP1) is efficient to identify patients with advanced fibrosis and cirrhosis. They examined the distribution of the algorithm scores through different stages of fibrosis to determine the correlation between the scores and the severity of the disease measured by histology. Their algorithm can be used in a wide range of liver fibrosis diseases to distinguish patients with mild or no fibrosis from those with clinically significant fibrosis. (Rosenberg et al., 2004).

Some more limitations of direct biomarkers have aroused. There is a tendency to find those biomarkers elevated in association with a high inflammatory activity, consequently, some cases of extensive matrix deposition may be overlooked due to low inflammation. They are not liver specific and also, serum markers levels depend on the clearance rates, influenced by the dysfunction of endothelial cells or renal function (Baranova et al. 2011).

Proteomics-derived biomarkers

New techniques based on mass spectrometry (MS) have emerged in the recent years. MS technology, thanks to its high sensibility, makes possible a deep analysis of the proteome and offers the possibility to describe new potential biomarkers. In the liver disease field, there is a high interest in the research of non-invasive biomarkers accurate enough to discern between the different fibrosis stages. A MS consists of three basic components:

- An ion source: the sample is fractioned into analytes and ionized. The most common used techniques are MALDI (matrix-assisted laser desorption/ionization) and ESI (electrospray ionization).

- A mass analyzer: the samples are separated by the mass-to-charge ratio. Depending also on the MS instrument, there are four different types of analyzers: TOF

(time of flight), ion trap, quadrupole and FTICR (Fourier transform ion cyclotron resonance).

- An ion detector.

Different combinations of the ion source and mass analyzer are possible, ESI-ion trap, ESI-Q/TOF, MALDI-TOF are the most common. Figure 4 shows a general diagram of a MS. In general, the sample is loaded, ionized and fragmented normally at the peptide bond site in the mass analyzer. The charged particles are separated according to their mass-to-charge by and electric or magnetic fields. A software transforms the results into a mass spectrum graph that represents the obtained mass-to charge ratio of the peptides and some instruments, in addition, make possible the determination of the aminoacid sequence. The last step requires the use of bioinformatics tools to classify the significantly obtained peaks with a decision tree classification (Bozdayi et al., 2012; Guerrera and Kleiner, 2005).

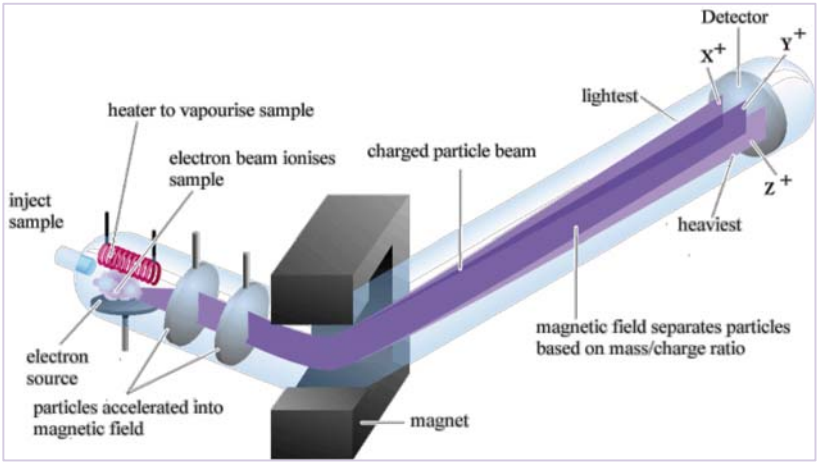

Figure 4. Mass spectrometer. Modified figure from Organic Chemistry 4e. Francis A. Carey, Mc Graw Hill.

2. The fibrogenesis process

Hepatic stellate cells

The hepatic stellate cells (HSC) were described by Kupffer in 1876 and referred to as “sternzellen”, star cells, thanks to a method based on gold chloride that was able to identify vitamin A droplets. Almost a century later, Ito described them as “fat storing cells” as and named them “Ito cells” (Ito, 1951), years later, other investigators

proposed the name of “lipocytes”. Finally, Wake revalidated Kupffer’s experiment in 1971 (Wake, 1971). In 1996 there was a consensus to standardize the name to “hepatic stellate cells”. Indeed, HSC are vitamin A droplet storing cells (retinoid) with an unquestionable role in liver fibrosis and repair. Their similarities with fibroblasts

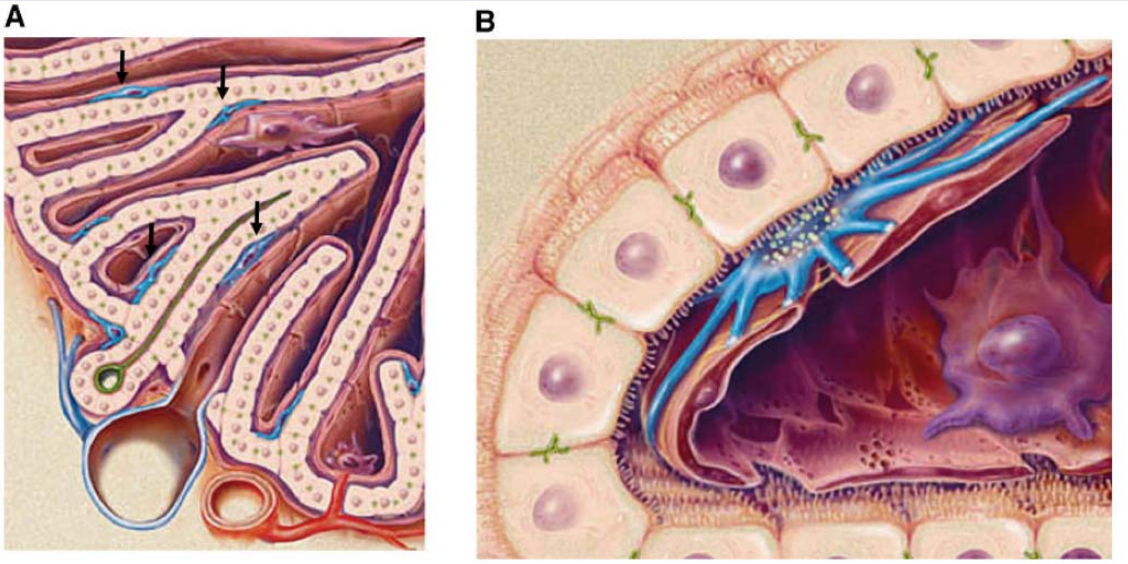

Figure 5. The hepatic stellate cell. Arrows indicate HSC position in the Disse space. Original figure from Friedman, 2008.

arose a lot of interest and many studies were conducted to deepen the knowledge about their function. HSC are located in the Disse space, between the basolateral surface of hepatocytes and the anti-luminal side of sinusoidal endothelial cells and they comprise a 15% of the total cell population in a normal liver (Figure 5A,5B).

HSC functions

In addition to the role of HSC in fibrogenesis, there is growing evidence that these enigmatic cells have other multiple functions. As shown on Figure 6, HSC are important immunoregulators during the initial phases of fibrosis. Activated cells release chemokines, such as monocyte chemotactic peptide (MCP-1), CCL21 or RANTES among others providing the ability to amplify the inflammatory response by stimulating the infiltration of blood cells into the tissue. HSCs can also function as antigen presenting cells stimulating lymphocyte proliferation or apoptosis and also by interacting with lymphocyte subsets including natural killer cells (NK), which function as cleaners of activated HSCs, but also CD4 and CD8 lymphocytes (Friedman, 2008, 2010).

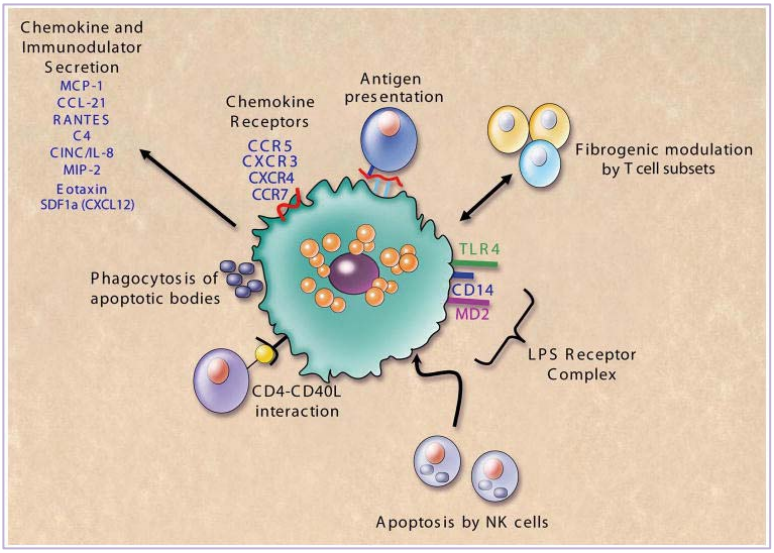

Figure 6. Immunoregulation by HSC. Original figure from Friedman, 2008.

CD8 T cells have more fibrogenic properties than CD4, which explains the increased rate of fibrosis in patients with HIV co-infection, where the CD4/CD8 ratio is reduced. Kupffer cells express toll-like receptors (TLRs), but surprisingly HSCs too, which means they can respond to pathogen-associated molecular patterns (PAMPs) clearly inducing its inflammatory phenotype. In particular, the expression of TLR4 and the bacterial lipopolysaccharide (LPS) receptor complex components CD14 and MD2 entail that HSCs interact with LPS inducing the expression of more chemokines (Paik et al., 2003). Phagocitosis of apoptotic bodies that result from apoptotic hepatocytes is also another known function carried out by HSCs. Those apoptotic bodies serve as activation stimuli of HSCs (Canbay et al., 2004).

As a result of all those functions, HSCs secrete a wide broad of substances and membrane receptors. Among those substances, the most remarkable are:

- Lipids: prostaglandins and leukotrienes.
- Growth factors: comprises a large group of factors like epidermal growth factor (EGF), hepatocyte growth factor (HGF), fibroblast growth factor (FGF), transforming growth factor-α (TGFα), insulin growth factor I and II (IGF), the most potent stellate cell mitogen platelet derived growth factor -A and –B (PDGF) together with its receptor PDGFRβ, vascular endothelial growth factor (VEGF) and its receptor and connective tissue growth factor (CTGF).

- Chemokines: MCP-1 and platelet activating factor (PAF), RANTES, C-X-C chemokine ligand 1 (CXCL1).
- Cytokines: the pro-inflammatory IL6, or the anti-inflammatory IL10, and the most important cytokine, TGFβ together with the receptor TGFβR1.
- Adhesion molecules: ICAM-1 and VCAM-1.
- Vasoactive factors: endothelin-1 (ET-1) a potent vasoconstrictor, its receptors ET_A and ET_B and its physiological antagonist, nitric oxide (NO).
- Matrix components: ECM turnover proteins, such as collagens, metalloproteinases (MMPs) and tissue inhibitor of metalloproteinases (TIMPs).
- Membrane receptors: and finally integrins and cannabinoid receptors (CB1 and CB2)

HSC activation

Stellate cell activation is a key event in fibrogenesis. The activation of these cells refers to a phenotypic change from a quiescent vitamin A-rich cells to activated myofibroblast-like proliferating, fibrogenic and contractile cells. Upon activation, HSC lose the characteristic vitamin A droplets and instead, express desmin, an intermediate filament typical of contractile cells and α-SMA, typical of vascular smooth muscle cells and myofibroblasts. Both have been widely studied and are consolidated markers of HSC activation in rodents. Induction of α-SMA is the most reliable HSC marker also in human cultured cells because it is absent in any other resident liver cell but vascular smooth muscle cells. A study demonstrated that the activation of HSC is also linked to a switch from E- to N-cadherin typical from endothelial cells (Lim et al., 2007). This finding suggests that HSC undergo epithelial to mesenchymal transition (Sicklick et al., 2006).

The source of the damage is diverse, leukocyte infiltration is the main trigger of HSC activation, but in metabolic diseases such as hemochromatosis infiltration of inflammatory cells is absent. Reactive oxygen species (ROS) are generated from lipid peroxidation, or from the induction of cytochrome P450 2E1 in hepatocytes in ASH or NASH. Ethanol, polyunsaturated fatty acids and iron also enhance the production of ROS.

Apoptosis of parenchymal cells is both a consequence and an important stimulus of activation of HSC. Stellate cells phagocyte the apoptotic bodies increasing NAPH oxidase (Zhan et al., 2006).

As previously mentioned, the release of immunomodulators by HSC induce an important inflammation response that enhances fibrogenesis from early stages.

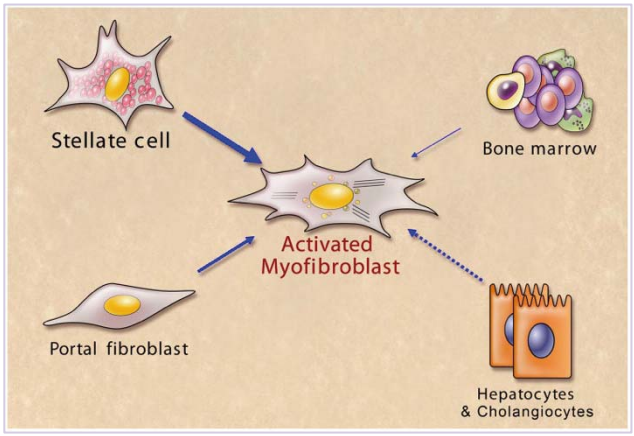

Figure 7. Sources of myofibroblasts in the liver. Original figure from Friedman, 2008.

Resident stellate cells are not the only cell types that contribute to the population of myofibroblast-like cells increase and accumulation. Other cells also take part in response to liver injury (Figure 7). Fibrocytes are fibroblasts that can originate from perfipheral blood (seen in lung fibrosis) or bone marrow cells. These cells migrate in response to chemokines secreted upon liver injury. There are some studies that proposed that circulating fibrocytes also might derive from bone marrow cells and contribute in small numbers to the collagen-producing cells in the liver (Kisseleva et al., 2006). Epithelial cells (EC) contribute to the myofibroblast population via epithelial-to-mesenchymal transition. Damaged epithelial/endothelial barrier lead to vascular thickening, tissue hypoxia and decrease in NO. EC also produce TGFβ and contributes to the recruitment of neutrophils from the blood vessels into the damaged tissue and macrophages phagocyte apoptotic bodies from apoptosing EC (Sicklick et al., 2006). In cholestatic liver injury, the most important source over HSC are portal fibroblasts with the ability to induce α-SMA expression and secretion of MCP-1 (Beaussier et al., 2007).

HSC activation consists of two main phases: initiation and perpetuation. A third phase that should not be overlooked is resolution of fibrosis, which might occur if the source of the damage subsides (see Figure 8).

- Initiation, or proinflammatory state is characterized by early changes in gene expression and phenotype of stellate cells with the active participation of all neighboring cells (Kupffer cells, sinusoidal endothelial cells and hepatocytes). Upon

liver tissue injury, cells surrounding stellate cells segregate paracrine stimuli that promote their activation. The molecular mechanisms underlying HSC activation point to TGFβ as the most important profibrogenic cytokine responsible for the stimulation of many genes involved in inflammation or ECM turnover. New collagen formation will change the ECM composition from type IV to type I and III, and the upregulation of both MMPs and TIMPs will lead to ECM disregulation. NFκB upregulation promotes HSC survival, therefore, increasing fibrosis.

- **Perpetuation** is characterized by the behavioral change in activated stellate cells and myofibroblast-like cells with the end point of increasing the accumulation of ECM. This stage comprises a complex orchestra of different events that occur simultaneously:

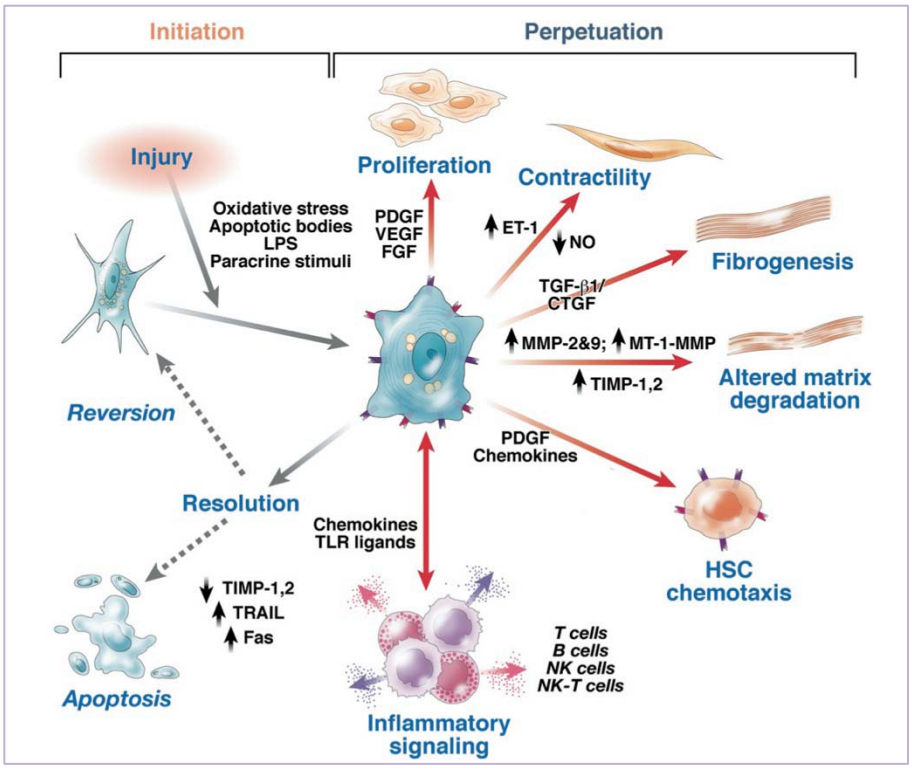

Figure 8. Hepatic stellate cell activation. Original figure from Friedman, 2008.

1) Proliferation: the most immediate and potent mitogenic factor released upon liver injury is PDGF together with its receptor PDGFRβ. Not only HSCs, but also Kupffer cells release this factor. The downstream cascade activates ERK, PI3-kinase among others, and activate Na^+/H^+ exchange channels. Other proliferating factors such as VEGF, thrombin and its receptor, EGF, FGF are also upregulated in this phase. With

all this stimuli, myofibroblast cells increase its numbers substantially compared to a normal liver.

2) Chemotaxis: chemoattractant chemokines are secreted to promote HSC migration towards the site of injury. PDGF also has chemotactic properties, as well as MCP-1, which induce macrophage infiltration to the tissue increasing the inflammatory response.

3) Fibrogenesis: if liver damage is sustained, HSC start to produce matrix components that lead to the characteristic liver stiffness of advanced cirrhosis. In this phase, the most important inducer of collagen synthesis is TGFβ (Gressner et al., 2002), secreted by the same HSC and surrounding cells. The TFGβ cascade include Smad proteins, which translocate into the nucleus and promote the transcription of other TFGβ target genes. The response of Smads differs between chronic or acute damage (Inagaki and Okazaki, 2007; Breitkopf et al., 2006), moreover, TGFβ also induces matrix formation by stimulating the production of collagens (Pinzani and Marra, 2001). Hepatocytes undergoing oxidative stress release profibrogenic factors for HSC (Svegliati Baroni et al., 1998). CTGF is another important fibrogenic factor regulated by TGFβ.

4) Contractility: contractility of stellate cells is the main cause of the increased portal resistance in the liver. Activated HSCs express contractile filaments including α-SMA and myosin. HSC are mainly located where collagenous bands develop and prevent normal blood flow by constricting sinusoids and in general, by contracting the whole liver. Calcium takes a major role in contraction, but the increase of ET-1 and the physiological antagonist, NO, decrease are the most important regulations of the contractibility of the liver. Other vasoactive factors such as AII, eicosanoids, atrial natriuretic peptide, somatostatin or carbon monoxide are also involved.

5) Matrix degradation: fibrosis is the result of an unbalance between matrix formation and degradation. Disruption of the balance of the normal liver leads to matrix accumulation. Collagen mRNA is highly upregulated, and collagen type IV is rapidly replaced by collagen type I and type III (Lindquist et al., 2000; Tsukada et al., 2006). HSCs secrete some of the MMPs important for the initial phases of fibrogenesis, such as MMP13, but other cells also contribute to their synthesis. MMPs inhibitors, the TIMPs, are highly upregulated repressing MMPs matrix degradation and taking the

balance to a net accumulation of ECM. TIMP1 has also an anti-apoptotic role towards HSC, participating in the increase of HSC population (Murphy et al., 2002).

6) Retinoid loss: one of the most characteristic phenotypic changes is the loss of retinoid droplets when HSC activate, but it is not completely clear if it is a requirement for the activation.

- Resolution or reversion of fibrosis occurs if the source of damage is ceased. This process is correlated with the decrease in TFGβ and other pro-inflammatory cytokines as well as ECM production, increased collagenase activity and decrease of myofibroblasts (Iredale et al., 1998). During reversion of fibrosis, myofibroblasts undergo apoptosis and senescence (Iredale et al., 1998; Krizhanovsky et al., 2008), but there is also a portion of those cells that escape cell death. A recent study evidences that a reversion from myofibroblasts to a similar quiescent HSC phenotype takes place

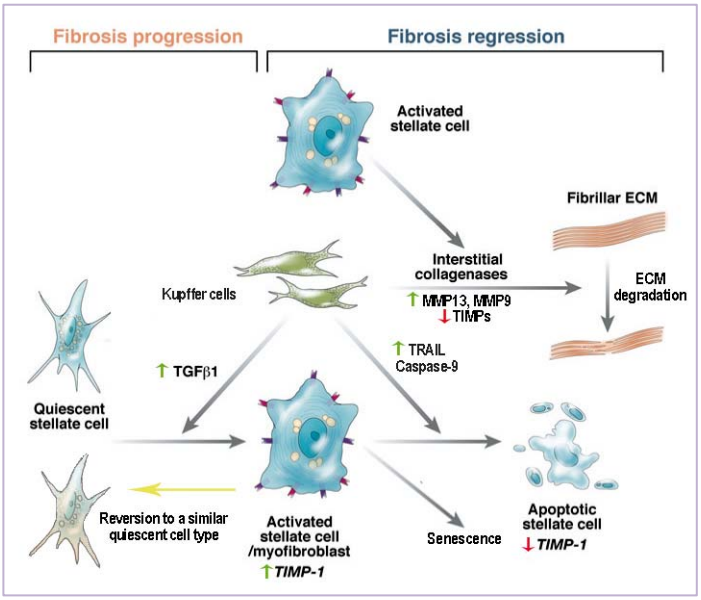

Figure 9. Fibrosis regression. Modified figure from Friedman, 2008.

(Kisseleva et al., 2012). Kupffer cells produce Caspase-9 and TRAIL (tumor necrosis factor–related apoptosis inducing ligand) which promote HSC apoptosis (Fischer et al., 2002). Increased collagenase activity is also an important step in fibrosis resolution. Kupffer cells also secrete MMP13 and MMP9, which degrade the collagen fibers and at the same time, TIMPs are downregulated (Fallowfield et al., 2007; Fisher et al., 2002). Figure 9 summarizes the progression process and illustrates the explained reversion steps. However, full recovery of the original architecture of the liver is not

accomplished in advanced fibrosis /cirrhosis stages, which is often referred as a “point of no return”.

3. Key target genes

Key genes involved in fibrogenesis are potential therapeutic targets, for this reason, in the last years many studies have aimed at modulating the expression of those genes. The most relevant genes in this work are the ones represented on Figure 10. PDGF is the main proliferation and chemotactic agent, TGFβ is the most important profibrogenic cytokine, MMPs and TIMPs are the responsible proteins of the ECM balance and collagens are the main matrix components.

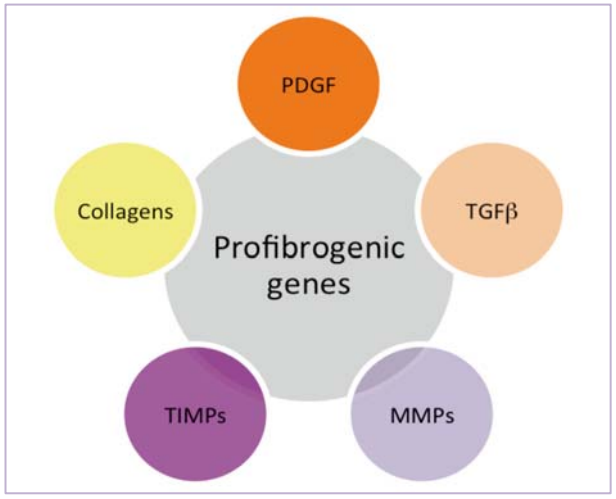

Figure 10. Key genes involved in fibrogenesis.

PDGF

PDGF is the most potent mitogen and second most potent cytokine after TGFβ involved in liver fibrogenesis and HSC activation. PDGF family consists of PDGF-A, PDGF-B, PDGF-C and PDGF-D, and their receptors PDGFRα and PDGFRβ. PDGF is secreted as homo- or heterodimers (PDGF-AA, -BB and –AB). Receptor affinity varies between the isoforms, PDGF-A and –C bind specifically to Rα, PDGF-B binds to both Rα and Rβ and PDGF-D binds only to Rβ (Bonner, 2004). Following liver damage, quiescent HSC activate into myofibroblast-like cells, and express PDGFRβ and PDGF to stimulate autocrine growth, chemotaxis and loss of retinoids. It is also known that TGFβ increases the mitogenic effect of PDGF-BB, but not –AA, due to the upregulation of PDGFRβ (Pinzani et al., 1995 and Bissell et al., 1995). In normal liver, PDGFRs expression is almost undetectable, however, after damage type β receptor is markedly upregulated, suggesting that PDGF-B is the main isoform involved during HSC

activation. In a more recenty study, PDGF-D also showed mitogenic and profibrogenic effects on HSC (Borkham-Kamphrost et al., 2007). Many studies have reported TGFβ as the main regulator of PDGFRβ in HSC, but also TGFβ released from other cells contribute to PDGF upregulation (Bissell et al., 1995). The main signaling pathway for PDGF is ERK/MAPK.

TGFβ

TGFβ is the most important cytokine that promotes wound-healing and repair. Overexpression of TGFβ in rodents has proved to increase fibrosis in many organs (Bataller and Brenner, 2005). Kupffer cells are the major source of TFGβ, which induces apoptosis of hepatocytes and at the same time activates HSC resulting in collagen synthesis. Before its complete activation, TGFβ undergoes posttranslational modifications. At first, it is secreted as a non-active preform and remains inactive while associated with LAP (latency associated peptide) and LTBP (latent TGFβ binding protein) and is activated by binding either to thromposponding-1 (TSP-1) or to αvβ6 integrin. TSP-1 is a glycoprotein implicated in cell adhesion, angiogenesis and remodeling of the ECM, and αvβ6 integrin is a matrix receptor in epithelial cells, and macrophages, and mediate cell adhesion, migration and connect all cytoskeletal proteins to the ECM. Other proteases such as plasmin or MMP2, 9 can also activate TFGβ.

TFGβ canonical signaling is mediated by Smad proteins, R-Smad (Smad 1-2-3-5-8), co-Smad (Smad 4) and inhibitory Smads (Smad 6-7). Smad 3 is known to be critical for hepatic fibrogenesis as well as fibrosis in other tissues. The complex Smad 3/4 translocate to the nucleus and initiate the transcription of target genes. CTGF is a recognized stimulator of TGFβ as it increases the affinity to the receptor TGFβRII and antagonizes Smad 7. Hepatocyte growth factor (HGF) is produced in response to elevated TGFβ and functions as a negative regulator by inhibiting Smad translocation to the nucleus. HGF is anti-fibrogenic, anti-inflammatory, pro-regenerative and inhibits myofibroblast differentiation. However, TGFβ also inhibits HGF, and with high levels of TGFβ during HSC activation, HGF is rather repressed.

Aside from MCP1 and MIP, TGFβ is also a potent chemoattractant of macrophages.

MMPs and TIMPs

In healthy livers, ECM formation and degradation is perfectly balanced. The enzymes responsible for the correct homeostasis of the ECM are the matrix metalloproteinases (MMPs) and their inhibitors, the tissue inhibitors of metalloproteinase's (TIMPs). Upon damage, the liver ECM homeostasis is deregulated by the activation of the HSCs and the production of profibrogenic cytokines and ECM components mainly by this same cell type (Figure 11). The upregulation of TIMPs result in the inhibition of MMP activity and consequently, matrix proteins accumulate in the extracellular space (Hemmann et al., 2007).

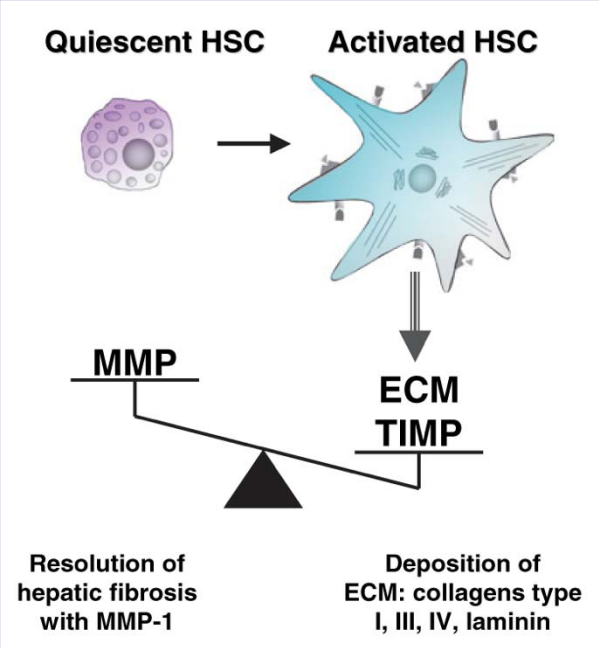

Figure 11. Deregulation of the normal ECM balance. Original figure from Kisseleva and Brenner, 2006.

The main cell type expressing MMPs are HSCs, myofibroblasts and Kupffer cells. These enzymes have a complex regulation. Aside from TIMPs, they are also regulated by different mechanisms at transcription level (by cytokines such as IL1α, TGFβ or TNFα,) by activation and cleavage of the proenzyme to an active form or by the action of endogenous proteinase inhibitors, such as α2 macroglobulins produced by hepatocytes (Cawston and Mercer, 1986; Visse and Nagase, 2003). The MMPs itself can be the responsible for other proMMP's activation, such as MMP3 or MMP2 in absence of TIMP2 (Knauper et al., 2002). The MMP family, with 23 different members described in humans, is able to degrade a wide broad of collagenous and non-collagenous substrates. They are classified into six groups according to their main substrate, sequence similarity and domain organization:

- Gelatinases: MMP2 (gelatinase A) and MMP9 (gelatinase B).
- Collagenases: MMP1 in humans and MMP13 in rodents, MMP8 and MMP18 in *Xenopus*.
- Stromelysins: MMP3 (stromelysin 1) and MMP10 (stromelysin 10).
- Matrilysins: MMP7 (matrilysin 1) and MMP26 (matrilysin 2).
- Metalloelastase: MMP12.
- Membrane-Type MMPs: six members compose this group, transmembrane-type I MMPs characterized by a C-terminal transmembrane domain (MMP14 or MT1-MMP, MMP15 or MT2-MMP, MMP16 or MT3-MMP and MMP24 or MT5-MMP) and the ones anchored to glycosyl phosphatidyl inositol in the surface of the cells (MMP17 or MT4-MMP and MMP25 or MT6-MMP).
- Other MMPs: there are few MMPs that are not classified in the above groups. MMP19 (important in rheumatoid arthritis), MMP20 (relevant for tooth formation), MMP22 (unknown action), MMP23 (expressed in reproductive tissues) and MMP28 (expressed in keratinocytes). MMP21 is expressed in *Xenophus* and MMP27 in *Gallus*.

MMP expression shows a dynamic expression during liver fibrogenesis. Figure 12 shows a schematic graph of the expression timings of MMPs and TIMPs during fibrogenesis.

Not all MMPs are expressed in the liver tissue, and is also noteworthy, that not the same MMPs are found in rodents and humans. MMP13 is considered the rodent homologue of human MMP1 due to its similarities in function and sequence (Knittel et al., 1999). TGFβ is known to repress the expression of MMP1, but interestingly not MMP13. In progressive liver fibrosis, MMP1/MMP13 is not significantly upregulated as fibrosis develops (Benyon et al.,

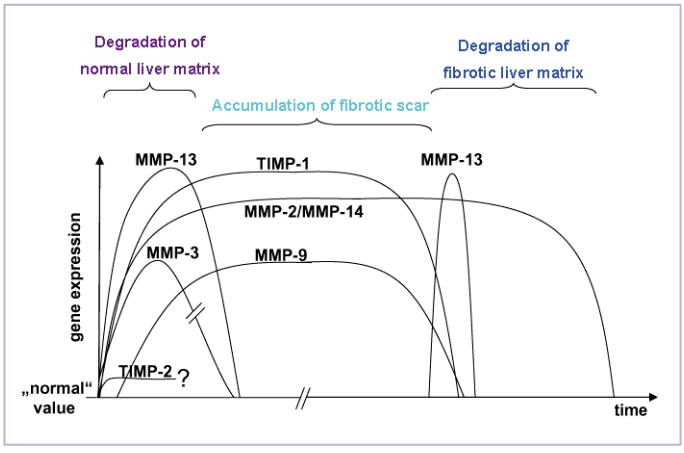

Figure 12. MMPs and TIMPs time expression. Figure modified from Hemman et al., 2007.

1996) in turn their direct inhibitor, TIMP1, is highly expressed. Several studies have reported that there is an enhanced MMP13 mRNA expression during resolution of CCl_4-induced liver fibrosis (Watanabe et al., 2000) and that MMP13 knockout mice showed a delay in resolution of liver fibrosis (Fallowfield et al., 2007). In this same study, the authors also observed that the main cellular source of MMP13 was scar-associated macrophages, and not any other liver cells.

MMP2 expression, together with MMP14, increases soon after HSC activation and is sustained during liver injury. MMP2 is specifically expressed and secreted by HSC. The activation of this metalloproteinase is particular as it takes place on the membrane and is mediated by a complex comprised of MMP2-MMP14 and TIMP2. Both MMP2 and MMP14 mRNA expression has shown a steady increase associated with the progression from mild to advanced cirrhosis (Zhou et al., 2004).

MMP9 has been more related to tissue inflammation than to the degree of fibrosis (Lichtinghagen et al., 2001). MMP9, produced mainly by Kupffer cells, is activated by MMP3 and is an important factor during the initial phase of HSC activation. Contradictory data exists about the expression levels of MMP9 in more advanced stages of fibrosis progression. Some studies have reported that MMP9 is elevated after an acute damage (Knittel et al., 2000), but not after a chronic liver injury induced by CCl_4 (Zhou et al., 2004). It has also been reported that MMP9 has an important role in reversion of fibrosis (Jiao et al., 2012).

MMP3 plays an important role activating other MMPs, and at the same time, can itself be activated by other proteases. This means that inflammation is an important trigger initiating the MMPs cascade. MMP3's most important substrate is laminin. This metalloproteinase has not been found to be relevant to assess fibrolysis in liver diseases, however it seems to be more valuable for alcoholic liver disease. Sinusoid and peri-sinusoidal areas are rich in laminin, and it has been found that during alcohol liver disease there are important pathological changes in those areas (Xu et al., 2004).

So far, only four TIMPs have been described: TIMP1, TIMP2, TIMP3 and TIMP4. TIMPs bind to MMPs through N terminal domain. There is a difference regarding the bond strength between a TIMP and a particular MMP. For instance, TIMP1 is specific for MMP9, while TIMP2 inhibits mainly MMP2. Each of them can interact with other

MMPs with less strength, there is only one exception, TIMP1 is unable to inhibit MMP14, MMP15 and MMP24. TIMPs are expressed by many cell types, and often are co-secreted with MMPs. TIMP1 is produced by activated HSC, as well as Kupffer cells and hepatocytes. Transcription is mainly regulated by TFGβ, which in turn inhibits MMP1 and MMP3 promoting the net accumulation of collagen. TIMP1, aside from inhibiting the degradation of newly formed collagen fibrils by MMPs, also is able to prevent the activation of pro-MMPs. Moreover, it has also been associated with other fibrotic diseases such as lung, kidney or pancreas. TIMP1 has been found to be strickingly upregulted in patients with HCV and HIV co-infection, suggesting that aside from being upregulated during fibrogenic processes, is also upregulated by inflammation (Mastroianni et al., 2002). In patients with HCV chronic liver disease, serum and mRNA levels of TIMP1 are correlated with the grade o fibrosis (Yata et al., 1999).

TIMP2 is expressed by HSC, Kupffer cells and myofibroblasts, but not in hepatocytes. Chronic liver damage induces a minor peak that lasts the first two days, but during chronic injury no significant increase was observed (Figure 12). In mice, TIMP2 is essential for MMP2 activation (Wang et al., 2000). In contrast to TIMP1, TIMP2 is inhibited by TFGβ.

TIMP3 has proapoptotic activity, in contrast to TIMP1 and 2, which are antiapoptotic (Guedez et al, 1998).

Last, TIMP4 is found in brain, heart, ovary and skeletal muscle. Little is known about this inhibitor in general and in the liver, no activity has been reported to date.

Collagens

Studies about collagen implication in the fibrosis processes started in the late 50's. Collagen deposition in fibrosis is the main cause of the changes in the architecture of the tissue leading to stiffness of the organ and its consequences. Researchers and clinicians have always been aware of the importance of expanding the knowledge about collagen formation and the importance of its degradation necessary for the resolution of the disease (Du et al., 1999).

In the liver, collagen type I, II and IV are the most abundant ECM components and are dramatically up regulated upon chronic liver damage. HSC, myofibroblasts and portal fibroblasts are the main source of procollagen mRNA expression. Several studies have confirmed that the expression of the different types of collagen has different timings. *In vitro* studies by Knittel et al. showed that upon HSC activation, there is a

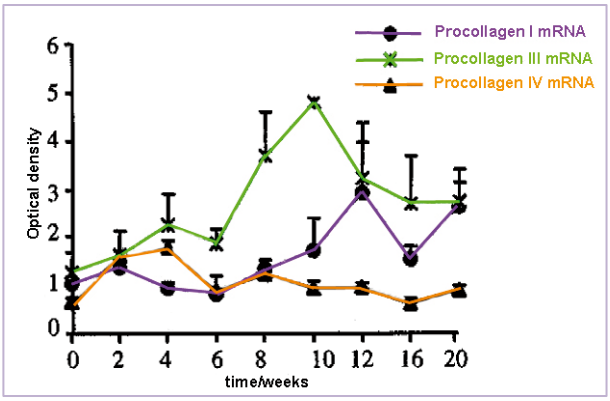

Figure 13. Dynamic changes of procollagen I, II and IV. Modified figure from Du et al., 1999.

different activation stage for each collagen type at both RNA and protein level. In freshly isolated HSC, the main collagen expressed is type IV, while collagen I is hardly detected. After a few days in culture, collagen I and III were highly upregulated while type IV declined (Du et al., 1999) (Figure 13).

The collagen fibers are located in the liver capsule, mesenchymal cells in portal areas and the walls of blood vessels (smooth muscle cells and endothelial cells of central veins).

4. The endocannabinoid system

General characteristics

Cannabis has been widely used as a psychoactive substance since ancient times and with medicinal purposes until the end of the 30's. The dangers of its abuse lead to many countries to prohibit the use of Marijuana as a therapy. In the last decades, the interest in these substances has stirred up once more with the description of the molecular structure of Δ^9-tetrahydrocannabinol (THC), the main psychoactive ingredient of Marijuana (Gaoni and Mechoulam, 1964). Endocannabinoids are lipid molecules derived from arachidonic acid involved in a wide variety of physiological

functions including, food intake, energy balance, pain, neuromodulation, cardiovascular homeostasis, immune and inflammatory responses and cell proliferation (Pacher et al., 2006; Reichenbach et al., 2010; Tam et al., 2011). The most studied endogenous cannabinoids are anandamide (Arachidonoyl ethanolamide, AEA) and 2-Arachidonoyl glycerol (2-AG). Several other endocannabinoids have also been described, N-Arachidonoyl dopamine (NADA), noladin ether (2-Arachidonoyl glycerol ether, 2-AGE) and virodhamine (O-Arachidonoyl ethanolamine, OAE). For Oleoylethanolamide (OEA) and palmitoylethanolamide (PEA) no known receptors have been described yet. All endogenous cannabinoids are eicosanoids and are not stored in the cells, they are synthetized on demand (Witting et al., 2004).

The effects of the endocannabinoids are mediated through two G protein-coupled receptors (GPCR), cannabinoid receptor 1 (CB1) and cannabinoid receptor 2 (CB2) (Figure 14). CB1 was first described by Matsuda et al. in 1990. It was found widely expressed in brain and in much lower concentrations in other peripheral tissues and cells (testis, spleen cells, leukocytes). CB2, the second cannabinoid receptor

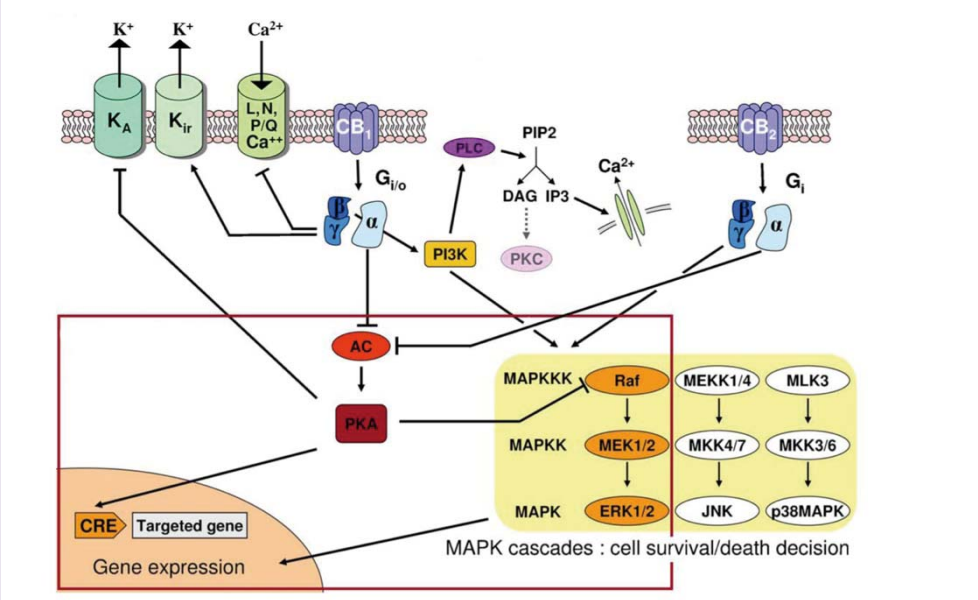

Figure 14. Cannabinoid receptors signaling pathways. Original figure from Bosier et al., 2010.

described (Munro et al., 1993), is mainly expressed in the immune system cells and peripheral tissues, but also in lower concentrations in the brain. CB1 and CB2 share only a 44% of their protein sequence and a 68% in the 7-transmembrane domains. Cannabinoid receptor signaling is rather complex. As G coupled-receptors, they inhibit adenylate cyclase activity (AC in the figure) with the consequent reduction of cAMP as

seen in experiments where pertussis toxin was able to reverse this effect (Howlett et al., 1986), they also inhibit different types of Ca^{2+} channels and stimulate certain K^{+} channels. Cannabinoids can also activate the signaling pathway of MAP kinases, including p44/42 MAP kinase, p38 kinase and JUN-terminal kinase and phosphatidylinositol-3-kinase pathway. Other pathways independent of G proteins have also been described for cannabinoids. CB2 transduces signals through the same pathways as CB1 with the exception of Ca^{2+} and K^{+} channels. AEA also interacts with the transient receptor potential vanilloid type 1 (TRPV1) that belongs to a large family of ion channels (Starowicz et al., 2007). Some studies have found evidence of another possible CB receptor, (Hájos et al., 2001) however further studies are needed to strengthen this hypothesis. GPR55, is an orphan receptor that has shown to be involved with the endocannabinoid system as it is able to recognize some endocannabinoid ligands and GPR119 has been reported to interact with OEA (Baker et al., 2006; Overton et al., 2006; Brown, 2007).

The endocanabinoid degradation is mediated by two enzymes, fatty acid amide hydrolase (FAAH) is responsible for the degradation of AEA (Glaser et al., 2003), while monoacyl glycerol liapse (MGL) degrades 2-AG (Saario et al., 2004).

The great interest in getting a better understanding on the mechanism of action of the endocannabinoid system have led investigators to develop synthetic agonists and antagonists (Table 1).

Table 1. Synthetic cannabinoid receptor agonists and antagonists. Adapted from Patcher et al., 2006.

CB1 selective		CB2 selective	
Agonists	**Antagonists**	**Agonists**	**Antagonists**
•R-(+)-methanandamide •Arachydonoyl 2' – choloroethylamide (ACEA) •O-1812 •2- Arachydonoyl glycerol ether	•SR1441716 •AM251 •AM281 •LY320135	•JWH015 •JWH133 •AM1241 •HU308	•SR144528 •AM630

Hepatic fibrosis and endocannabinoids

The first studies reporting endocannabinoid implication in liver diseases where published in 2001 by Garcia et al. The study revealed that AEA had a role in systemic and portal hemodynamics. Few years later, Siegmund et al., observed that AEA was able to induce apoptosis of HSC in vitro, proposing AEA as a possible antifibrogenic therapy. The same year, Julien et al. carried out the first study with clear results of CB2 receptors implication in liver disease. The group demonstrated that CB2 had an antifibrogenic role in liver fibrosis triggering growth inhibition and apoptosis of non-parenquimal cells. CB2 knockout mice where found to develop liver fibrosis after CCl_4-induced liver damage compared to wild type animals. In the same study, the analysis of human liver biopsies from various etiologies by immunohistochemistry showed that CB2 is not expressed in normal livers, but it is present in cirrhotic livers in non-parenchymal cells and in fibrotic septa. In culture, activated HSC and myofibroblasts presented high expression levels of this receptor, but not in non-activated and parenquimal cells. Thanks to those findings, CB2 has emerged as a possible antifibrotic target for future possible therapies.

In our laboratory, Muñoz et al. treated cirrhotic rats with ascites with a selective CB2 agonist (JWH133) for 9 days. We observed that the stimulation of CB2 receptors improved the systemic hemodynamics, decreased the number of infiltrating cells, reduced the number of activated HSC (measured by the amount of α-SMA), increased apoptosis of non-parenchymal cells and significantly decreased fibrosis compared to vehicle rats.

Further studies regarding CB2 receptors role in the liver, aside from their implication in fibrogenesis associated with chronic liver diseases, revealed they were also involved in ischaemia/reperfusion (I/R)-induced liver injury and hepatic encephalopathy-associated with acute liver failure. CB2 receptors limit liver injury induced by I/R (Bátkai et al., 2007; Rajesh et al., 2007) by reducing cell infiltration, reduced lipid peroxidation and expression of proinflammatory cytokines and chemokines. In addition, KO mice for the CB2 receptor where more susceptible to damage after I/R. CB2 also seem to play a role in hepatic encephalopathy. In the animal model of fulminant liver failure induced by tioacetamide, CB2 and 2-AG brain

levels where increased. The administration of different CB ligands including THC, HU-308, 2-AG or Rimonabant improved neurological dysfunction. Dagon et al., attributed this CB2 effect to the stimulation of brain AMP-activated kinase, a key regulator in energy balance and cognitive function.

A recent study by Teixeira-Clerc et al., added a new role of CB2 to the list as a key factor during liver regeneration using a model of partial hepatectomy in mice. KO mice for CB2 receptors had a delayed liver regeneration rate compared to wild type animals. The treatment of wild type mice with the CB2 agonist JWH-133 reduced liver injury and increased liver regeneration.

In parallel, many other investigators studied the role of CB1 receptors and interestingly, the effect was the opposite of the CB2 receptors, the stimulation of CB1 during liver fibrosis exerted a profibrogenic role (Teixiera-Clerc et al., 2006). The antagonism of CB1 receptor was able to attenuate liver damage induced in different rodent animal models of liver disease.

CB1 is the main effector of THC in brain, for this reason many studies were conducted at this level and a potent antagonist known as Rimonabant (SR141716A) (Rinaldi-Carmona et al., 1994), was developed and commercialized for human use to treat obesity. Soon after its commercialization, the drug was removed from the market in some countries due to an increase in depression and suicide rate in those patients (Christensen et al., 2007). This fact arose controversies for the use of CB1 antagonists as therapeutics, due to the possibility of side effects of the drug on the brain. Despite that, many studies have been conducted in rodent model animals testing the efficiency of blocking CB1. In a recent study by Giannone et al., the treatment of cirrhotic rats with established ascites with Rimonabant, was associated with a liver fibrosis decrease. Moreover, CB1 receptor stimulation decreased iNOS and ET1 expression, proinflammatory cytokines such as PDGF and TGFβ, as well as ECM turnover genes expression, as seen when analyzing TIMP1, MMP2, MMP9 and MMP13 expression. This demonstrated that the reversal of advanced fibrosis is also possible with the pharmacological antagonism of CB1 receptors, despite of the possible brain side effects.

Further study of CB2 involvement in liver fibrosis seems to be more appealing as it is unlikely that CB2 will cause side effects as CB1. However, as the stimulation of

CB1 receptors has proved to be a good antifibrogenic strategy, more research on CB1 antagonists that does not cross the blood-brain barrier could also open more possibilities to new antifibrogenic treatments (Wu et al., 2011).

Inflammation and endocannabinoids

CB2 receptors are highly expressed in the cells from the immune system, for this reason, there has been a great interest in unraveling the role of the endocannabinoid system regarding the immune regulation. Investigators were not disappointed with the findings, as CB2 has proved to be a key component and a potent regulator of immune responses. The cells from the immune system express 10 to 100 times more CB2 than CB1 receptor (Galièque et al., 1995). Among all immune cells, CB2 expression varies from the highest to the lowest as follows: B cells > NK cells > macrophages > polymorphonuclear cells > CD4 T cells > CD8 T cells. CB2 plays a role regulating immunity through in cell migration, proliferation and different effector functions of various immune cells. AEA is poorly expressed outside the brain, in contrast, 2-AG is detected in many peripheral tissues. Therefore, 2-AG is considered the main CB2 receptor ligand (Sugiura and Waku, 2002).

The endocannabinoid system is capable of inducing immune suppression, this fact arose great interest in these molecules as a possible treatment and many synthetic cannabinoids have been used on clinical trials (Klein, 2005). *In vitro* migration assays have shown that 2-AG was able to induce migration of different cell types such as monocytes, neutrophils and eosinophils among others, this effect was reverted when the cells were treated with the CB2 antagonist SR144528 (Rinaldi-Carmona et al., 1998). However the migration effect was not the same when using synthetic cannabinoids, in that case, they inhibited cell migration. There is a similar situation regarding cell proliferation, some studies support that endocannabinoids promote cell proliferation while others have observed the opposite effect. Although it is not completely clear, seems like CB2-dependent mechanisms induce apoptosis of the immune cells. On the contrary, several studies support the evidence that CB2 inhibit cytokine production.

CB2 receptors have also a role in inflammatory and autoimmune diseases, arthritis, inflammatory bowel disease, nervous tissue inflammation and vascular inflammation (cardiovascular disease and atherosclerosis).

Hemodynamic dysfunction and endocannabinoids

Several studies investigating the cardiovascular dysfunction in advanced liver disease demonstrated the implication of the endocannabinoid system. A study from our laboratory by Ros et al. demonstrated that the administration of the selective CB1 antagonist, SR141716A, increased arterial pressure and total peripheral resistance in cirrhotic rats with ascites, and that this effect probably mediated by circulating blood cells acting via CB1 receptors. Bátkai et al., in a parallel study, also observed that the CB1 receptor blockade in bile-duct ligated rats and CCl_4-induced cirrhotic rats normalized blood pressure, reduced portal hypertension and mesenteric blood flow. AEA is increased in cirrhotic patients and in experimental cirrhosis produced hypotension and mesenterial arteriolar vasodilation.

Neurological and metabolic disorders and the endocannabinoid system

One of the major complications in liver cirrhosis is hepatic encephalopathy. The patients with advanced cirrhosis may present neurological disorders associated with an acute or chronic liver failure. There are some studies that sought to investigate the implication of the endocannabinoid system in this pathology. Mice treated with tioacetamide (TAA) develop an acute fulminant liver failure, and the administration of a CB2 agonist or a CB1 antagonist improved the neurological score, activity and cognitive functions (Avraham et al., 2006). Another interesting finding from the same group was that endocannabinoids regulate AMP-activated kinase, a major intracellular energy sensor involved in the compensatory response to liver failure.

5. The apelin system

General characteristics of apelin and APJ

Apelin is a peptide that was described and isolated in 1998 by Tatemoto et al. It is the only known ligand to date of the orphan angiotensin-like receptor receptor 1 (AGTRL-1), later renamed as APJ. Apelin received the name after APJ endogenous ligand, the mature form of apelin consists of 36 aminoacids, apelin-36, but two more isoforms have been described, apelin-13 and apelin-17, with 13 and 17 aminoacids, respectively. The smaller the isoform, the better affinity for the receptor it presents (Hosoya et al. 2000). The common precursor, preproapelin, was cloned in human cells as well as in other animal species (Brindle et al., 2006; Tatemoto et al., 2001).

APJ is a 7-transmembrane G coupled protein-receptor. There is a 31% homology with the angiotensin receptor 1 (AT1), but angiotensin does not bind APJ. The primary structure is conserved between human, bovine, rat and mouse, suggesting a highly conserved sequence in evolution (Tatemoto et al. 1998). However, there might exist functional differences between species, as APJ is highly expressed in rat lungs, but not in humans (Habata et al., 1999; Edinger et al., 1998).

The transcriptional regulation of the apelin seems to be modulated by cytokine release associated with phospho-stat3 (Han et al., 2008). In adipocytes, it is upregulated by the co-activator PPARγ co-activator 1alpha (PGC-1alpha) (Mazzucotelli et al., 2008) and TNFα (Daviaud et al., 2006) and under hypoxic conditions it is regulated by the hypoxia inducible factor 1α (HIF1α) (Ronkainen et al., 2007; Eyries et al. 2008). A very recent publication added some new information on apelin. Bone morphogenic protein seems to downregulate apelin expression in endothelial and vascular cells (Poirier et al., 2012). The transcriptional regulation of APJ, on the other hand, is still not completely understood.

Apelin and APJ are widely expressed in peripheral tissues of adult and embryo (Figure 15). In rodents, the highest levels were found in heart and lungs, and in lower levels in skeletal muscle, brain, kidney and ovary. In all these tissues, the specific localization was in the vascular and endothelial cells. (Medhurst et al., 2003; Horiuchi et al., 2003; Scott et al., 2007).

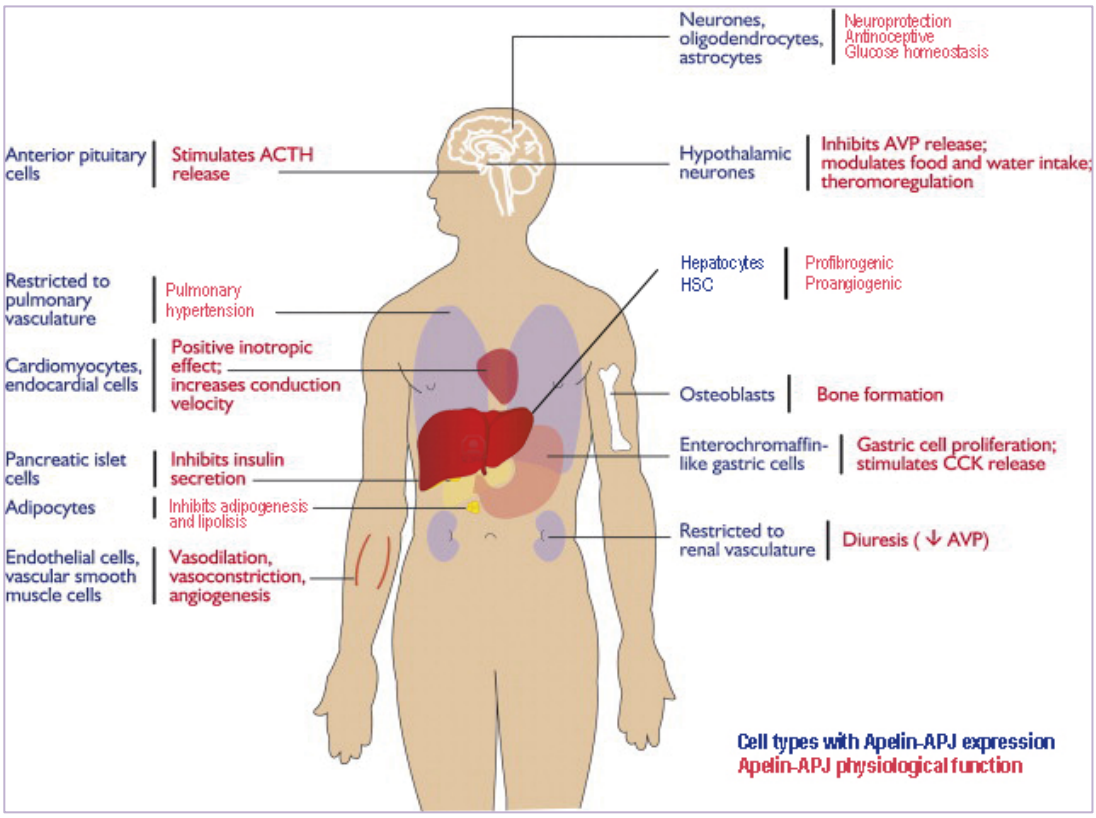

Figure 15. Expression and physiological functions of the apelin-APJ system. Modified figure from Japp and Newby, 2008.

Apelin has been attributed many physiological roles thanks to the wide distribution of this peptide and receptor in different tissues. The remarkable specific expression found in blood vessels, suggests that apelin-APJ system has an important role in angiogenesis and vascular formation (Kidoya and Takakura, 2012). Indeed, apelin was found to be involved in normal vessel development, regulation of apoptosis, regulation of NO-dependent vasodilation and improving cardiac contractility (Lee et al., 2000). The apelin-APJ system seems to have an opposite role to the renin-angiotensis system. Apelin signaling can block AII action by increasing NO production (Ishida et al., 2004; Chun et al., 2008; Siddiquee et al., 2011). Similar results were found in a previous study, where intravenous injection of apelin induced the reduction of blood pressure, associated with the intracellular activation of NO (Tatemoto et al., 2001). In pulmonary hypertension, apelin attenuated vasoconstriction in isolated rat arteries (Andersen et al., 2011). Apelin was also described in a number of studies as an important factor protecting against cardiovascular disease (Koguchi et al., 2012). It has a positive inotropic effect both *in vitro* and *in vivo* (Katugampola et al. 2001; Berry et al., 2004; Dai et al., 2006).

Other roles have been attributed to apelin-APJ, such as diabetes and adipose tissue or inflammation. Apelin was found upregulated in obese and hyperinsulinemic humans and mice, and it was able to restore glucose tolerance and increased glucose utilization (Dray et al., 2008). Apelin has also a role in inflammation in kindey, gastrointestinal tract or atherosclerosis (Malyszko et al., 2008; Han et al., 2008; Lu et al., 2012). A recent study added a new function of apelin, that is the implication in the lymphatic system by stabilizing endothelial lymphatic cells (Sawane et al., 2011). The most relevant role for apelin for the current doctoral thesis is the role of apelin described in liver fibrosis by our laboratory and confirmed later by others (Principe et al., 2008; Tiani et el., 2009; Melgar-Lesmes et al., 2010; Melgar-Lesmes et al., 2011).

Apelin and liver fibrosis

In the last few years, our laboratory has showed great interest in the study of the role of the endogenous apelin system in liver fibrosis and associated complications. We first described the role of apelin in hepatic remodeling and cardiovascular and renal complications associated with advanced liver disease (Principe et al., 2008). Apelin was found upregulated in the hepatic tissue of cirrhotic rats with ascites across the fibrotic septa, while APJ was localized mainly in the parenchyma. Circulating levels of apelin were also elevated in both cirrhotic patients and cirrhotic rats. The antagonism of the apelin receptor with F13A reduced fibrosis formation, vessel density, improved cardiac performance and renal function and produced the loss of ascites.

Apelin was also analyzed in a rat portal hypertension model. Treatment with the apelin receptor antagonist, F13A, markedly reduced splanchnic neovascularization, formation of portosystemic collateral vessels and decreased the expression of proangiogenic factors such as VEGF, PDGF and angiopoietin 2 in portal hypertensive rats (Tiani et al., 2009).

Our group continued with the characterization of the apelin system *in vitro.* Melgar-Lesmes et al. investigated the role of apelin in human tissue and in human hepatic stellate cells (LX2) under fibrogenic-related gene induction and hypoxia. Apelin was found to be an important factor in the regulation of AII and ET1 mediated effects

on HSC. This effect was confirmed *in vivo* by the selective blockade of AII and ET1 in CCl_4-treated rats. In both cases, the inactivation of this profibrogenic genes normalized apelin expression.

The most recent publication focused on APJ and its upregulation by hypoxia and proinflammatory factors such as LPS or TNF in human hepatocytes (HepG2) and HSC cells (LX2), further strengthening the role of the apelin system in hepatic cirrhosis (Melgar-Lesmes et al. 2011).

AIMS

Liver fibrosis degree assessment is the most valuable parameter in the diagnosis of patients with liver disease. The most used technique to determine liver fibrosis stage is the biopsy and despite the potential complications, it is still frequently used to assign a proper treatment of patients with HCV. In the last years, there has been a constant research of new non-invasive biomarkers of liver fibrosis in order to substitute the invasive biopsy. Indirect biomarkers include basic laboratory blood tests parameters (AST, platelet count, bilirubin etc.) and although the analysis reflects well the alteration in the hepatic function, the greatest limitation is that these biomarkers do not provide information about the changes in the ECM. Direct biomarkers, on the other hand, include collagens and other matrix proteins involved in the ECM turnover, which provide more accurate information about the fibrosis stage. During the fibrogenesis process, many substances such as ECM products and cytokines are released to the blood flow, which could be used as potential biomarkers. In the clinical practice there are many studies that by combination of three or more direct biomarkers have achieved good prognosis scores in HCV patients.

The most characteristic feature of fibrogenesis is ECM deregulation. The normal ECM balance leans towards matrix production and accumulation, which causes normal liver tissue architecture disruption into a fibrotic one. MMPs are the classical degrading enzymes of collagen and other ECM fibers, and they are upregulated during fibrogenesis as well as their inhibitors, the TIMPs. Degradation products of collagen, such as PIIINP or PICP are well known to be increased in serum of patients with liver disease and have been tested in several studies. Degradation of collagen fibers by MMPs generates specific cleavage fragments that can also be considered as potential biomarkers. Specifically, MMP9 cleavage of collagen type III produces a new described fragment, CO3-610, which has shown to be correlated with total collagen content of the livers of intraperitoneal CCl_4-treated rats (Barascuk et al., 2010). Considering all this background information, the main aims of this first study were the following:

- To evaluate whether the circulatory levels of CO3-610 could be used as a new effective serum biomarker to assess liver fibrosis progression in rats treated by CCl_4 inhalation during different periods of time and with different degrees of fibrosis.

- To assess if CO3-610 is correlated with the systemic hemodynamics and portal hypertension worsening that characterize fibrosis to cirrhosis progression.

Hepatic fibrogenesis is triggered upon liver damage, whatever the source, when the damage persists, inflammation becomes chronic and the liver architecture is altered by an excessive matrix deposition. Liver fibrosis is the initial cause of major complications in liver disease, which become more accused in advanced fibrosis and cirrhosis. Liver stiffness causes alterations in the intrahepatic vasoreactivity, inducing vasoconstriction, which in turn, induce portal hypertension and increased hepatic resistance. As a compensatory effect, there is an increase in the collateral circulation resulting in a decrease of the systemic blood pressure. In addition, liver cirrhosis ultimately results in hepatic failure with a high risk of hepatocarcinoma. For this reason, treatments focused on the prevention of fibrosis progression are of great interest.

Endocannabinoids are lipid-based molecules that participate in a wide range of physiological functions including neuroprotection, energy balance, cardiovascular homeostasis or immune and inflammatory responses among others. Cannabinoid receptors have been reported to be involved in liver fibrosis in several studies in the last few years. Specifically, CB2 receptor stimulation has antifibrogenic effects in experimental fibrosis (Julien et al., 2005; Muñoz-Luque et al., 2008), while CB1 has profibrogenic properties (Teixeira-Clerc et al., 2006). CB1 receptors are widely expressed in the brain, for this reason, non-desirable side effects have been attributed to this receptor. On the other hand, CB2 receptors are found expressed mainly in peripheral tissues, especially in the immune system. It is for this reason that CB2 receptor studies have attracted more attention lately, as no side effects have been associated to date.

Another endogenous system that has emerged in the last decade is the apelin system. Although its implication in other pathologies such as cardiovascular disease is well known, only recently our group has described its role in hepatic cirrhosis. Apelin is a 36-aminoacid peptide with proangiogenic properties that has also been found increased in serum and liver tissue of cirrhotic patients. Apelin receptor (APJ) blockade

with a specific antagonist has reverted apelin effects, improving fibrosis and angiogenesis in cirrhotic rats with ascites.

For this second study, the set aims were:

- To investigate new therapeutic strategies focused on preventing fibrosis progression in rats chronically treated with increasing doses of CCl_4, such as stimulation of the endocannabinoid and blockade of the apelin systems.

- To determine if both antifibrogenic strategies have positive effects on systemic and portal hemodynamics and liver function.

- To assess gene expression changes in a selected group of genes involved in fibrosis, inflammation and ECM turnover after chronic stimulation of CB2 receptors with a selective agonist AM1241, and APJ blockade with the antagonist F13A.

In connection to the second study of this thesis, (see results of the 2nd article), PDGFRβ expression was modulated by two different antifibrogenic agents, showing clear evidence that this receptor is a potential therapeutic target for liver fibrosis. In concrete, this third study was focused on PDGFRβ and the effect of its signaling disruption by an adenovirus encoding for a dominant-negative soluble PDGFRβ. It has been already mentioned that the perpetuation of the activated state of HSCs induce the release of cytokines and profibrogenic genes, but also an increase of their cell membrane receptors and an enhanced downstream signaling. The sequential activation of the PDGF signaling pathway includes the activation of ERK1 and ERK2, which translocate into the nucleus and trigger the proliferative response. For this reason, targeting the PDGF system by inhibitors of tyrosine kinase receptors is an attractive therapeutic strategy for liver fibrosis. The main drawback is that the PDGF system signaling pathway is common with other growth factors that may have beneficial effects in other cells within the same tissue. In order to avoid inhibiting general tyrosine kinase receptors, there is the option of recurring to dominant-negative transgenic strategies. Truncated membrane-bound receptors with a non-functional tyrosine kinase domain have proved to disrupt *in vitro* signaling of multiple receptor isoforms by competing for ligand binding (Celli et al., 1998; Qi et al., 1999;

Borkham-Kamphorst et al., 2004). Therefore, the main aims of this third study were the following:

- To assess the relationship between the activation of PDGFRβ, hemodynamic dysfunction and progression of hepatic fibrosis in CCl_4-treated rats with different degrees of fibrosis.
- To analyze the hemodynamic and antifibrotic effects produced by the adenoviral transduction of a dominant-negative soluble form of PDGFRβ (sPDGFRβ) in fibrotic rats.

The second study of this thesis has contributed to widen the knowledge on CB2 receptors and their role in fibrosis progression. In this fourth study, we sought to assess further data on the role of the endocannabinoid system in inflammation. As mentioned in the introduction, CB2 receptors are mainly expressed in peripheral tissues, especially in the immune system cells. Cannabinoids can modulate cytokine and chemokine production, therefore, they could be used as anti-inflammatory drugs to treat chronic inflammatory diseases. Moreover, the endocannabinoids AEA and 2-AG have been shown to enhance chemotaxis of leukocytes, further supporting the evidence of CB2 implication in inflammation. In addition, cirrhotic patients with ascites have altered host-defense mechanisms and increased susceptibility to bacterial infections, which can lead to SBP in patients with advanced liver disease and increase the mortality rate of those patients. This work sought to investigate the relationship between LPS-induced sepsis in liver cirrhosis and the endocannabinoid system.

The main aims of this fourth study are summarized as follows:

- To assess whether LPS regulates the CB2 expression in a human monocytic cell line (U937) at both mRNA and protein levels.
- To determine the mRNA expression level of CB2 receptors in isolated circulating monocytes and peritoneal macrophages from the ascites fluid of cirrhotic patients with or without SBP.

- To study if LPS treatment produced any effect on the migratory activity of U937 cells towards the endocannabinoids AEA and 2-AG.

- To evaluate if the effects on the transcriptome in U937 cells triggered by LPS are specific by adding polymixin B, an antibiotic that prevents LPS signaling.

This thesis includes four individual studies, the first three have been published and are in press and the fourth one has been sent for review to the journal Gut.

RESULTS

1st Article: Circulating CO3-610, a degradation product of collagen III, closely reflects liver collagen and portal pressure in rats with fibrosis.

Non-invasive liver fibrosis assessment in order to substitute liver biopsy has been the aim of physicians for many years, for this reason, it is of great interest to find new efficient serum biomarkers that are able to asses accurately the fibrosis stage and ideally predict fibrosis progression. Previous studies have already showed that CO3-610 had a significant correlation with the total amount of collagen in the livers of BDL and CCl_4-treated rats (Veidal et al., 2010; Vassiliadis et al., 2011). For the present study, we used an experimental liver fibrosis rat model with different CCl_4-inhalation periods of time in order to obtain different grades of fibrosis and cirrhosis (as explained in the material and methods section of the 1st article). Mean arterial pressure and portal pressure was measured in all animals, as well as the % of fibrosis area, and gene expression of ECM turnover genes. The results of this study are summarized below:

1. Fibrosis quantification and staging

The individual response to the CCl_4 treatment varies between animals. For this reason, to assess more accurately the differences between CO3-610 levels in rats with different fibrosis grades, the animals were classified into four groups according to the % of fibrosis obtained by Sirius red staining quantification instead of the weeks of CCl_4 treatment duration. The groups were the following: 1) Control animals (non-treated animals had non-appreciable alteration in liver histology presented < 1% of fibrosis), 2) mild and moderate fibrosis (fibrotic area between 1-6% of the total liver biopsy), 3) severe fibrosis (fibrotic area between 6-11%) and 4) cirrhosis (> 11%). Figure 1 shows representative Sirius red stained liver slices of a control, mild/moderate, severe and cirrhotic rat. There is an evident progression of collagen accumulation and liver architecture deregulation characterized by the initial formation of fibrotic septa and regenerative nodules in severe fibrotic rats that becomes more evident in cirrhotic animals. Liver function parameters such as AST and ALT also showed a progressive worsening along with fibrosis progression (Table 1).

2. CO3-610 is detected in serum of cirrhotic rats and increases in parallel with liver fibrosis progression

Immunoprecipitation analysis showed that CO3-610 was only found as a single 25 kDa band in cirrhotic animals and almost no signal was detected in healthy rat serum, as shown in Figure 2.

CO3-610 serum levels were measured by ELISA in the four groups of rats. No significant differences were found between untreated (control) rats and rats with mild/moderate fibrosis (<6% of fibrosis area). However, there was a parallel increase in the circulating serum levels of CO3-610 and fibrosis progression, reaching maximum levels in cirrhotic rats (Figure 3A). Overall, the collagen content analyzed by histology was closely correlated with the increase of serum CO3-610 (Figure 3B).

3. Serum CO3-610 values closely correlate with portal hypertension

In order to analyze whether CO3-610 could be used as an indicator of hemodynamic worsening, mean arterial pressure and portal pressure were measured in a representative group of animals. The progressive disruption of the architecture of the liver led to systemic and portal hemodynamics deterioration. CO3-610 levels were significantly correlated with the systemic hemodynamics worsening, but the most interesting finding of this investigation was that the correlation between CO3-610 and portal pressure showed a strong correlation in fibrotic/cirrhotic animals (Figure 4).

4. Collagen types I and III are overexpressed in the hepatic tissue of CCl_4-treated rats

Collagen 1α2 and 3α1 mRNA expression was enhanced in fibrotic/cirrhotic rats as expected, but the expression pattern differed between the two transcripts. Figure 5A, shows the mRNA expression results obtained by Real Time PCR. Both collagen 1α2 and 3α1 were upregulated up to the same amount in fibrotic rats, but in cirrhotic rats, collagen 1α2 was more than 20 times higher compared to controls, while collagen 3α1 remained at the same level as fibrotic rats. However, when analyzing the specific hepatic content of collagen type III by immunohistochemistry (Figure 5B), we observed a progressive deposition of collagen type III fibers in the hepatic tissue of fibrotic/cirrhotic animals.

5. Genes involved in ECM turnover are induced in the liver of CCl_4-treated rats

Chronic hepatic injury induces the upregulation of ECM turnover genes, which causes the disruption of the normal balance of matrix deposition/degradation. MMPs and their inhibitors, the TIMPs, are the proteins that orchestrate the ECM turnover. We analyzed the mRNA expression of MMP2, the most relevant metalloproteinase in liver, MMP9, the responsible for the generation of CO3-610 from collagen type III, and both inhibitors of metalloproteinases, TIMP1 and TIMP2 (Figure 5C). MMP2 expression was paralleled with fibrosis progression, but MMP9 was only upregulated in fibrotic animals, while in cirrhotic rats mRNA levels drastically fell to non-significant compared to control animals. Both TIMP1 and TIMP2 mRNA levels were increased in fibrotic and cirrhotic rats compared to controls. TIMP1 was 10 times higher in fibrotic rats reaching a maximum of 15-fold in cirrhotic animals, while TIMP2 was only increased by 2-fold and 5-fold in fibrotic and cirrhotic animals, respectively.

Segovia-Silvestre *et al. Fibrogenesis & Tissue Repair* 2011, **4**:19
http://www.fibrogenesis.com/content/4/1/19

Fibrogenesis & Tissue Repair

RESEARCH Open Access

Circulating CO3-610, a degradation product of collagen III, closely reflects liver collagen and portal pressure in rats with fibrosis

Toni Segovia-Silvestre[1*], Vedrana Reichenbach[2], Guillermo Fernández-Varo[2], Efstathios Vassiliadis[1], Natasha Barascuk[1], Manuel Morales-Ruiz[2], Morten A Karsdal[1] and Wladimiro Jiménez[2,3]

Abstract

Background: Hepatic fibrosis is characterized by intense tissue remodeling, mainly driven by matrix metalloproteinases. We previously identified CO3-610, a type III collagen neoepitope generated by matrix metalloproteinase (MMP)-9, and tested its performance as a fibrosis marker in rats with bile-duct ligation. In this study, we assessed whether CO3-610 could be used as a surrogate biomarker of liver fibrosis and portal hypertension in carbon tetrachloride-induced experimental fibrosis.

Results: For this study, 68 Wistar rats were used. Serum CO3-610 was measured by ELISA. Liver fibrosis was quantified by Sirius red staining. Serum hyaluronic acid (HA) was measured with a binding-protein assay. Gene expression of collagens I and III, Mmp2 and Mmp9, and tissue inhibitors of matrix metalloproteinase 1 (Timp1) and 2(Timp2) was quantified by PCR. Hemodynamic measurements were taken in a subgroup of animals. A close direct relationship was found between serum CO3-610 and hepatic collagen content ($r = 0.78$; $P < 0.001$), superior to that found for serum HA ($r = 0.49$; $P < 0.05$). CO3-610 levels in rats with severe fibrosis (43.5 ± 3.3 ng/mL, $P < 0.001$) and cirrhosis (60.6 ± 4.3 ng/mL, $P < 0.001$) were significantly higher than those in control animals (26.6 ± 1.3 ng/mL). Importantly, a highly significant relationship was found between serum CO3-610 and portal hypertension ($r = 0.84$; $P < 0.001$). Liver Mmp9 expression increased significantly in fibrotic animals but decreased to control levels in cirrhotic ones.

Conclusions: Circulating CO3-610 behaves as a reliable indicator of hepatic remodeling and portal hypertension in experimental fibrosis. This peptide could ultimately be a useful marker for the management of liver disease in patients.

Background

Identification of non-invasive biochemical markers of liver fibrosis is a major challenge for scientists and clinicians dealing with hepatic diseases. The degree of liver fibrosis has emerged as the primary determinant in the diagnosis, prognosis and management of patients with chronic liver diseases [1,2]. Furthermore, the probably availability of antifibrotic treatments in the near future 3 emphasizes the necessity of having accurate tools that allow the sequential evaluation of changes in collagen turnover induced by these drugs.

Liver biopsy (LB) is the gold standard method for the diagnosis of liver fibrosis, providing a unique source of information on fibrosis and assessment of histology. Even for patients in whom serologic tests point to a specific liver disease, LB can give valuable additional information regarding staging, prognosis and management [4]. However, LB can be painful and carries a risk, albeit slight, of complications, some of which may be life-threatening, and therefore it is often reserved for cases in which clinical cirrhosis or the diagnosis of the type of liver disease is unclear. The size and quality of the biopsy, interpretation of histology, and the heterogeneity of fibrosis deposition between patients are variables that can lead to errors and inaccurate assessment of fibrosis [5]. In the past few years, the list of non-invasive

* Correspondence: segovia.silvestre.t@gmail.com
[1]Nordic Bioscience A/S, Herlev, Denmark
Full list of author information is available at the end of the article

Segovia-Silvestre *et al. Fibrogenesis & Tissue Repair* 2011, **4**:19
http://www.fibrogenesis.com/content/4/1/19

surrogate markers of liver fibrosis has increased progressively. Indirect biomarkers, such as platelet count or liver transaminases, reflect alterations in hepatic function but not changes in extracellular matrix (ECM) turnover [6,7]. By contrast, direct biomarkers are thought to be involved in the deposition or removal of the ECM. The extensive deposition of fibrous tissue, together with the active remodeling and recurrent scarring that develops during fibrosis, results in increased serum levels of the constituents and degradation products of fibrous tissue [7,8]. This group includes collagens, proteoglycans, matrix glycoproteins, HA, matrix metalloproteinases (MMPs) and their inhibitors (tissue inhibitors of matrix metalloproteinases; TIMPs), and several cytokines involved in fibrosis signaling pathways. The most extensively studied collagen-derived markers in liver fibrosis are the N-terminal propeptide of type III procollagen (PIIINP) and type IV collagen [8-11]. Indirect and direct markers of liver fibrosis have been validated alone or in combination in different groups of patients with differing degrees of hepatic dysfunction. However, wide agreement on the most suitable biomarker of liver fibrosis is far from being reached.

Recently, a new strategy based on the identification of neoepitopes arising from the cleavage of ECM components by matrix proteolytic enzymes has been proposed [12]. This strategy assumes that collagen cleavage occurs at significant levels only during the gross alterations in ECM homeostasis seen during fibrosis. Neoepitopes, which are cleared into the circulation in peptide fragments, are almost completely absent under healthy conditions, and detectable only when active fibrosis is ongoing. This, in turn, raises the possibility of discriminating between different degrees of disease activity. Based on this approach, we recently identified CO3-610, a specific peptide fragment of type III collagen generated by MMP-9, as a potential liver fibrosis biomarker, and developed an ELISA assay to quantify it in serum [13]. Initial tests of this assay, particularly its performance in rats with bile-duct ligation (BDL) have been previously reported [14].

In the present study we assessed whether the circulating levels of CO3-610 could be used as a surrogate marker of liver fibrosis and portal hypertension in experimental fibrosis induced by carbon tetrachloride (CCl_4) in rats.

Results

Fibrosis quantification and staging

The liver of animals treated with CCl_4 had a finely granulated surface macroscopically. As anticipated, the individual response to the fibrosis-induction protocol varied widely from animal to animal. Hence, based on histological analysis, CCl_4-treated rats were staged into three groups according to the percentage of fibrotic area compared with the total area of the LB: mild and moderate fibrosis (defined as the fibrotic area being < 6% of the total; n = 33), severe fibrosis (6 to 11%; n = 15) and cirrhosis (> 11%; n = 20). Control rats displayed no appreciable alterations in liver histology, and had an almost negligible amount of fibrous tissue. However, in fibrotic rats, there was progressive accumulation of ECM as a consequence of the continuous liver injury, evolving from a slight deposition of fibrosis mainly in the portal area (mild/moderate fibrosis) to numerous and thicker septa resulting from the longer exposure to CCl_4 (severe fibrosis). Finally, most of the animals exposed to the toxin for the longest periods developed cirrhosis, characterized by the formation of regenerative nodules of liver parenchyma separated by fibrotic septa. Figure 1 shows representative Sirius red staining of tissue from a control rat, a rat with mild/moderate fibrosis, a rat with severe fibrosis and a rat with cirrhosis.

The fibrotic/cirrhotic rats included in the study had important alterations in liver-function tests, being more pronounced in the group of rats with cirrhosis (Table 1). These animals also had a moderate but significant alteration in extracellular fluid homeostasis, as reflected by hyponatremia.

CO3-610 is a 25 kDa circulating fragment of collagen type III detected in the serum of cirrhotic rats

Western blotting analysis of serum samples from cirrhotic and control rats precipitated with the anti-CO3-610 antibody was carried out (Figure 2). No signal was detected in healthy animals, but a clear specific band at a molecular mass of approximately 25 kDa was visible in blots of serum from cirrhotic rats. These results indicate that a single molecular entity is detected with the CO3-610 antibody, in contrast to other serum collagen ELISA assays reported previously, in which several fragments of collagen were measured simultaneously [15].

Serum CO3-610 values rose in parallel with liver fibrosis

No difference was found between serum levels of CO3-610 between control rats and those with mild/moderate fibrosis (26.6 ± 1.3 ng/ml versus 28.5 ± 1.6 ng/ml, respectively) (Figure 3A). However, progression of liver fibrosis was associated with a parallel increase in the circulating levels of the collagen III-derived epitope; values significantly increased in rats with severe fibrosis (43.5 ± 3.3 ng/ml, $P < 0.001$) and reached maximum levels in rats with cirrhosis (60.6 ± 4.3 ng/ml, $P < 00.01$). There was a close direct relationship between CO3-610 values and hepatic collagen content in CCl_4-treated rats ($r = 0.78$; $P < 0.001$) (Figure 3B). These differences were clearly greater than those obtained by calculating the correlation coefficient between serum hyaluronic acid

Segovia-Silvestre *et al. Fibrogenesis & Tissue Repair* 2011, **4**:19
http://www.fibrogenesis.com/content/4/1/19

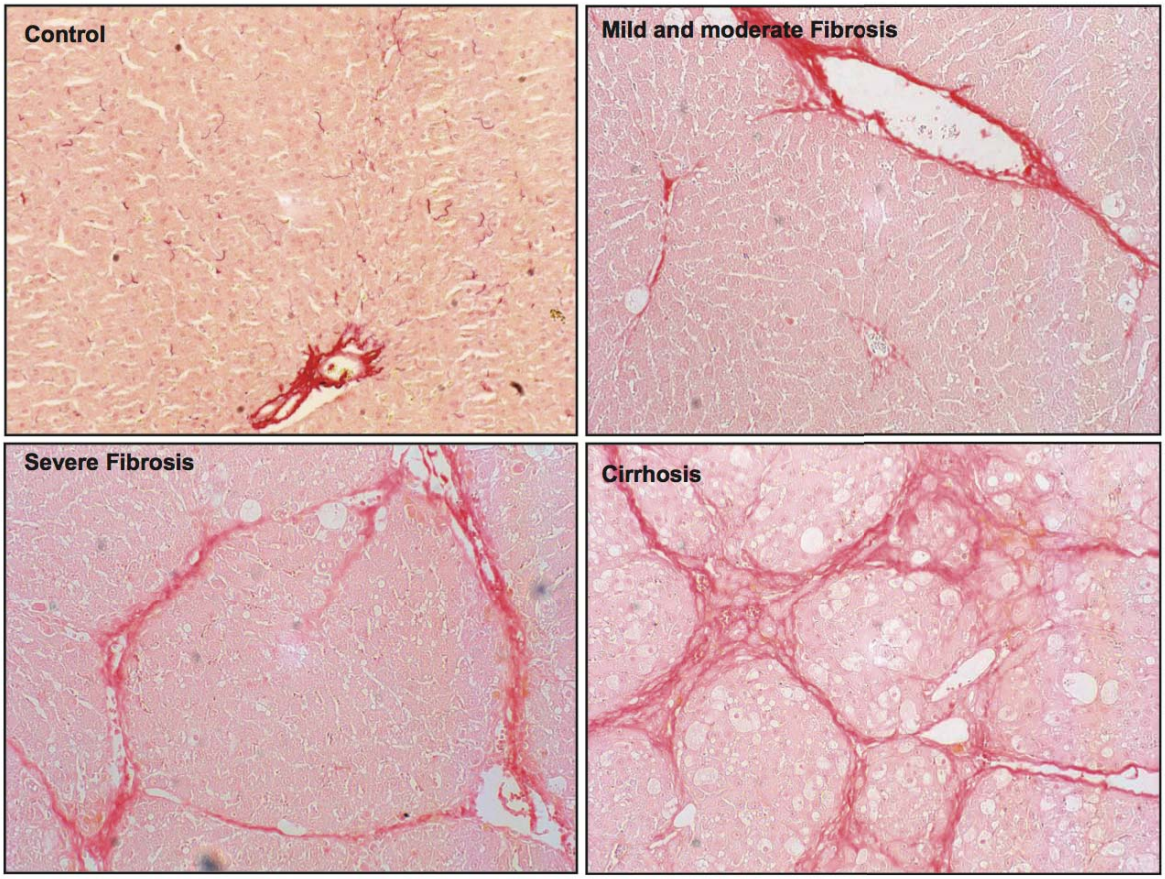

Figure 1 Classification of the study animals based on liver-collagen content. Photomicrographs of liver sections stained with Sirius red are representative of control and treatment groups. Rats under CCl_4 inhalation treatment were classified based on the evidence into three different groups according to the histological quantification of their liver-collagen content: mild/moderate fibrosis (< 6% fibrotic area), severe fibrosis (6 to 11% fibrotic area) and cirrhosis (> 11% fibrotic area). Original magnification ×100.

Table 1 Body weight, liver-function test results and serum electrolyte values in the rats of the study

	Control (n = 20)	Fibrosis		
		Mild/moderate (n = 33)	Severe (n = 15)	Cirrhosis (n = 20)
Body weight, g	399 ± 8	369 ± 6	367 ± 9	383 ± 9
ALT, U/L a	12.8 ± 1	88.6 ± 31.8	138.1 ± 71*	119.6 ± 31.5***
AST, U/L b	117 ± 23	219 ± 27	355 ± 92**	512 ± 69***
LDH, U/L c	1093 ± 106	1455 ± 154*	1386 ± 134*	917 ± 112
Albumin, g/l	36.1 ± 0.5	34.9 ± 0.5	33.3 ± 1.0	29.0 ± 0.8***
Serum Na^+, mEq/l	142 ± 1.6	142.6 ± 0.5	142.9 ± 0.4	141.5 ± 0.5*
Serum K^+, mEq/l	5.7 ± 0.2	6.0 ± 0.1	5.7 ± 0.1	4.8 ± 0.2
Serum osmolality, mOsm/Kg	292 ± 6	294 ± 3	291 ± 3	289 ± 1

[a] Alanine aminotransferase.
[b]Aspartate aminotransferase.
[c]Lactate dehydrogenase.
*P < 0.05; **P < 0.01 and ***P < 0.001 compared with control rats (one-way ANOVA with Newman-Keuls *post hoc* test and Kruskal–Wallis test with Dunn *post hoc* tests as appropriate).

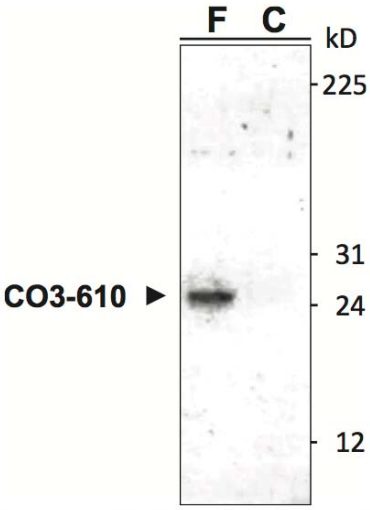

Figure 2 Immunoprecipitation of CO3-610 type III collagen fragment from rat serum. CO3-610 was precipitated with monoclonal antibodies from serum of a cirrhotic (F) rat treated with CCl_4 for 19 weeks and an untreated age-matched control (C) rat and detected by western blotting as a single discrete protein band of 25 kDa. The numbers on the right are the molecular masses of Full-Range Rainbow Markers (Mr 12,000 to 225,000) from GE Healthcare (Little Chalfont, United Kingdom). The figure is representative of three independent experiments.

(HA) (a well-established serum marker of liver fibrosis) and the hepatic collagen content in fibrotic/cirrhotic rats (r = 0.49; P < 0.05).

Serum CO3-610 values closely correlate with portal hypertension

Further insight into the suitability of CO-610 as a surrogate indicator of hepatic fibrosis was gained by measuring mean arterial pressure (MAP) and portal pressure (PP) in 20 of the 68 CCl_4-treated rats included in the protocol. This subset of animals did not differ from the whole group of fibrotic/cirrhotic rats in terms of fibrosis staging (seven rats with mild/moderate fibrosis, three rats with severe fibrosis and ten rats with cirrhosis), range of CO3-610 values (37.3 ± 5.6 ng/ml, 55.1 ± 6.3 ng/ml and 72.2 ± 6 ng/ml, respectively) or correlation coefficient with hepatic collagen content (r = 0.71; P < 0.001). As previously observed, the increased disruption in the hepatic architecture was associated with a progressive deterioration in systemic hemodynamics. In fact, animals with cirrhosis had frank hypotension (MAP 96.5 ± 2.4 mmHg; P < 0.001) compared with control rats (MAP 124.6 ± 2.4 mmHg). Accordingly MAP inversely correlated with serum CO3-610 values in CCl_4-treated rats (r = -0.59; P < 0.01) (Figure 4A). However, the most interesting finding of this investigation was that the serum concentration of CO3-610 depicted a higher direct relationship with the degree of portal hypertension in fibrotic/cirrhotic animals (r = 0.84; P < 0.001) (Figure 4B).

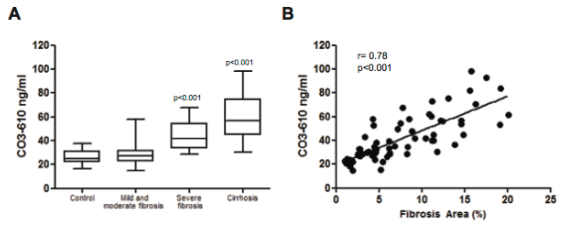

Figure 3 CO3-610 serum levels in experimental fibrosis induced by chronic administration of carbon tetrachloride in rats. (A) Serum concentrations of CO3-610 in control (untreated) rats (n = 20), and rates with mild/moderate fibrosis (n = 33), severe fibrosis (n = 15) and cirrhotic (n = 20). The box contains the values between the 25th and 75th percentiles, and the horizontal line is the median. Whiskers show the range of the data. Significance is denoted versus the control animals. **(B)** Correlation of CO3-610 serum levels with histological quantification of liver fibrosis in all CCl_4-treated rats.

Collagen types I and III are overexpressed in the hepatic tissue of CCl_4-treated rats

As expected, the expression of collagen 1α2 (Col1α2) and 3α1 (Col3α1) mRNA was generally enhanced in fibrotic/cirrhotic rats, but the pattern and degree of changes clearly differed between the two transcripts (Figure 5A). Collagen 1α2 mRNA expression increased in parallel with the worsening of the liver disease. In cirrhotic rats this enhancement was around 20 times higher than that in controls. This increase in the expression of collagen 3α1 mRNA reached its peak in the animals with fibrosis, and there was no worsening of this level in the liver of rats with cirrhosis. Because CO3-610 is a degradation product of collagen type III, we next examined the hepatic content of collagen type III in the liver of CCl_4-treated rats. Gene activation of collagen 3α1 mRNA was associated with a progressive deposition of collagen III fibers in the hepatic tissue of animals with induced fibrosis/cirrhosis protocol (Figure 5B),

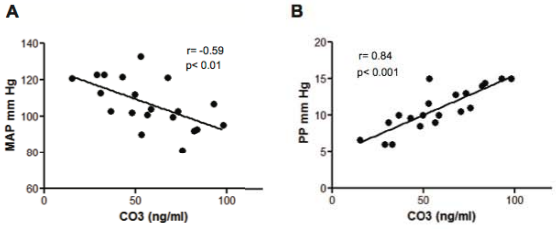

Figure 4 Correlation of CO3-610 serum levels with portal pressure (PP) and mean arterial pressure (MAP) in a group of 20 CCl_4-treated rats.

Segovia-Silvestre *et al. Fibrogenesis & Tissue Repair* 2011, **4**:19
http://www.fibrogenesis.com/content/4/1/19

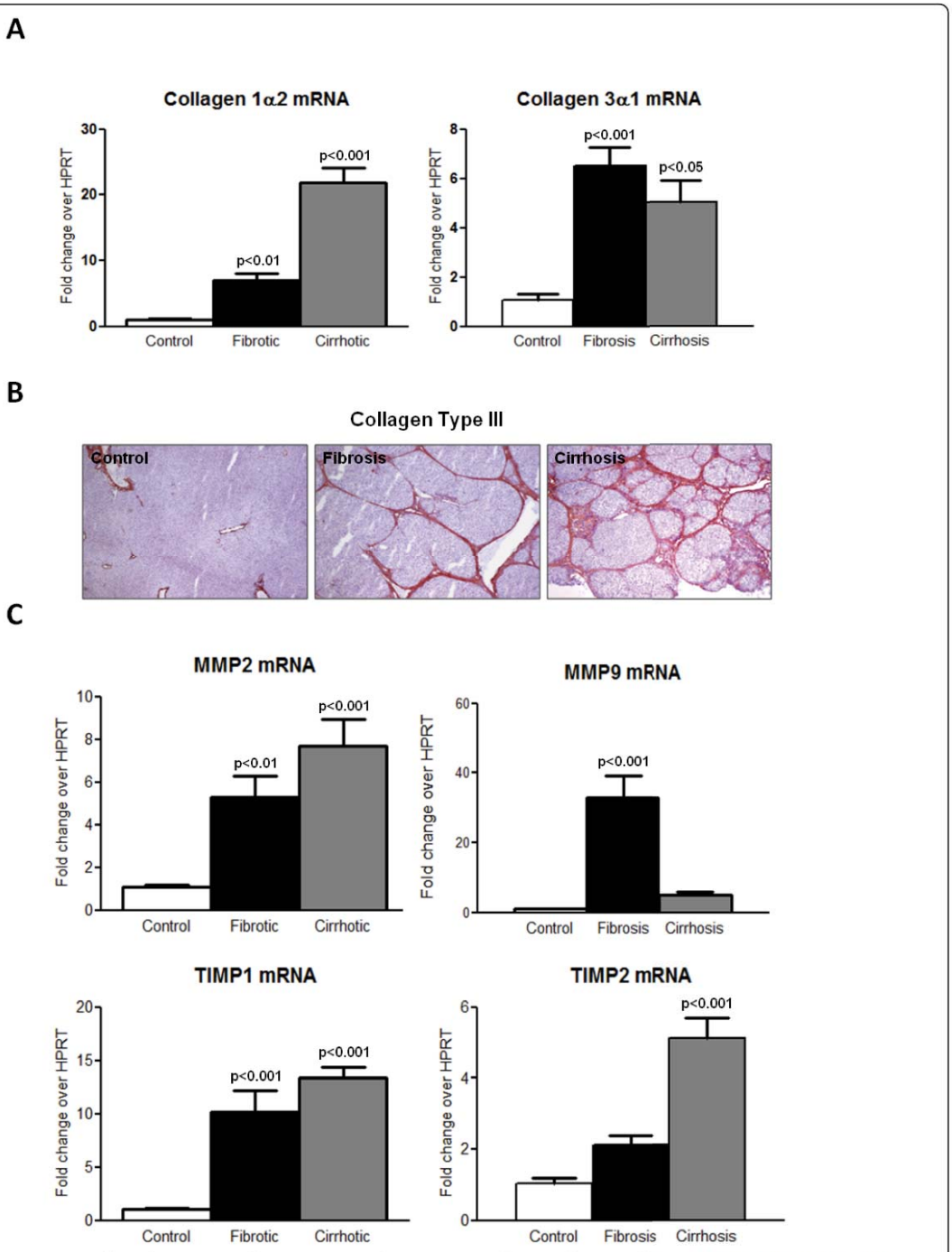

Figure 5 Hepatic expression of predominant collagen types and turnover regulators of extracellular matrix (ECM) in the study rats. Animals were grouped as control, fibrosis and cirrhosis. Rats with mild, moderate and severe fibrosis were analyzed together as the fibrosis group. **(A)** Collagens I and III transcription levels quantified by real-time PCR. **(B)** Immunolocalization of collagen type III in liver tissue. **(C)** Hepatic gene expression of matrix metalloproteinase (Mmp)-2 and Mmp9, and tissue inhibitor of matrix metalloproteinase (Timp)-1 and Timp2 by real-time PCR. Data are expressed as mean ± SEM of the group, and $P \leq 0.05$ was considered significant (on top of the columns). Significance is denoted versus the control group.

Segovia-Silvestre *et al. Fibrogenesis & Tissue Repair* 2011, **4**:19
http://www.fibrogenesis.com/content/4/1/19

Genes involved in ECM turnover are induced in the liver of CCl_4-treated rats

Following hepatic injury, increased matrix deposition of collagen fibers results from an altered balance between the activity of cleavage proteases such as MMPs and their endogenous inhibitors, the TIMPs. Therefore, we sought to determine expression of the rat genes Mmp2, Mmp9, Timp1 and Timp2 in the liver of CCl_4-treated rats with different degrees of cirrhosis (Figure 5C). Reverse transcriptase PCR analysis revealed marked Mmp2 and Mmp9 mRNA overexpression in fibrotic rats compared with control animals. A similar degree of Mmp2 mRNA expression was apparent in cirrhotic rats; however, the abundance of the Mmp9 transcript was clearly attenuated in this group of animals. Timp1 and -2 mRNAs were also significantly overexpressed in the liver of CCl_4-treated rats, with the higher intensity being found in cirrhotic animals.

Discussion

It has recently been reported that human MMP-9 can perform the initial cleavage of native collagens I and III, with a clear substrate preference for type III over type I [16]. A number of specific sequences of type III collagen generated by MMP-9 have been identified previously [17]. One of these, the neoepitope CO3-610, is also produced in rodents [13]. We previously reported that CO3-610 levels are significantly increased in response to BDL in Sprague-Dawley rats [14]. Rats had serum levels 2.3 times higher than those of matched sham controls at 2 and 4 weeks after surgery. Similarly, when we investigated how CO3-610 responds to CCl_4 intraperitoneal injection, we found that serum levels doubled after 4 weeks of treatment, and remained significantly higher than those of controls until week 8 [18].

In the present study, we found that fibrosis induced by CCl_4 inhalation in Wistar rats also resulted in increased expression of the 25 kDa CO3-610 circulating fragment (Figure 2). The fragment could be quantified by serum ELISA, and used to differentiate the stages of hepatic fibrosis in this experimental group. In particular, the study marker could discriminate advanced fibrosis from cirrhosis, and both from mild/moderate fibrosis and normal liver conditions (Figure 3A). This suggests that CO3-610 may be of use in advanced disease diagnosis, in the prognosis of liver-related events (hepatic coma or liver-related death), or as a marker of treatment efficacy in patients with cirrhosis. In the diagnosis of advanced fibrosis, CO3-610 seems to add little extra value to the already existing serum and imaging markers; however, as a marker of treatment efficacy, it merits further research considering that currently the greatest limitation in bringing new antifibrotic drugs to the clinic is the lack of clinical trial end points [7]. In contrast to our previous studies in models of acute liver disease [14,18] in which CO3-610 levels quickly responded to the treatment in the context of high associated mortality, this study allowed us to observe how CO3-610 levels correlated with histological fibrosis along a wide range of fibrosis values (Figure 3B), and how CO3-610 can effectively discriminate stages of severe fibrosis and cirrhosis from mild/moderate or no fibrosis, and between both advanced stages of disease (Figure 3A).

A key finding in this paper is the relationship between serum CO3-610 and PP, which was the strongest of all variables studied. The assessment of hemodynamic parameters, together with liver biopsy examination, is a very important tool for staging and prognosis in liver disease. Furthermore, a recent study in patients with hepatitis C virus after liver transplantation determined that a hepatic venous pressure gradient value of 6 mm Hg or higher was accurate at identifying patients at risk of disease progression (area under the curve 0.96) [19]. To our knowledge, HA is the only serum marker that has been confirmed as an independent predictor of portal hypertension in patients with liver disease [20]. In our study, compared with HA measurements in serum, there was a stronger relationship between CO3-610 and hepatic collagen content during fibrosis, This is important because HA is an ECM component whose serum levels are closely associated with matrix deposition, and it is generally considered one of the best available liver fibrosis biomarkers. HA has been thoroughly studied in both preclinical and clinical settings, and continues to be tested in human liver disease as part of algorithmic models that include other serum markers and clinical variables [8,21,22].

Interstitial collagens type I and III are the main components of the scar matrix that replaces the basal membrane of the subendothelial space of Disse and sinusoid during liver fibrosis [23,24]. Type I collagen transcription is considered a sensitive marker of active fibrogenesis, with increased levels seen at an early stage in the process [25,26]. In the study group, Col1α2 transcription behaved as a quantitative index of fibrosis progression, whereas type III collagen transcription was activated in fibrosis, but remained at similar levels in cirrhosis (Figure 5A). This differential profile is not apparent when animals are grouped according to the time course of CCl_4 exposure [24]. Type III collagen protein accumulation continued to increase in cirrhotic tissue (Figure 5B), probably due to decreases in interstitial collagen degradation in advanced disease. Changes in the activities of MMPs are considered one of the main factors contributing to excess collagen deposition in liver fibrosis [27]. We found a general overexpression of both gelatinases during fibrosis (Figure 5C), in agreement with previous reports [28-30]. However, rat Mmp9

Segovia-Silvestre *et al. Fibrogenesis & Tissue Repair* 2011, **4**:19
http://www.fibrogenesis.com/content/4/1/19

gene expression was no longer induced in cirrhotic animals, but returned to control values. Similar expression profiles have been published in previous reports [31,32], with Mmp9 increases being associated with early liver injury and inflammatory reaction, but not with the stage of fibrosis, and they disappeared in advanced fibrosis. Instead, Mmp2 levels increased with tissue inflammation, and were sustained at later stages. It is thought that the initial role of MMP-9 in liver fibrosis is the degradation of the normal basolateral matrix, and that subsequent decreases in ECM breakdown by MMP-9 lead to ECM accumulation and exacerbation of liver fibrosis. CCl_4 treatment also induced increases in rat Timp1 and -2 expression (Figure 5C). Interestingly, Timp2 increases were significant only in cirrhotic rats. Taken together, these results suggest that rat liver Mmp9 production and activity may reach their peak during fibrosis, but not cirrhosis. However, relevant Mmp9 activity also depends upon release of the latent form of the enzyme from cellular stores, and is heavily regulated by interactions with different tissue factors [33].

Conclusions

The results presented in this paper indicate that the type III collagen neoepitope CO3-610 closely correlates with hepatic collagen content and portal pressure in rats with fibrosis. Taking into account that the CO3-610 amino acid sequence is identical in rodent and human type III collagen, our findings suggest that this peptide could ultimately be a useful non-invasive biomarker of fibrosis in patients with liver disease.

Methods

The study was performed according to the criteria of the investigation and ethics committee of the Hospital Clinic, Barcelona, Spain.

Induction of cirrhosis in rats and experimental procedures

The study was performed on 68 male Wistar rats with different degrees of fibrosis and 20 control Wistar rats (Charles-River, Saint Aubin les Elseuf, France). Fibrosis was induced by repetitive CCl_4 inhalation [34]. The rats were fed *ad libitum* with standard chow and given water containing phenobarbital 0.3 g/L as drinking fluid. Animals were exposed to a CCl_4 vapor atmosphere twice a week, starting with 0.5 minutes per exposure. The duration of exposure was increased by 1 minute after every three session until it reached 5 minutes, which was used until the end of the investigation. To examine the effects of variable degrees of hepatic fibrosis, the CCl_4-treated rats were examined at weeks 8 (n = 13), 13 (n = 26), 16 (n = 13) and 19 (n = 16) after starting the fibrosis-induction protocol. For the analysis of results, all treated animals were grouped according to thresholds of histological fibrosis (Figure 1). Control rats were studied after similar periods of phenobarbital administration alone.

When scheduled, animals were anesthetized and a hemodynamic study was performed when indicated. A subgroup of 20 rats was selected to perform these measurements before termination to measure MAP and PP. A blood sample was then obtained from all animals to measure osmolality, electrolytes, standard parameters of liver function, and serum concentrations of HA and CO3-610. Thereafter, the animals were killed by isofluorane overdose (Forane, Abbott Laboratories S.A., Madrid, Spain), and hepatic samples were obtained from the middle liver lobe, which were immediately frozen in liquid nitrogen until further analysis of mRNA expression, or fixed in 10% buffered formalin for further analysis with hematoxylin and eosin stain, Sirius red stain and immunohistochemistry.

Hemodynamic measurements

Rats were anesthetized with barbiturate 100 mg/kg body weight (Inactin®; Sigma-Aldrich Chemie Gmbh, Steinherim, Germany) and a polyvinyl catheter (PE-50; ; Becton-Dickinson, Franklin Lakes, NJ, USA) was implanted in the left femoral artery. The arterial catheter was connected to a very sensitive transducer (Hewlett Packard, Avondale, PA, USA) that was calibrated before each study. Hemodynamic parameters were allowed to equilibrate for 30 minutes, and MAP and heart rate values were recorded for two periods of 30 minutes. Each value represented the average of two measurements. A midline abdominal incision (20 mm) was made, and a PE-50 catheter was placed in the portal vein through an ileocolic vein. After verifying free blood reflux, the catheter was fixed to the mesentery with cyanoacrylate glue, and PP was measured. Animals were killed by isofluorane overdose, and tissue specimens were collected.

Quantification of fibrosis

Liver sections 4 μm thick were stained in 0.1% Sirius red F3B (Sigma-Aldrich, St. Louis, MO, USA) in saturated picric acid (Sigma-Aldrich). The relative fibrotic area, expressed as a percentage of total liver area, was assessed by analyzing 36 fields of Sirius red-stained liver sections per animal. Each field was acquired at 10× magnification with a microscope (E600; Nikon, Tokyo, Japan) and digital camera (RT-Slider Spot; Diagnostic Instruments, Sterling Heights, MI, USA). Results were analyzed using imaging software (ImageJ, NIH). To evaluate the relative fibrosis area, the measured collagen area was divided by the net field area and then multiplied by 100. Subtraction of the vascular luminal area

Segovia-Silvestre *et al. Fibrogenesis & Tissue Repair* 2011, **4**:19
http://www.fibrogenesis.com/content/4/1/19

from the total field area yielded the net fibrosis area [35].

CO3-610 immunoprecipitation from serum

Serum samples from rats treated with CCl_4 for 19 weeks and from non-treated animals were analyzed in parallel. Briefly, 1.5 μg/well of biotinylated anti-CO3-610 antibody was used to coat streptavidin 96-well plates (Thermo Scientific Pierce, Rockford, IL, USA). Serum samples (125 μL) were diluted 1:1 in immunoprecipitation buffer, added to the wells, and incubated for 1 hour at room temperature. Antibody-antigen complexes were removed from non-specific binding, and the antigen eluted from the plates according to the manufacturer's instructions. For western blotting analysis, 1.4 μl of DTT 1 mol/l was added to 35 μL of each eluted sample, and then heated for 5 minutes at 95°C. The heated samples were loaded onto 15% SDS gels, resolved, and transferred to nitrocellulose membranes using 60 mA for 90 minutes. Membranes were blocked overnight in 5% milk, and incubated for a further 2.5 hours with horseradish peroxidase-labeled anti-CO3-610 antibody (diluted 1:100). After three washes of 10 minutes each, membranes were incubated for a further 1 hour with anti-mouse IgG HRP-linked secondary antibody (diluted 1:5000) followed by another three washes of 10 minutes each. Membranes were then developed with autoradiography films (GE Healthcare, Piscataway, NJ, USA) for 30 minutes.

CO3-610 quantification in serum

Details on the design and production of the monoclonal antibody against CO3-610 and the development of the serum CO3-610 ELISA assay have been previously published [13]. In brief, 100 μl of 2.5 ng/mL C-term biotinylated peptide NB51 (KNGETGPQGP) in PBS-Tris-borate-EDTA were used to coat streptavidin plates for 30 minutes at 20°C on a 300 rpm shaker, and then removed with washing buffer. Serum samples (20 μl) were diluted eightfold in incubation buffer (10 mmol/l: 400 mmol/l Tris:Bis-Tris buffer) and added to the plates. Next, 100 μL of CO3-610 peroxidase conjugated antibody solution (1:40,000 dilution) was added to the plates and left to incubate overnight at 4°C, on a 300 rpm shaker. The next day, plates were washed five times in washing buffer, then 100 μl of 3,3',5,5'-tetramethylbenzidine was added, and the plates incubated in darkness for 15 minutes at 20°C on a 300 rpm shaker. The reaction was stopped with the addition of 100 μL of stop solution, and plates were read on an ELISA reader at 450 nm, with 650 nm as reference.

Messenger RNA expression of Col1α2, Col3α1, Mmp2, Mmp9, Timp1 and TIMP2

Total RNA was extracted from frozen liver specimens of control and fibrotic rats (RNeasy Kit; Qiagen, Hilden, Germany), then 1 μg of total RNA was reverse transcribed using a complementary DNA synthesis kit (High-Capacity cDNA Reverse Transcription Kit; Applied Biosystems, Foster City, CA, USA). RNA concentration was determined by spectrophotometric analysis (ND-100 Spectrophotometer, Nanodrop Technologies Inc., Wilmington, DE, USA). Total RNA (1 μg) was reverse transcribed using the same complementary DNA synthesis kit described above. Specific primers and probes used for the different genes studied were designed to include intron spanning, using the Universal Probe Library Assay Design Center through the ProbeFinder software (version 2.45; Roche Diagnostics, Indianapolis, IN, USA; https://www.roche-applied-science.com/sis/rtpcr/upl/index.jsp). The primers used are shown in Table 2. Primers for rat were designed according to GenBank sequences (NM_053356.1, NM_032085.1, NM_053819.1, NM_021989.2, NM_031054.2, NM_031055.1 and NM_012583.2, respectively) and probes were designed using ProbeFinder software as above.

Real-time quantitative PCR reactions were performed in duplicate and analyzed (Light Cycler 480; Roche Diagnostics). The PCR reaction mix was 10 μl total volume, comprising 1:8 cDNA dilution, 200 nmol/l primer dilution, 100 nmol/l pre-validated nine-mer probe (Universal ProbeLibrary, Roche Diagnostics) and a master kit (FastStart Taqman Probe Master Kit; Roche Diagnostics). The hypoxanthine phosphoribosyltransferase 1 gene (Hprt1) was used as a reference gene for normalization (Table 2), and water was used as negative control.

Relative quantification was calculated using the comparative threshold (CT) cycle, which is inversely related to the abundance of mRNA transcripts in the initial sample. The mean of CT duplicate measurements was used to calculate ΔCT as the difference in CT for target

Table 2 Primers used for PCR

Primer name		Sequence 5'→3'
Col1α2	Left	AGACCTGGCGAGAGAGGAGT
	Right	ATCCAGACCGTTGTGTCCTC
Col3α1	Left	TCCCCTGGAATCTGTGAATC
	Right	TGAGTCGAATTGGGGAGAAT
Timp1	Left	CATGGAGAGCCTCTGTGGAT
	Right	TGTGCAAATTTCCGTTCCTT
Timp2	Left	GACAAGGACATCGAATTTATCTACAC
	Right	CCATCTCCTTCCGCCTTC
Mmp2	Left	GCGCTTTTCTCGAATCCAT
	Right	GGGTATCCATCTCCATGCTC
Mmp9	Left	CCTGAAAACCTCCAACCTCA
	Right	GAGTGTAACCATAGCGGTACAGG
Hprt1	Left	GACCGGTTCTGTCATGTCG
	Right	ACCTGGTTCATCATCACTAATCAC

and reference. The relative quantity of product was expressed as fold-induction of the target gene compared with the reference gene according to the formula $2^{-\Delta\Delta CT}$, where ΔΔCT represents ΔCT values normalized with the mean ΔCT of control samples.

Type III collagen immunohistochemical analysis

Sections of frozen liver tissue 5 μm thick were cut and fixed in acetone for 10 minutes, then dried overnight at room temperature. Slides were washed in water for 5 minutes. Anti-type III collagen ab7778 primary antibody (Abcam, Cambridge, UK) was diluted 1:50 with 1% bovine albumin, and incubated on the slides for 30 minutes at room temperature, then removed with 0.1% Triton X-100 in PBS (two washes of 5 minutes each). Slides were then incubated with secondary horseradish peroxidase Envision anti-rabbit IgG antibody (Dako, Glostrup, Denmark) for 30 minutes, and washed with 0.1% Triton X-100 (2 × 5 minutes). Red staining was produced by incubation with 3-amino-9-ethyl carbazole substrate (Vector Laboratories, Burlingame, CA, USA) for 30 minutes. Slides were counterstained with Meyers hematoxylin.

Other measurements and statistical analysis

Serum levels of HA were quantified with an enzyme-linked binding-protein assay according to the manufacturer's instructions (Corgenix Inc, Westminster, CO, USA). Serum osmolality was determined from osmometric depression of the freezing point (Osmometer 3300; Advanced Instruments, Needham Heights, MA, USA) and Na^+ and K^+ concentrations by flame photometry (IL 943; Instrumentation Laboratory, Lexington, MA, USA). Serum albumin, alanine transaminase and lactate dehydrogenase were measured by a chemical analyzer (ADVIA 2400; Siemens Healthcare Diagnostics, Tarrytown, NY, USA). Quantitative data were analyzed using GraphPad Prism 5 (GraphPad Software, Inc., San Diego, CA, USA). Differences between mean values obtained from CCl_4-treated and control groups were analyzed using one-way ANOVA with Newman-Keuls *post hoc* test, and Kruskal–Wallis test with Dunn *post hoc* tests when appropriate. Correlations between serum CO3-610 values and the rest of the variables studied were analyzed with the Pearson two-tailed test. Data was expressed as mean ± SEM, and $P \leq 0.05$ was considered significant.

List Of Abbreviations

Mmp/MMP, matrix metalloproteinase (rat and human, respectively); HA, hyaluronic acid; PIIINP, human N-terminal propeptide of type III procollagen; Timp/TIMP tissue inhibitor of metalloproteinase (rat and human, respectively); LB, Liver biopsy; ECM, extracellular matrix; BDL, bile-duct ligation; MAP, mean arterial pressure; PP, portal pressure; Col1**α**2, collagen type I alpha 2 in rat; Col3**α**1, collagen type III alpha 1in rat; Hprt1, hypoxanthine-guanine phosphoribosyltransferase 1 in rat; ELISA, enzyme-linked immunosorbent assay; PBS, phosphate-buffered saline

Acknowledgements

This work was supported in part by grants from the Dirección General de Investigación Científica y Técnica (SAF09-08839 to WJ and SAF07-63069 to MMR) and from the Agència de Gestió d'Ajuts Universitaris I de Recerca (SGR 2009/1496). CIBERehd is funded by the Instituto de Salud Carlos III (Spain).

Author details

[1]Nordic Bioscience A/S, Herlev, Denmark. [2]Biochemistry and Molecular Genetics, Hospital Clinic, IDIBAPS, CIBERehd, Barcelona, Spain. [3]Department of Physiological Sciences I, Medical School, University of Barcelona, Barcelona, Spain.

Authors' contributions

TSS and WJ designed and conceived the study. TSS performed the CO3-610 measurements and immunoprecipitation, VR and GFV performed HA measurements, quantitative PCR and hemodynamic measurements. MMR performed the liver-collagen quantification. NB supervised and ensured CO3-610 assay performance. SV, MMR and MAK participated in data interpretation and manuscript preparation. TSS, VR and WJ wrote the manuscript. All authors read and approved the final manuscript.

Competing interests

TSS, EV and NB are full-time employees at Nordic Bioscience, and MAK owns stocks at Nordic Bioscience. Nordic Bioscience is currently applying for a patent relating to the use of CO3-610 as a fibrosis biomarker. The other authors declare no competing interests.

Received: 26 May 2011 Accepted: 3 August 2011
Published: 3 August 2011

References

1. Castera L, Pinzani M: **Biopsy and non-invasive methods fot the diagnosis of liver fibrosis: does it take two to tango?** *Gut* 2010, **59**:861-866.
2. Castera L, Pinzani M: **Non invasive assessment of liver fibrosis: are we ready?** *Lancet* 2010, **375**:1419-1420.
3. Friedman SL: **Mechanisms of hepatic fibrogenesis.** *Gastroeneterology* 2008, **134**:1655-1669.
4. Bravo AA, Sheth SG, Chopra S: **Liver biopsy.** *N Engl J Med* 2001, **344**:495-500.
5. Afdhal NH, Nunes D: **Evaluation of liver fibrosis: a concise review.** *Am J Gastroenterol* 2004, **99**:1160-1174.
6. Gressner AM, Gao CF, Gressner OA: **Non-invasive biomarkers for monitoring the fibrogenic process in liver: a short survey.** *World J Gastroenterol* 2009, **15**:2433-2440.
7. Talwalkar JA: **Antifibrotic therapies–emerging biomarkers as treatment end points.** *Nat Rev Gastroenterol Hepatol* 2010, **7**:59-61.
8. Carrion JA, Fernandez-Varo G, Bruguera M, Garcia-Pagan JC, Garcia-Valdecasas JC, Perez-Del-Pulgar S, *et al*: **Serum fibrosis markers identify patients with mild and progressive hepatitis C recurrence after liver transplantation.** *Gastroenterology* 2010, **138**:147-158.
9. Guechot J, Laudat A, Loria A, Serfaty L, Poupon R, Giboudeau J: **Diagnostic accuracy of hyaluronan and type III procollagen amino-terminal peptide serum assays as markers of liver fibrosis in chronic viral hepatitis C evaluated by ROC curve analysis.** *Clin Chem* 1996, **42**:558-563.
10. Guechot J, Loria A, Serfaty L, Giral P, Guiboudeau J, Poupon R: **Serum Hyaluronan as a marker of liver fibrosis in chronic viral hepatitis C: effect of alpha-interferon therapy.** *J Hepatol* 1995, **22**:22-26.
11. Shimizu I, Omoya T, Takaoka T, Wada S, Wada H, Taoka M, *et al*: **Serum amino-terminal propeptide of type III procollagen and 7S domain of type IV collagen correlate with hepatic iron concentration in patients with chronic hepatitis C following alpha-interferon therapy.** *J Gastroenterol Hepatol* 2001, **16**:196-201.
12. Veidal SS, Bay-Jensen AC, Tougas G, Karsdal MA, Vainer B: **Serum markers of liver fibrosis: combining the BIPED classification and the neo-epitope approach in the development of new biomarkers.** *Dis Markers* 2010, **28**:15-28.
13. Barascuk N, Veidal SS, Larsen L, Larsen DV, Larsen MR, Wang J, *et al*: **A novel assay for extracellular matrix remodeling associated with liver**

fibrosis: An enzyme-linked immunosorbent assay (ELISA) for a MMP-9 proteolytically revealed neo-epitope of type III collagen. *Clin Biochem* 2010, **43**:899-904.
14. Veidal SS, Vassiliadis E, Barascuk N, Zhang C, Segovia-Silvestre T, Klickstein L, *et al*: **Matrix metalloproteinase-9-mediated type III collagen degradation as a novel serological biochemical marker for liver fibrogenesis.** *Liver Int* 2010, **30**:1293-1304.
15. Jensen CH, Hansen M, Brandt J, Rasmussen HB, Jensen PB, Teisner B: **Quantification of the N-terminal propeptide of human procollagen type I (PINP): comparison of ELISA and RIA with respect to different molecular forms.** *Clin Chim Acta* 1998, **269**:31-41.
16. Bigg HF, Rowan AD, Barker MD, Cawston TE: **Activity of matrix metalloproteinase- against native collagen types I and III.** *FEBS J* 2007, **274**:1246-1255.
17. Zhen EY, Brittain IJ, Laska DA, Mitchell PG, Sumer EU, Karsdal MA, *et al*: **Characterization of metalloprotease cleavage products of human articular cartilage.** *Arthritis Rheum* 2008, **58**:2420-2431.
18. Vassiliadis E, Vang Larsen D, Elgaard Clausen R, Veidal SS, Barascuk N, Larsen L, *et al*: **Measurement of CO3-610, a potential liver biomarker derived from matrix metalloproteinase-9 degradation of collagen type III, in a rat model of reversible carbon-tetrachloride-induced fibrosis.** *Biomarkers Insight* 2011, **6**:49-58.
19. Blasco A, Forns X, Carrion JA, Garcia-Pagan JC, Gilabert R, Rimola A, *et al*: **Hepatic venous pressure gradient identifies patients at risk of severe hepatitis C recurrence after liver transplantation.** *Hepatology* 2006, **43**:492-499.
20. Yachida S, Wakabayashi H, Okano K, Suzuki Y: **Prediction of posthepatectomy hepatic functional reserve by serum hyaluronate.** *Br J Surg* 2009, **96**:501-508.
21. Nobili V, Parkes J, Bottazzo G, Marcellini M, Cross R, Newman D, *et al*: **Performance of ELF serum markers in predicting fibrosis stage in pediatric non-alcoholic fatty liver disease.** *Gastroenterology* 2009, **136**:160-167.
22. Fontana RJ, Goodman ZD, Dienstag JL, Bonkovsky HL, Naishadham D, Sterling RK, *et al*: **Relationship of serum fibrosis markers with liver fibrosis stage and collagen content in patients with advanced chronic hepatitis C.** *Hepatology* 2008, **47**:789-798.
23. Rojkind M, Giambrone MA, Biempica L: **Collagen types in normal and cirrhotic liver.** *Gastroenterology* 1979, **76**:710-719.
24. Nakatsukasa H, Nagy P, Evarts RP, Hsia CC, Marsden E, Thorgeirsson SS: **Cellular distribution of transforming growth factor-beta 1 and procollagen types I, III, and IV transcripts in carbon tetrachloride-induced rat liver fibrosis.** *J Clin Invest* 1990, **85**:1833-1843.
25. Castilla A, Prieto J, Fausto N: **Transforming growth factors beta 1 and alpha in chronic liver disease. Effects of interferon alfa therapy.** *N Engl J Med* 1991, **324**:933-940.
26. Annoni G, Weiner FR, Zern MA: **Increased transforming growth factor-beta 1 gene expression in human liver disease.** *J Hepatol* 1992, **14**:259-264.
27. Hemmann S, Graf J, Roderfeld M, Roeb E: **Expression of MMPs and TIMPs in liver fibrosis – a systematic review with special emphasis on anti-fibrotic strategies.** *J Hepatol* 2007, **46**:955-975.
28. Takahara T, Furui K, Funaki J, Nakayama Y, Itoh H, Miyabayashi C, *et al*: **Increased expression of matrix metalloproteinase-II in experimental liver fibrosis in rats.** *Hepatology* 1995, **21**:787-795.
29. Milani S, Herbst H, Schuppan D, Grappone C, Pellegrini G, Pinzani M, *et al*: **Differential expression of matrix-metalloproteinase-1 and -2 genes in normal and fibrotic human liver.** *Am J Pathol* 1994, **144**:528-537.
30. Kossakowska AE, Edwards DR, Lee SS, Urbanski LS, Stabbler AL, Zhang CL, *et al*: **Altered balance between matrix metalloproteinases and their inhibitors in experimental biliary fibrosis.** *Am J Pathol* 1998, **153**:1895-1902.
31. Knittel T, Mehde M, Grundmann A, Saile B, Scharf JG, Ramadori G: **Expression of matrix metalloproteinases and their inhibitors during hepatic tissue repair in the rat. Histochem.** *Cell Biol* 2000, **113**:443-453.
32. Gieling RG, Wallace K, Han YP: **Interleukin-1 participates in the progression from liver injury to fibrosis.** *Am J Physiol Gastrointest Liver Physiol* 2009, **296**:G1324-1331.
33. Vempati P, Karagiannis ED, Popel AS: **A biochemical model of matrix metalloproteinase 9 activation and inhibition.** *J Biol Chem* 2007, **282**:37585-37596.
34. Clària J, Jiménez W: **Renal dysfunction and ascites in carbon tetrachloride-induced cirrhosis in rats.** In *The Liver and the Kidney* Edited by: Arroyo V, Schrier RW, Rodés J, Ginès P. Boston: Blackwell Science 1999, 379-396.
35. Muñoz-Luque J, Ros J, Fernández-Varo G, Tugues S, Morales-Ruiz M, Alvarez CE, *et al*: **Regression of fibrosis after chronic stimulation of cannabinoid CB2 receptor in cirrhotic rats.** *J Pharmacol Exp Ther* 2008, **324**:475-483.

doi:10.1186/1755-1536-4-19
Cite this article as: Segovia-Silvestre *et al.*: **Circulating CO3-610, a degradation product of collagen III, closely reflects liver collagen and portal pressure in rats with fibrosis.** *Fibrogenesis & Tissue Repair* 2011 **4**:19.

2nd Article: Prevention of fibrosis progression in CCl_4-treated rats: role of the hepatic endocannabinoid and apelin systems.

Targeting critical molecules involved in fibrosis progression, inflammation and/or angiogenesis open new possibilities for preventing liver fibrosis progression to advanced stages. In order to prevent fibrosis progression, antifibrogenic strategies need to focus on reducing myofibroblastic cell accumulation by blocking proliferation factors or inducing apoptosis of those cells, but also targeting ECM turnover genes, by inhibiting matrix synthesis and promoting matrix degradation. Both the endocannabinoid and apelin systems are actively implicated in liver fibrosis. Previous studies have demonstrated that CB2 receptors have antifibrogenic effects by inhibiting myofibroblast cell growth and inducing apoptosis. This antifibrogenic role was confirmed in $CB2^{-/-}$ knockout mice, which showed increased fibrosis compared to wild type (Julien et al., 2005). CB2 receptor stimulation was able to reverse liver fibrosis in cirrhotic rats with ascites, together with a decrease in inflammatory cell infiltration and an increase in non-parenchymal cell apoptosis (Muñoz-Luque et al., 2008). Apelin has an important role in neovascularization, regulating the vascular tone and myocardial contractility; it is actually one of the most potent positive inotropic agents. The apelin system's role in liver fibrosis has been recently described in our laboratory (Principe et al., 2008). Cirrhotic patients have elevated circulating levels of this peptide, and the blockade of the receptor with a specific antagonist improved liver fibrosis, systemic hemodynamics and reduced angiogenesis and ascites volume in cirrhotic rats.

For this study, we used CCl_4-treated rats for 13 weeks, to allow enough time for animals to develop fibrosis. The animals were assigned randomly into 5 groups: 1) a control group, 2) a group treated with a selective CB2 agonist, AM1241 and 3) the corresponding vehicle group, and 4) a group treated with an apelin receptor antagonist, F13A and 5) the corresponding vehicle.

1. Liver function tests, mean arterial pressure and portal pressure in treated and non-treated fibrotic rats

As anticipated, vehicle animals from both experimental groups presented the classical alteration of liver function parameters (Table 1), as well as, hyoptension and

portal hypertension. Of note, is that only chronic administration of CB2 receptor agonist improved AST and ALT levels in serum, and no other significant changes in biochemical parameters were observed in the rest of treated rats by either AM1241 or F13A. However, both treatments ameliorated the hemodynamic function increasing mean arterial pressure (MAP), splanchnic perfusion pressure (SPP) and decreasing portal pressure (PP) compared to vehicle-treated rats.

2. Effect of CB2 receptor activation and APJ blockade on liver fibrosis in fibrotic rats

Sirius red staining quantification of liver samples showed that vehicle rats had visible fibrosis formation with significant collagen accumulation in the periportal and perivenular areas and thin portal-to-portal septa formation. Both CB2 stimulation and APJ blockade treatments prevented the excessive accumulation of matrix fibers produced in vehicle rats. Figure 1 shows representative images of control, vehicle and treated rats, as well as, a quantification of the % of fibrotic area, which resulted in a >50% reduction in treated animals.

3. Effects od CB2 receptor activation and APJ blockade on infiltrating cells, vessel desity, apoptosis and activated caspase-3 expression

CB2 stimulation and APJ blockade were able to prevent immune cell infiltration and angiogenesis of new blood vessels compared to vehicle animals (Figure 2 and 3). Both antifibrogenic agents had a significant effect on apoptosis of the hepatic cells measured by TUNEL assay as shown on Figure 4A, 4B. The apoptotic cells were located in the marginof fibrous septa and parenchyma. These results were supported with the protein quantification of Caspase-3 (Figure 4C, 4D). Both treatments decreased the activated Caspase-3 expression in the hepatic tissue of fibrotic rats.

4. Effect of CB2 receptor activation and APJ blockade on mRNA of hepatic profibrogenic genes and protein expression of PDGFRB and TIMP1

The mRNA expression of a panel of key profibrogenic genes involved in cytokine signaling (PDGFRβ and TGFβ), HSC activation (α-SMA), collagen accumulation (Col1α2) and ECM turnover genes (MMP2, MMP9, TIMP1 and TIMP2) was analyzed by Real

Time PCR (Table 2). CCl_4-induced liver damage upregulated all the genes analyzed as expected. Both AM1241 and F13A treatments decreased the expression of PDGFRβ, and also the HSC activation marker α-SMA. The most interesting finding, was that both treatments had a strong effect on ECM turnover genes in favor of ECM degradation. Table 3 shows the ratios between MMP/TIMP mRNA expression. Compared to vehicle animals, treated rats with either AM1241 or F13A showed an increased MMP9/TIMP1 and MMP9/TIMP2 ratio. Finally, PDGFRβ and TIMP1 expression, as they seem to be the major contributory genes, was confirmed by assessing protein levels by western blot. The results supported mRNA expression results, protein leveles of both genes were downregulated in treated rats (Figure 5).

1521-0103/12/3403-629–637$25.00
THE JOURNAL OF PHARMACOLOGY AND EXPERIMENTAL THERAPEUTICS
Vol. 340, No. 3
188078/3749549
JPET 340:629–637, 2012

Prevention of Fibrosis Progression in CCl_4-Treated Rats: Role of the Hepatic Endocannabinoid and Apelin Systems

Vedrana Reichenbach, Josefa Ros, Guillermo Fernández-Varo, Gregori Casals, Pedro Melgar-Lesmes, Teresa Campos, Alexandros Makriyannis, Manuel Morales-Ruiz, and Wladimiro Jiménez

Service of Biochemistry and Molecular Genetics, Hospital Clínic, Barcelona, Spain (V.R., J.R., G.F.-V., G.C., P.M.-L., T.C., M.M.-R., W.J.); Institut d'Investigacions Biomèdiques August Pi i Sunyer, Barcelona, Spain (V.R., J.R., G.F.-V., P.M.-L., M.M.-R., W.J.); Centro de Investigación Biomédica en Red de Enfermedades Hepáticas y Digestivas, Barcelona, Spain (G.F.-V., M.M.-R., W.J.); Center for Drug Discovery, Northeastern University, Boston, Massachusetts (A.M.); and Department of Physiological Sciences I, University of Barcelona, Barcelona, Spain (W.J.)

Received September 15, 2011; accepted December 6, 2011

ABSTRACT

Endocannabinoids behave as antifibrogenic agents by interacting with cannabinoid CB2 receptors, whereas the apelin (AP) system acts as a proangiogenic and profibrogenic mediator in the liver. This study assessed the effect of long-term stimulation of CB2 receptors or AP receptor (APJ) blockade on fibrosis progression in rats under a non-discontinued fibrosis induction program. The study was performed in control and CCl_4-treated rats for 13 weeks. Fibrosis-induced rats received a CB2 receptor agonist (*R,S*)-3-(2-iodo-5-nitrobenzoyl)-1-(1-methyl-2-piperidinylmethyl)-1*H*-indole (AM1241) (1 mg/kg b.wt.), an APJ antagonist [Ala^{13}]-apelin-13 sequence: Gln-Arg-Pro-Arg-Leu-Ser-His-Lys-Gly-Pro-Met-Pro-Ala (F13A) (75 μg/kg b.wt.), or vehicle daily during the last 5 weeks of the CCl_4 inhalation program. Mean arterial pressure (MAP), portal pressure (PP), hepatic collagen content, angiogenesis, cell infiltrate, and mRNA expression of a panel of fibrosis-related genes were measured in all animals. Fibrosis-induced rats showed increased hepatic collagen content, reduced MAP, portal hypertension, and increased expression of the assessed messengers in comparison with control rats. However, fibrotic rats treated with either AM1241 or F13A had reduced hepatic collagen content, improved MAP and PP, ameliorated cell viability, and reduced angiogenesis and cell infiltrate compared with untreated fibrotic rats. These results were associated with attenuated induction of platelet-derived growth factor receptor β, α-smooth muscle actin, matrix metalloproteinases, and tissue inhibitors of matrix metalloproteinase. CB2 receptor stimulation or APJ blockade prevents fibrosis progression in CCl_4-treated rats. The mechanisms underlying these phenomena are coincident despite the marked dissimilarities between the CB2 and APJ signaling pathways, thus opening new avenues for preventing fibrosis progression in liver diseases.

Introduction

Inflammation and remodeling are orchestrated responses ultimately directed to promoting tissue repair after organ injury. However, maintenance of the injury results in the activation of a profibrogenic cascade of events in chronic liver disease that finally leads to cirrhosis. Cirrhosis is a major determinant of morbidity and mortality and predisposes to hepatic failure and primary liver cancer. Therefore, halting the progression of fibrosis to cirrhosis has largely been considered to be a foremost goal in patients with liver disease (Friedman, 2010). Inflammation is an early event in the history of the disease. It occurs before the onset of significant clinical manifestations and becomes chronic during the evolution of the illness, particularly in patients with viral infection (Marra, 1999). This dynamic inflammatory state has been associated with liver fibrogenesis and fibrosis in experimental cirrhosis (Muñoz-Luque et al., 2008). In addition,

This work was supported by the Dirección General de Investigación Científica y Técnica [Grants SAF09-08839, SAF07-63069] (to W.J. and M.M.-R., respectively); Agència de Gestió d'Ajuts Universitaris i de Recerca [Grant SGR 2009/1496]; Dirección General de Investigación Científica y Tecnológica [Grant BES-2004-5186] (to P.M.-L.); and Instituto de Salud Carlos III ["Contrato Post Formación Sanitaria Especializada" FIS CM07/00043] (to G.C.). Centro de Investigación Biomédica en Red-Enfermedades Hepáticas y Digestivas was founded by the Instituto de Salud Carlos III (Spain).

This work was previously presented in part at the following conferences: Reichenbach V, Ros J, Fernández-Varo G, Muñoz-Luque J, Morales-Ruiz M, Makriyannis A, and Jiménez W (2008) Chronic stimulation of cannabinoid CB2 receptor represses fibrosis progression in CCl_4-treated rats. *59th Annual Meeting of the American Association for the Study of Liver Diseases*; 2008 Oct 31–Nov 4; San Francisco, CA. American Association for the Study of Liver Diseases, Alexandria, VA. Reichenbach V, Ros J, Fernández-Varo G, Casals G, Melgar-Lesmes P, Pauta M, Morales-Ruiz M, and Jiménez W (2010) Activation of the hepatic apelin system is of major relevance in early stages of liver fibrosis. *International Liver Conference 2010*; 2010 Apr 14–18; Vienna, Austria. European Association for the Study of the Liver, Geneva, Switzerland.

Article, publication date, and citation information can be found at http://jpet.aspetjournals.org.

http://dx.doi.org/10.1124/jpet.111.188078.

JPET PHARMACOLOGY AND EXPERIMENTAL THERAPEUTICS aspet

many inflammatory mediators have direct angiogenic activities and, in turn, angiogenesis contributes to the perpetuation and the amplification of the inflammatory state by promoting the recruitment of inflammatory cells in the neovasculature (Morales-Ruiz and Jiménez, 2005; Tugues et al., 2007). Therefore, inflammation, fibrogenesis, and angiogenesis are three closely related phenomena in chronic liver disease.

Under this scenario, suitable targets for anti-fibroproliferative therapies should include molecules that are critical in fibrosis progression and also possess inflammatory and/or angiogenesis-related properties. In this regard, two recently characterized endogenous hepatic systems are attracting increasing attention, namely the hepatic endocannabinoid and apelin systems. Endocannabinoids are lipid-related molecules participating in a wide range of physiological functions including neuroprotection, pain and motor function, energy balance and food intake, cardiovascular homeostasis, immune and inflammatory responses, and cell proliferation (Pacher et al., 2006; Reichenbach et al., 2010; Tam et al., 2011). These effects are mediated by interaction with two different types of receptors, the CB1 and CB2 receptors. Of interest, the CB1 receptor in the liver has been shown to mediate profibrogenic effects (Teixeira-Clerc et al., 2006) and has also been implicated in the pathogenesis of alcoholic and nonalcoholic liver disease (Hézode et al., 2008; Jeong et al., 2008). On the other hand, CB2 receptor agonism shows opposite antifibrogenic and anti-inflammatory effects in hepatic and nonhepatic tissue (Muñoz-Luque et al., 2008; Akhmetshina et al., 2009) and protects against liver ischemia-reperfusion injury (Horváth et al., 2011). Previous studies by our laboratory have demonstrated that the proangiogenic peptide, apelin (AP), is up-regulated in HSCs of patients with cirrhosis (Melgar-Lesmes et al., 2010). Furthermore, this peptide behaves as a paracrine mediator of fibrogenesis-related gene induction in human HSCs (Melgar-Lesmes et al., 2010), and apelin receptor (APJ) blockade has shown to be effective in reducing hepatic fibrosis and angiogenesis in rats with cirrhosis (Principe et al., 2008). Recent studies have also suggested that the apelin system is involved in inflammation and in endothelial cell proliferation (Masri et al., 2004; Daviaud et al., 2006).

In the present investigation, we sought to examine new therapeutic strategies to prevent the progression of fibrosis in injured livers of rats chronically receiving increasing doses of CCl_4. We assessed the changes in messenger expression of a panel of genes involved in inflammation and/or tissue remodeling and the antifibrogenic, antiangiogenic, and anti-inflammatory effects induced by either long-term administration of a specific CB2 receptor agonist or a selective APJ receptor antagonist in rats with experimentally induced fibrosis.

Materials and Methods

Induction of Fibrosis in Rats. Studies were performed in 47 male adult Wistar rats (Charles River Laboratories, Saint Aubin les Elseuf, France). Rats with fibrosis ($n = 37$) and control rats ($n = 10$) were fed ad libitum with standard chow and water containing phenobarbital (0.3 g/l) as drinking fluid. Fibrosis was induced by CCl_4 inhalation as described previously (Clària and Jiménez, 1999). In brief, animals were exposed to a CCl_4 vapor atmosphere twice a week, starting at 0.5 min/exposure. The duration of the exposure was increased by 1 min after every three sessions until it reached 5 min, which was used until the end of the investigation. Rats with fibrosis were studied 13 weeks after the start of the fibrosis induction protocol. Control rats were studied after a similar period of phenobarbital administration. The study was performed according to the criteria of the investigation and ethics committees of the Hospital Clínic Universitari.

Selective Activation of CB2 Receptors in Fibrotic Rats. The hemodynamic and gene expression effects of CB2 receptor activation were assessed in 20 rats with fibrosis. Ten animals were randomly assigned to a daily subcutaneous injection of a specific CB2 agonist, (*R,S*)-3-(2-iodo-5-nitrobenzoyl)-1-(1-methyl-2-piperidinylmethyl)-1*H*-indole (AM1241) at a dose of 1 mg/kg per day b.wt.) (Malan et al., 2001). In parallel, 10 rats received a solution of ethanol-Cremophor ELP-saline (1:1:18) as vehicle. AM1241 or vehicle was administered from the 9th to the 13th week after the start of the fibrosis induction protocol.

APJ Blockade in Fibrotic Rats. The hemodynamic and gene expression effects of APJ blockade were assessed in 17 rats with fibrosis. Seven animals were randomly assigned to a daily subcutaneous injection of an APJ antagonist, [Ala^{13}]-apelin-13 sequence: Gln-Arg-Pro-Arg-Leu-Ser-His-Lys-Gly-Pro-Met-Pro-Ala (F13A) at a dose of 75 μg/kg per day b.wt. (Phoenix Pharmaceuticals, Belmont, CA), and 10 rats received 1 ml/kg per day of saline solution as vehicle. F13A or vehicle was administered from the 9th to the 13th week after the start of the fibrosis induction protocol.

Hemodynamic Studies. Rats with fibrosis and control rats were anesthetized with Inactin (50 mg/kg b.wt.; Sigma-Aldrich Chemie GmbH, Taufkirchen, Germany) and prepared with a polyvinyl-50 catheter in the left femoral artery. The animals were prepared for measurements of hemodynamic parameters as described previously (Ros et al., 2005). Hemodynamic parameters were allowed to equilibrate for 30 min, and values of mean arterial pressure (MAP), portal pressure (PP), and heart rate were recorded. Splanchnic perfusion pressure (SPP) was defined as MAP − PP. At the end of the study, the animals were exsanguinated and a blood sample (6–9 ml) was taken to measure standard parameters of hepatic and renal function.

Quantification of Fibrosis and Apoptosis in Hepatic Tissue. Liver sections (4 μm) were stained in 0.1% Sirius red F3B (Sigma-Aldrich Chemie GmbH) in saturated picric acid (Sigma-Aldrich Chemie GmbH). Relative fibrosis area (expressed as a percentage of total liver area) was assessed by analyzing 32 fields of Sirius red-stained liver sections per animal. Each field was acquired at 10× magnification (Eclipse E600; Nikon, Kawasaki, Kanagawa, Japan) and then analyzed using the morphometry software ImageJ (version 1.37). To evaluate the relative fibrosis area, the collagen area measured was divided by the net field area and then multiplied by 100. Subtraction of vascular luminal area from the total field area yielded the final

ABBREVIATIONS: AP, apelin; HSC, hepatic stellate cell; APJ, apelin receptor; AM1241, (*R,S*)-3-(2-iodo-5-nitrobenzoyl)-1-(1-methyl-2-piperidinylmethyl)-1*H*-indole; F13A, [Ala^{13}]-apelin-13 sequence: Gln-Arg-Pro-Arg-Leu-Ser-His-Lys-Gly-Pro-Met-Pro-Ala; MAP, mean arterial pressure; PP, portal pressure; SPP, splanchnic perfusion pressure; TUNEL, terminal deoxynucleotidyl transferase dUTP nick-end labeling; PDGFRβ, platelet-derived growth factor receptor β; TGFβR1, transforming growth factor β receptor 1; Col1α2, collagen-Iα2; α-SMA, α-smooth muscle actin; TIMP, tissue inhibitor of matrix metalloproteinase; MMP, matrix metalloproteinase; HPRT, hypoxanthine guanine phosphoribosyltransferase; vWF, von Willebrand factor; AST, aspartate aminotransferase; ALT, alanine aminotransferase; ANOVA, analysis of variance; ECM, extracellular matrix; PDGF, platelet-derived growth factor; Col1, collagen type 1; C_T, comparative threshold cycle.

JPET PHARMACOLOGY AND EXPERIMENTAL THERAPEUTICS aspet

calculation of the net fibrosis area. The amount of fibrosis measured in each animal was analyzed, and the average value is presented as a percentage.

To determine the degree of hepatic apoptosis, we used the terminal deoxynucleotidyl transferase dUTP nick-end labeling (TUNEL) assay to detect cell death using a fluorescein-FragEL DNA Fragmentation Detection Kit (Calbiochem, San Diego, CA) according to the manufacturer's protocol. To quantify and compare the rates of cell death between groups, a semiquantitative scoring method was used. For each sample, the number of TUNEL-positive cells was counted per 200× high-power field. At least eight representative fields were evaluated for each experimental group, from which an average value was calculated.

Hepatic Messenger Expression of a Panel of Profibrogenic Genes in Fibrotic Rats. Liver specimens were obtained from each animal, washed in 0.1% diethyl pyrocarbonate-treated phosphate-buffered saline salt solution (140 mM NaCl, 8.5 mM Na_2HPO_4, and 1.84 mM $Na_2HPO_4 \cdot H_2O$, pH 7.4), immediately frozen in dry ice, and stored in liquid nitrogen. Liver samples from treated and untreated animals were also fixed in 10% buffered formalin for further hematoxylin and eosin and immunostaining analysis. Total RNA was extracted from the middle liver lobe of control and fibrotic rats using a commercially available kit (RNAeasy; QIAGEN, Hilden, Germany). The RNA concentration was determined by spectrophotometric analysis (ND-100 spectrophotometer; Thermo Fisher Scientific, Waltham, MA). One microgram of total RNA was reverse-transcribed using a cDNA synthesis kit (High-Capacity cDNA Reverse Transcription Kit; Applied Biosystems, Foster City, CA). Specific primers and probes used for the different genes studied were designed to include intron spanning using the Universal ProbeLibrary Assay Design Center through ProbeFinder version 2.45 software (Roche Diagnostics, Indianapolis, IN; https://www.roche-applied-science.com/sis/rtpcr/upl/index.jsp). A panel of selected profibrogenic genes was analyzed. The panel included the following: platelet-derived growth factor receptor β (PDGFRβ) (probe 69; left 5′-GCGGAAGCGCATCTATATCT-3′ and right 5′-GCGGAAGCGCATCTATATCT-3′), transforming growth factor β receptor 1 (TGFβR1) (probe 53; left 5′-AAGGCCAAATATTCCCAACA-3′ and right 5′-ATTTTGGCCATCACTCTCAAG-3′), collagen-Iα2 (Col1α2) (probe 95; left 5′-AGACCTGGCGAGAGAGGAGT-3′ and right 5′-ATCCAGACCGTTGTGTCCTC-3′), α-smooth muscle actin (α-SMA) (probe 78; left 5′-CATCAGGAACCTCGAGAAGC-3′ and right 5′-AGCCATTGTCACACACCAGA-3′), tissue inhibitor of matrix metalloproteinases type 1 (TIMP1) (probe 95; left 5′-CATGGAGAGCCTCTGTGGAT-3′ and right 5′-TGTGCAAATTTCCGTTCCTT-3′), TIMP2 (probe 73; left 5′-GACAAGGACATCGAATTTATCTACAC-3′ and right 5′-CCATCTCCTTCCGCCTTC-3′), matrix metalloproteinase 2 (MMP2) (probe 60; left 5′-CTCCACTACGCTTTTCTCGAAT-3′ and right 5′-TGGGTATCCATCTCCATGCT-3′), and MMP9 (probe 53; left 5′-CCTGAAAACCTCCAACCTCA-3′ and right: 5′-GAGTGTAACCATAGCGGTACAGG-3′). Hypoxanthine-guanine phosphoribosyltransferase (HPRT) (probe 95: left 5′-GACCGGTTCTGTCATGTCG-3′ and right 5′-ACCTGGTTCATCATCACTAATCAC-3′) was used as the reference gene. Primers were designed according to rat sequences (GenBank codes NM_031525.1, NM_012775.2, NM_053356.1, NM_031004.2, NM_053819.1, NM_021989.2, NM_031054.2, NM_031055.1, and NM_012583.2, respectively). Real-time quantitative polymerase chain reaction was analyzed in duplicate and performed with the LightCycler 480 (Roche Diagnostics). A 10-μl total volume reaction of diluted 1:8 cDNA, 200 nM primer dilution, 100 nM prevalidated 9-mer probe (Universal ProbeLibrary) and FastStart TaqMan Probe Master (Roche Diagnostics) were used in each polymerase chain reaction reaction. A fluorescence signal was captured during each of the 45 cycles (denaturizing for 10 s at 95°C, annealing for 20 s at 60°C, and extension for 1 s at 72°C). HPRT was used as a reference gene for normalization, and water was used as a negative control. Relative quantification was calculated using the comparative threshold cycle (C_T), which is inversely related to the abundance of mRNA transcripts in the initial sample. The mean C_T of duplicate measurements was used to calculate ΔC_T as the difference in C_T for target and reference. The relative quantity of product was expressed as fold induction of the target gene compared with the reference gene according to the formula $2^{-\Delta\Delta C_T}$, where $\Delta\Delta C_T$ represents ΔC_T values normalized with the mean ΔC_T of control samples.

Western Blot Analysis of Activated Caspase-3, PDGFRβ, and TIMP1. Hepatic tissue from treated and nontreated rats was individually homogenized as described previously (Muñoz-Luque et al., 2008). To detect PDGFRβ, TIMP1, and activated caspase-3, 80 μg of total denatured proteins were loaded on a 7% (PDGFRβ) and 12% (TIMP1 and caspase-3) SDS-polyacrylamide gel (Mini-PROTEAN III; Bio-Rad Laboratories, Hercules, CA). Gels were transferred for 2 h to nitrocellulose membranes of 0.45 μm for PDGFRβ and to 0.2 μm for TIMP1 and caspase-3 and blocked with 5% nonfat milk for PDGFRβ and 1% bovine serum albumin for TIMP1 and caspase-3 in TTBS buffer at room temperature for 2 h. All membranes were stained with Ponceau S Red as a control for protein loading and were then incubated overnight at 4°C with rabbit polyclonal anti-PDGFRβ (1:1000; Cell Signaling Technology, Danvers, MA), anti-TIMP1 (1:1000; Abcam, Cambridge, UK), and anti-activated caspase-3 (1:300 dilution; Abcam) for 24, 24, or 48 h, respectively. The bands were visualized by chemiluminescence (Lumi-Light Western blotting substrate; Roche Diagnostics).

Immunodetection of CD68 and von Willebrand Factor. Liver sections from cirrhotic rats underwent microwave antigen retrieval to unmask antigens hidden by cross-linkage occurring during tissue fixation. Endogenous peroxidase activity was blocked by hydrogen peroxide pretreatment for 10 min and with 5% goat serum for 45 min. The sections were then stained with mouse anti-CD68 (1:150; AbD Serotec, Oxford, UK) or with rabbit anti-vWF (1:500; Dako Denmark A/S, Glostrup, Denmark) and incubated for 1 h at room temperature or overnight at 4°C, respectively. The LSAB 2 System-HRP (Dako Denmark A/S) was used for antigen detection, and antigen visualization was achieved with streptavidin peroxidase and counterstained with hematoxylin.

Measurements and Statistical Analysis. Serum osmolality was determined from osmometric depression of the freezing point (Osmometer 3300; Advanced Instruments, Needham Heights, MA) and Na^+ and K^+ concentrations by flame photometry (IL 943; Instrumentation Laboratory, Lexington, MA). Serum albumin, aspartate aminotransferase (AST), alanine transaminase (ALT), and lactate dehydrogenase were measured with the ADVIA 2400 Instrument (Siemens Healthcare Diagnostics, Tarrytown, NY). Quantitative data were analyzed using GraphPad Prism 5 (GraphPad Software, Inc., San Diego, CA), and statistical analysis of the results was performed by one-way analysis of variance (ANOVA) with the Newman-Keuls post hoc test and the Kruskal-Wallis test with the Dunn post hoc test when appropriate. Data are expressed as means ± S.E.M. and were considered significant at $p < 0.05$.

Results

Liver Function Tests, Mean Arterial Pressure, and Portal Pressure in Treated and Nontreated Fibrotic Rats. Table 1 shows the biochemical tests of liver function, serum electrolytes, and systemic hemodynamics in fibrotic rats. As anticipated, in both experimental groups, fibrotic animals receiving vehicle showed the characteristic alterations of liver function tests, arterial hypotension, and significant portal hypertension. Chronic administration of the CB2 receptor agonist resulted in an approximately 50% reduction of ALT and AST levels in serum. No any other significant effects were observed in the biochemical parameters measured between vehicle-treated rats and rats receiving either the CB2 receptor agonist or the APJ antagonist. Of note,

JPET PHARMACOLOGY AND EXPERIMENTAL THERAPEUTICS aspet

TABLE 1

Body weight, standard liver function, serum electrolytes, and systemic hemodynamics in fibrotic rats receiving vehicle or treated with the CB2 agonist AM1241 or the APJ antagonist F13A

Results are given as means ± S.E.

Parameter	Control (n = 10)	CCl_4-Treated Rats			
		CB2 Stimulation		APJ Blockade	
		Vehicle (n = 10)	AM1241 (n = 10)	Vehicle (n = 10)	F13A (n = 7)
Body weight, g	399 ± 8	415 ± 7	403 ± 12	379 ± 10	380 ± 7
AST, U/l	117 ± 23	582 ± 58†††	295 ± 46***	373 ± 72††	431 ± 113
ALT, U/l	12.8 ± 1	326 ± 29†††	199 ± 60*	276 ± 89††	282 ± 46
Lactate dehydrogenase, U/l	1093 ± 106	1127 ± 94	1176 ± 344	1016 ± 178	1851 ± 619
Albumin, g/l	36.1 ± 0.5	29.3 ± 1.5†††	30.5 ± 0.7	29.2 ± 0.96†††	30.1 ± 0.8
Serum Na^+, mEq/l	142 ± 1.6	141 ± 1	142 ± 1	142 ± 1	143 ± 1
Serum K^+, mEq/l	5.1 ± 0.2	4.9 ± 0.2	4.9 ± 0.1	4.7 ± 0.2	5.0 ± 0.2
Serum osmolality, mOsmol/kg	292 ± 6	296 ± 1	296 ± 2	303 ± 3	302 ± 3
MAP, mm Hg	121 ± 1	111 ± 3††	126 ± 2**	110 ± 3††	124 ± 2**
PP, mm Hg	5.6 ± 0.2	10.2 ± 0.4†††	7.6 ± 0.8**	11.3 ± 0.6†††	7.5 ± 0.6***
SPP, mm Hg	117 ± 2	99 ± 3†††	117 ± 4***	100 ± 4†††	116 ± 2*
Heart rate, beats/min	395 ± 15	399 ± 13	424 ± 8	410 ± 12	421 ± 8

* $p < 0.05$, compared with vehicle-treated rats (one-way ANOVA with the Newman-Keuls post hoc test and the Kruskal-Wallis test with the Dunn post hoc test when appropriate).
** $p < 0.01$.
*** $p < 0.001$.
† $p < 0.001$, compared with control rats.
†† $p < 0.01$.
††† $P < 0.001$.

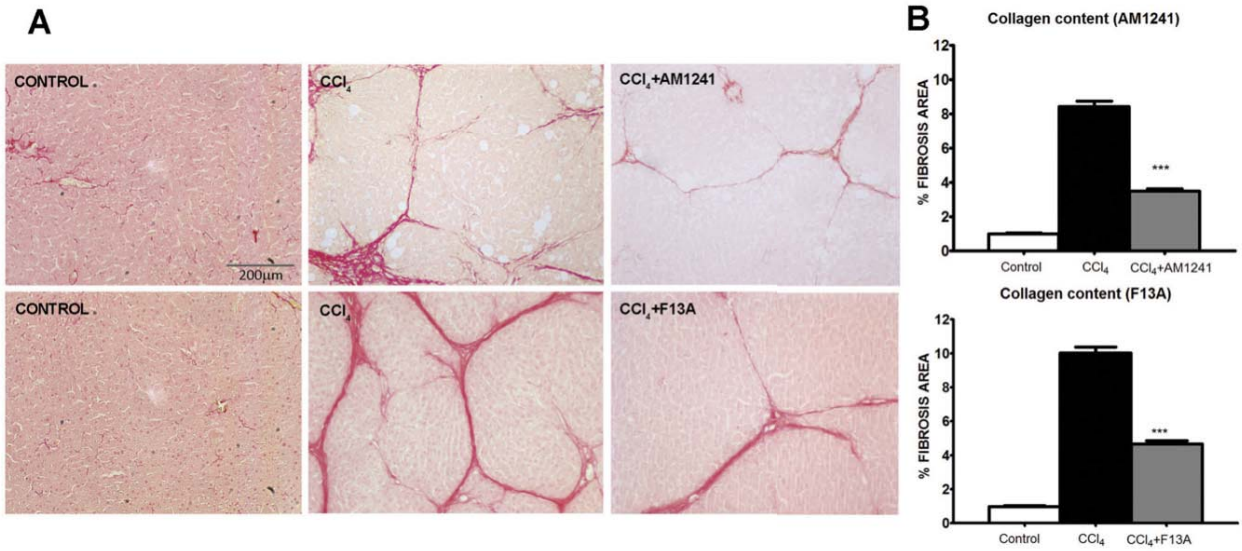

Fig. 1. A, effect of CB2 receptor activation (AM1241) and APJ blockade (F13A) on liver fibrosis. Sirius red staining of representative liver sections obtained from control rats, rats treated with vehicle, and rats receiving AM1241 (1 mg/kg per day b.wt.) or F13A (75 µg/kg per day b.wt.). Original magnification, 100×. Quantification of relative fibrosis area was assessed in 32 fields/animal. B, bars on the right show the quantitative measurement of relative fibrosis in all the animals. Results are given as means ± S.E. ***, $p < 0.001$.

however, long-term administration of AM1241 and F13A was associated with a significant amelioration in hemodynamic function as reflected by higher MAP and SPP and lower PP in fibrotic treated rats than in fibrotic rats receiving vehicle.

Effect of CB2 Receptor Activation and APJ Blockade on Liver Fibrosis in Fibrotic Rats. Sirius red, a dye that selectively binds collagen proteins, was used to stain the collagen fibrils in the liver of CCl_4-treated rats (Jiménez et al., 1985). As shown in Fig. 1, both groups of rats had remarkable fibrosis showing initial stages of the characteristic pattern of perivenular and periportal deposition of connecting tissue with development of thin portal-to-portal septa and slight evidence of architectural distortion resulting in micronodular fibrosis. However, biopsy samples obtained from fibrotic rats receiving AM1241 and from fibrotic rats receiving F13A displayed thinner septa and more preserved hepatic parenchyma than those from nontreated fibrotic animals. This result was confirmed by the morphometric analysis of all Sirius red-stained sections in which both hepatic samples of rats collected after CB2 receptor stimulation and liver biopsy samples obtained after APJ blockade showed a significant reduction in the percentage of fibrosis area compared with that in sections of the corresponding vehicle-treated fibrotic rats (Fig. 1).

Effects of CB2 Receptor Activation and APJ Blockade on Infiltrating Cells, Vessel Density, Apoptosis, and Activated Caspase-3 Expression. To assess the density of infiltrating macrophages/monocytes in the liver tissue of both vehicle and treated rats, CD68-positive cells were quantified in the parenchymal area and the periportal area. The amount of in-

JPET PHARMACOLOGY AND EXPERIMENTAL THERAPEUTICS aspet

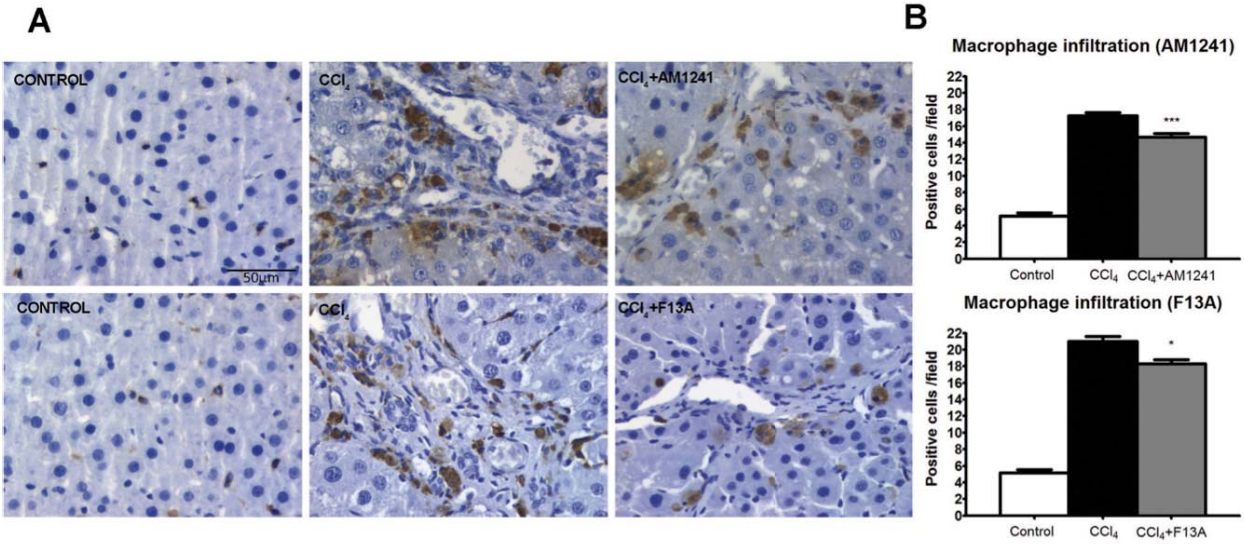

Fig. 2. A, effect of CB2 receptor activation (AM1241) and APJ blockade (F13A) on infiltrating cells. CD68 staining of representative liver sections obtained from control rats, rats treated with vehicle, and rats receiving AM1241 (1 mg/kg per day b.wt.) or F13A (75 μg/kg per day b.wt.). Positive cells were determined by counting the number of CD68-positive stained cells in 20 independent fields/animal. Original magnification, 400×. B, bars on the right show the quantitative measurement of infiltrating cells in all the animals. Results are given as means ± S.E. *, $p < 0.05$; ***, $p < 0.001$.

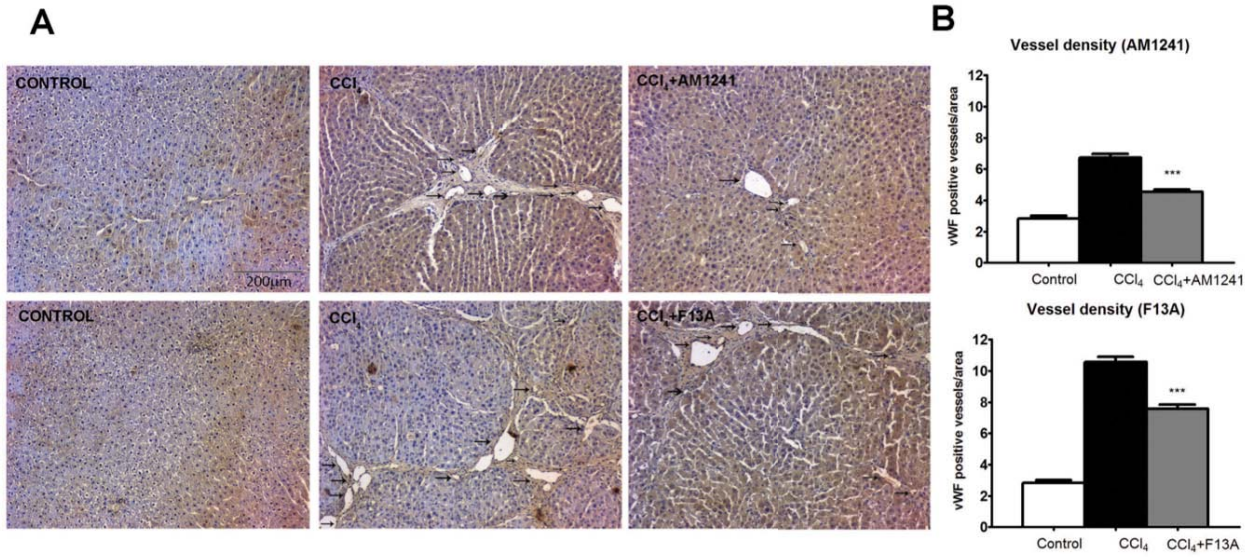

Fig. 3. A, effect of CB2 receptor activation (AM1241) and APJ blockade (F13A) on vessel density. Immunolocalization of vWF was used to quantify vessel density in liver sections obtained from control rats, rats receiving vehicle, or rats treated with either AM1241 (1 mg/kg per day b.wt.) or F13A (75 μg/kg per day b.wt.). Positive staining was determined counting vWF-positive stained vessels in 20 independent fields/animal. Original magnification, 100×. B, bars on the right show the quantitative measurement of vessel density in all animals. Results are given as means ± S.E. ***, $p < 0.001$.

filtrated cells was significantly higher in CCl_4-treated rats compared with that in controls. Chronic treatment with the CB2 receptor agonist or the APJ antagonist significantly decreased the number of CD68-positive cells in the liver of fibrotic rats (Fig. 2). Next, to evaluate whether AM1241 or F13A treatment may exert an antiangiogenic effect, anti-vWF antibody was used to quantify the number of vessels. There was a significant decrease in the amount of blood vessels in both AM1241- and F13A-treated animals compared with that for vehicle (Fig. 3). To explore whether antifibrogenic treatments may modify apoptosis, we performed in situ detection of nuclear DNA fragmentation by the TUNEL assay in liver sections of treated and nontreated fibrotic rats. As a positive control of the TUNEL assay, apoptosis was induced by incubation of liver sections with DNase I. No staining was observed in the negative control in which the terminal deoxynucleotidyl transferase enzyme was omitted (data not shown). Liver sections from fibrotic rats showed positive TUNEL staining cells with immunoreactivity localized to the margin of the fibrous septa and parenchyma (Fig. 4). However, the number of positive cells for TUNEL staining significantly decreased in hepatic sections of animals treated with AM1241 and F13A compared with the vehicle group (6 ± 1 versus 3 ± 0 positive cells/field, $p < 0.001$ and 5 ± 0 versus 3 ± 1 positive cells/field, $p < 0.001$, respectively). Finally, we measured the amount of active caspase-3 in livers of control, vehicle-treated, AM1241-treated, or F13A-treated animals. As shown in Fig. 4, the amount of activated caspase-3 was significantly higher in fibrotic rats than in controls. Of interest,

JPET PHARMACOLOGY AND EXPERIMENTAL THERAPEUTICS aspet

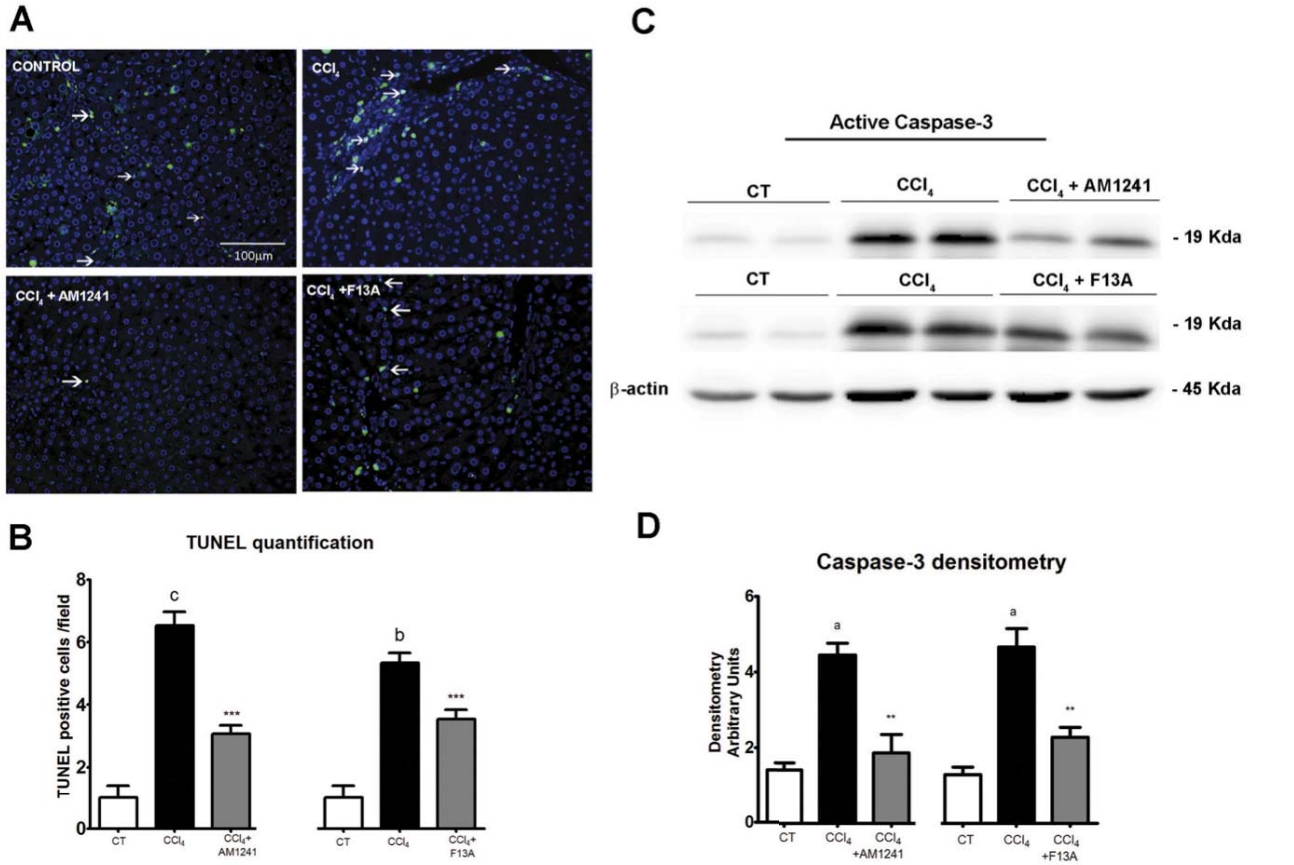

Fig. 4. Effect of CB2 receptor activation and APJ blockade on apoptosis. A, representative TUNEL assay in hepatic tissue of control rats and fibrotic rats receiving vehicle (CCl_4) or treated with the CB2 receptor agonist (CCl_4 + AM1241) or the APJ antagonist (CCl_4 + F13A). The number of positive cells was determined by counting the number of positively stained cells in eight independent fields per animal (original magnification, 200×). B, bars at the bottom show the quantitative measurement of TUNEL-positive cells in all animals. C, Western blot for activated caspase-3 on liver tissue of control rats (CT), fibrotic rats receiving vehicle (CCl_4), and fibrotic rats treated with either AM1241 (CCl_4 + AM1241, 1 mg/kg per day b.wt.) or F13A (CCl_4 + F13A, 75 μg/kg per day b.wt.) for 5 weeks. Eighty micrograms of protein was loaded per lane. D, bars at the bottom show the densitometric analysis of all the samples normalized to β-actin. Results are given as means ± S.E. a, $p < 0.05$; b, $p < 0.01$; c, $p < 0.001$ versus control; **, $p < 0.01$; ***, $p < 0.001$ versus CCl_4.

both CB2 receptor stimulation and APJ blockade significantly reduced activated caspase-3 expression in the hepatic tissue of fibrotic rats. These findings indicate that chronic in vivo CB2 stimulation or APJ blockade prevents proangiogenic and apoptotic phenomena in the liver of CCl_4-induced fibrotic rats.

TABLE 2

Gene expression of PDGFRβ, TGFβR1, Col1α2, α-SMA, MMP2, MMP9, TIMP1, and TIMP2, measured in the hepatic tissue of reference control rats and in fibrotic rats receiving vehicle or treated with the CB2 agonist AM1241 or the APJ antagonist F13A

Results are given as means ± S.E.

Genes (*fold change*)	Control (n = 10)	CCl_4-Treated Rats			
		CB2 Stimulation		APJ Blockade	
		Vehicle (n = 10)	AM1241 (n = 10)	Vehicle (n = 10)	F13A (n = 7)
PDGFRβ	1.02 ± 0.11	3.74 ± 0.81†	1.22 ± 0.27**	4.87 ± 0.92†††	2.36 ± 0.37*
TGFβR1	1.08 ± 0.21	1.46 ± 0.40	0.64 ± 0.06	2.05 ± 0.15*†	1.81 ± 0.35
Col1α2	1.04 ± 0.12	9.40 ± 1.31††	7.42 ± 1.61	9.80 ± 1.95†††	6.23 ± 1.39
α-SMA	1.10 ± 0.02	9.19 ± 1.70††	3.57 ± 0.89**	6.39 ± 0.48†	2.27 ± 1.30*
MMP2	0.97 ± 0.08	8.13 ± 1.39††	4.35 ± 0.82*	9.49 ± 1.23††	5.56 ± 0.73*
MMP9	1.04 ± 0.07	20.05 ± 4.12††	23.5 ± 5.42	14.46 ± 3.88††	14.32 ± 1.18
TIMP1	1.05 ± 0.18	12.42 ± 1.90††	6.28 ± 1.10**	8.97 ± 1.39†††	3.43 ± 0.56**
TIMP2	1.02 ± 0.08	3.11 ± 0.35†††	1.89 ± 0.15**	3.56 ± 0.53††	2.42 ± 0.36

* $p < 0.05$, compared with vehicle-treated rats (one-way ANOVA with the Newman-Keuls post hoc test and the Kruskal-Wallis test with the Dunn post hoc test when appropriate).
** $p < 0.01$.
*** $p < 0.001$.
† $p < 0.05$, compared with control rats.
†† $p < 0.01$.
††† $p < 0.05$.

JPET PHARMACOLOGY AND EXPERIMENTAL THERAPEUTICS aspet

Effect of CB2 Receptor Activation and APJ Blockade on mRNA of Hepatic Profibrogenic Genes and Protein Expression of PDGFRβ and TIMP1. For further insight into the effect of AM1241 and F13A in fibrotic rats, we measured hepatic mRNA expression of a panel of selected genes involved in cytokine signaling (TGFβR1 and PDGFRβ), collagen synthesis (Col1α2), stellate cell activation (α-SMA), and extracellular matrix (ECM) turnover (MMP2, MMP9, TIMP1, and TIMP2) (Table 2). After 13 weeks of CCl_4 treatment, all the genes analyzed were up-regulated in fibrotic rats compared with control animals. TGFβR1 was the least, albeit significantly, activated transcript (approximately a 2-fold increase), whereas the most intensely up-regulated messengers were those related to ECM turnover, such as MMP9 and TIMP1. The antifibrogenic properties displayed by AM1241 and F13A were paralleled by a decrease in mRNA expression in these genes. In fact, both the CB2 agonist and the APJ antagonist inhibited PDGFRβ expression and significantly reduced the degree of activation of HSCs as shown by the decrease in the mRNA expression of α-SMA. However, the most interesting finding was that both treatments significantly altered the expression balance of the transcripts involved in ECM turnover, thus favoring ECM degradation. In fact, although neither AM1241 nor F13A treatment modified MMP9 expression, both compounds induced a significant reduction in TIMP abundance, which, in turn, resulted in a marked increase in the MMP/TIMP gene expression ratio (Table 3).

TABLE 3

MMP/TIMP ratios calculated from the mRNA expression of MMP2, MMP9, TIMP1, and TIMP2 in liver tissue of fibrotic rats receiving vehicle or treated with the CB2 agonist AM1241 or the APJ antagonist F13A

Results are given as means ± S.E.

Gene Ratio	CCl_4-Treated Rats			
	CB2 Stimulation		APJ Blockade	
	Vehicle	AM1241	Vehicle	F13A
MMP2/TIMP1	0.91 ± 0.24	0.88 ± 0.21	1.43 ± 0.27	1.56 ± 0.12
MMP2/TIMP2	2.66 ± 0.48	2.18 ± 0.27	2.80 ± 0.26	2.09 ± 0.13
MMP9/TIMP1	1.79 ± 0.40	4.56 ± 0.96*	2.13 ± 0.54	4.91 ± 1.0*
MMP9/TIMP2	6.75 ± 1.36	15.7 ± 3.47*	4.39 ± 1.04	9.14 ± 3.35

* $p < 0.05$; unpaired Student's t test.

Because inhibition of mRNA expression of PDGFRβ and TIMP1 appeared to be major contributory factors to the antifibrotic properties of both AM1241 and F13A treatments, we next assessed whether CB2 receptor stimulation or APJ blockade was also associated with lower hepatic abundance of PDGFRβ and TIMP1 proteins. As shown in Fig. 5, PDGFRβ and TIMP1 expression were significantly reduced in fibrotic rats treated with AM1241 or F13A compared with fibrotic animals treated with vehicle.

Discussion

The results of this investigation indicate that chronic administration of either AM1241 or F13A reduces hepatic collagen deposition in rats under a non-discontinued fibrosis induction program. These findings indicate that long-term CB2 receptor stimulation or signaling disruption of the hepatic apelin system prevents fibrosis progression in CCl_4-

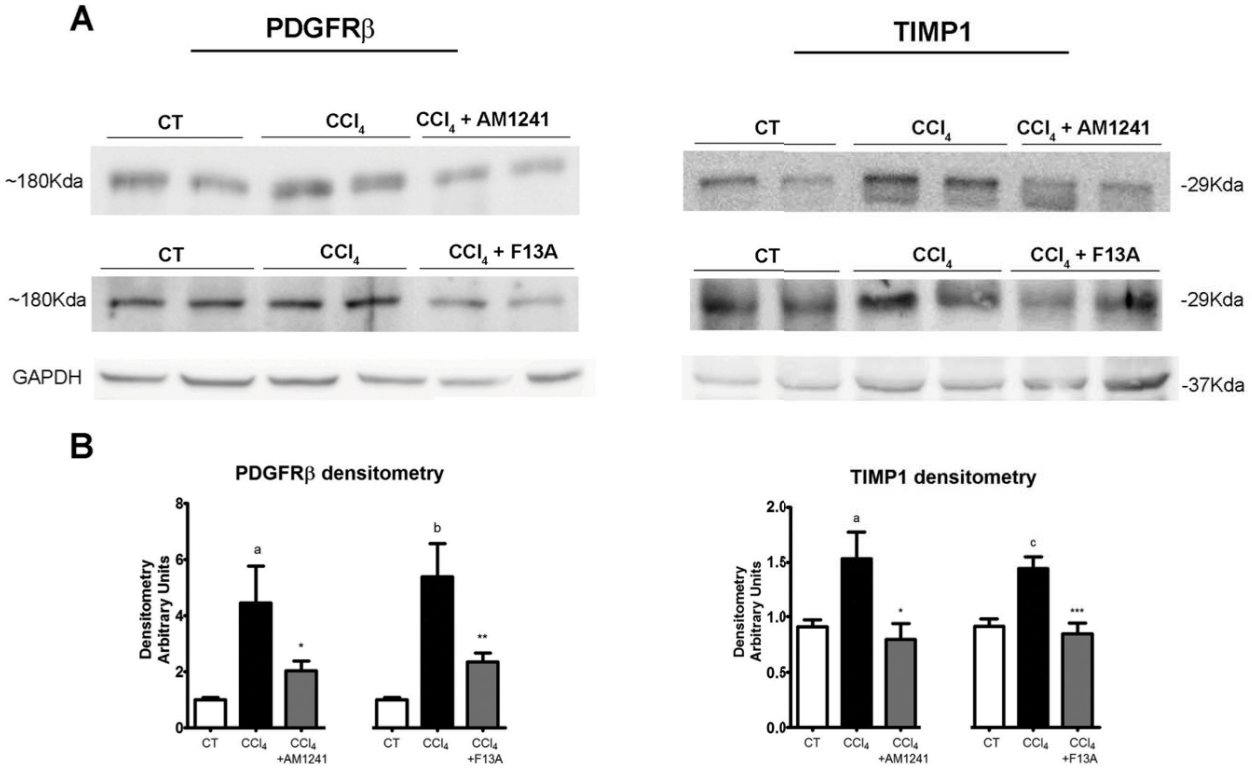

Fig. 5. A, effect of CB2 receptor activation and APJ blockade on protein expression of PDGFRβ and TIMP1. Representative Western blot for PDGFRβ and TIMP1 in liver tissue of control rats (CT), fibrotic rats receiving vehicle (CCl_4), and fibrotic rats treated with either AM1241 (CCl_4 + AM1241, 1 mg/kg per day b.wt.) or F13A (CCl_4 + F13A, 75 μg/kg per day b.wt.) for 5 weeks. Eighty micrograms of protein was loaded per lane. B, bars at the bottom show the densitometric analysis of all the samples normalized to GAPDH. Results are given as means ± S.E. a, $p < 0.05$; b, $p < 0.01$; c, $p < 0.001$ versus control; *, $p < 0.05$; **, $p < 0.01$; ***, $p < 0.001$ versus CCl_4.

JPET PHARMACOLOGY AND EXPERIMENTAL THERAPEUTICS aspet

treated rats. Our results also indicate that the molecular mechanisms ultimately underlying these phenomena are coincident despite the marked dissimilarities between the CB2 and APJ signaling pathways, thus opening new avenues for preventing fibrosis progression in liver diseases.

In fact, the chronic administration of either AM1241 or F13A to rats under a CCl_4-induced fibrosis/cirrhosis protocol resulted in significantly decreased hepatic collagen deposition, which was associated with a significant amelioration in systemic and portal hemodynamics, reduced angiogenesis, inflammatory infiltrate, and apoptosis compared with that in rats under the same fibrosis induction protocol but treated with vehicle. Moreover, animals receiving the CB2 agonist also showed signs of attenuated liver inflammation as indicated by decreased serum AST and ALT enzymes. All these changes were framed by reduced expression of messengers related to PDGF signaling, HSC activation, and ECM turnover.

Our group and others have previously described the antifibrogenic properties of CB2 receptor stimulation in experimental models of advanced liver disease (Julien et al., 2005; Liu et al., 2008; Muñoz-Luque et al., 2008). Whereas the experimental design of these studies focused on fibrosis regression, here we assessed whether CB2 agonism is able to prevent fibrosis progression even under conditions of maintaining the hepatic injury. We administered the CB2 receptor agonist AM1241 to rats under a fibrosis induction protocol. AM1241 is among the most selective receptor agonists currently available. For CB2 and CB1 receptors, the binding affinity (K_i) is 3.4 and 239.4 nM, respectively, and previous experiments have provided pharmacological and biochemical evidence that AM1241 selectively activates the CB2 receptor in vivo in mice, rats, and human cell lines (Malan et al., 2001; Ibrahim et al., 2003; Yao et al., 2006). The absence of central effects induced by CB2 agonism has been the major rationale to propose this mechanism as an antifibrogenic therapy. However, previous studies showed that pharmacological activation of the CB2 receptor signaling pathway may also induce inflammation in adipose tissue but not in the liver (Deveaux et al., 2009). In agreement with these findings, treatment with the CB2 agonist, in addition to stopping fibrosis progression and angiogenesis, was also associated with decreased serum levels of AST and ALT and reduced inflammatory infiltrate. An interesting finding of this study was that in contrast to what we had previously found in cirrhotic rats (Muñoz-Luque et al., 2008), administration of AM1241 inhibited apoptosis in fibrotic animals. Although we do not have any experimental data to explain this phenomenon, we believe that it is probably related to the different degrees of active fibrogenesis between the two groups of CCl_4-treated animals. In fact, in the former study, the rats had fully established cirrhosis and the active fibrogenesis was much lower than that in the animals of the current investigation that were within the initial phases of fibrosis development (Gressner et al., 2007; Iredale, 2007). There are a number of potential mechanisms mediating the effects of CB2 receptor stimulation on hepatic fibrosis. They are probably related to the strong abundance of these receptors in nonparenchymal and biliary cells located within and at the edges of fibrotic septa that directly mediate growth arrest and antifibrotic and proapoptotic actions in hepatic cells (Julien et al., 2005; Liu et al., 2008). Whatever the case, however, our results indicate that selective pharmacological activation of the CB2 receptor is effective in preventing fibrosis progression in experimental liver disease.

There is much experimental evidence indicating that the hepatic apelin system is an important mediator of the initiation and maintenance of the inflammatory and fibrogenic processes occurring in the cirrhotic liver (Principe et al., 2008; Melgar-Lesmes et al., 2010, 2011). In fact, AP is selectively expressed in HSCs of humans and rats with cirrhosis and markedly stimulates PDGFRβ, collagen type 1 (Col1), and cell viability in LX-2 cells, a human cell line of activated stellate cells. In contrast, APJ blockade significantly regressed hepatic fibrosis and angiogenesis in cirrhotic animals and prevented the induction of PDGFRβ and Col1 expression induced by profibrogenic agents in LX-2 cells. In the current investigation, we chemically disrupted APJ signaling using F13A. This is an analog of apelin-13 in which the phenylalanine at the C terminus of the peptide is substituted by an alanine residue that behaves as an AP-specific antagonist (Melgar-Lesmes et al., 2010). Interaction of this competitive antagonist with APJ fully abolishes the biological activity of AP (Lee et al., 2005).

Acquisition of a proliferative, proinflammatory, and contractile phenotype by quiescent stellate cells is the most characteristic response of activated HSCs to chronic liver injury. Our experiments indicate that the APJ antagonist exerts its antifibrogenic effect by acting on different steps of this process. Chronic administration of F13A strongly reduced α-SMA, a well accepted marker of hepatic myofibroblasts, suggesting that APJ antagonism in vivo represses the activation of HSCs in CCl_4-treated rats.

The current investigation indicates that in addition to favoring cell viability, CB2 stimulation or APJ blockade also interferes with the production of profibrogenic mediators produced during chronic liver injury and the concomitant tissue repair. In this regard, the inhibitory effect on PDGF signaling shared by both AM1241 and F13A is noteworthy, considering that PDGF is the most potent proproliferative cytokine for HSCs (Pinzani et al., 1989; Friedman, 2008).

Pharmacological stimulation of the CB2 receptor or inhibition of AP activity also appears to affect the synthesis of molecules implicated in ECM remodeling. The net deposition of scar tissue depends on the balance between synthesis and degradation. The latter reflects the relative activity of MMPs and their inhibitor TIMPs, which are mainly produced by HSCs and other inflammatory cells (Iredale, 2007; Friedman, 2008). In experimental and human cirrhosis, fibrosis appears to be the result not only of excessive ECM synthesis but also of reduced degradation, which is caused by the up-regulation of TIMPs, inactivating the concurrently secreted MMPs (Iredale, 2007). According to these mechanisms, the untreated fibrotic rats in our experiments presented a marked induction of Col1α2 gene expression as well as a significant up-regulation of the MMPs. This result can be explained as a compensatory mechanism designed to eliminate the excess of scar tissue. However, the concomitant TIMP induction overwhelmed MMP activity, thereby leading to a net ECM deposition in the liver. ECM remodeling is indeed regulated by the balance between MMPs and TIMPs rather than by their absolute levels (Iredale, 2007). Therefore, several investigations have proposed that the inhibitory activity of TIMPs is the leading regulator of the remodeling process (Arthur,

JPET PHARMACOLOGY AND EXPERIMENTAL THERAPEUTICS aspet

2000; Iredale, 2007). In our study, treatment with both AM1241 and F13A was associated with a significant increase in the MMP/TIMP ratio in agreement with the inhibition of fibrosis progression. This altered balance was due to TIMP1 inhibition rather than to a further activation of MMPs and further supports the concept that TIMP activity is a major regulator of the ECM degradation pattern in the injured liver by controlling the activity of the secreted MMPs.

Tissue repair is a homeostatic response toward tissue injury, in which multiple and complex proinflammatory, proangiogenic, and profibrogenic processes are activated. In the liver, maintenance of tissue aggression results in the perpetuation of these phenomena, the wound-healing response progressively leading to advanced fibrosis and eventually cirrhosis. Breaking this vicious circle is a major challenge to stopping fibrosis in patients with liver disease. In the current investigation, we have shown that stimulation of CB2 receptors or blocking the activity of the hepatic apelin system is able to attenuate collagen deposition in CCl_4-treated rats through common mechanisms. In fact, despite the marked differences in the signaling pathways driving endocannabinoids and AP antifibrogenic effects, both inhibit PDGFRβ expression and alter MMP/TIMP balance by decreasing TIMP1 messenger and protein abundance. These results, therefore, point to PDGF signaling and TIMP1 activity as major targets for future antifibrotic therapies.

Authorship Contributions

Participated in research design: Reichenbach, Ros, Melgar-Lesmes, and Jiménez.

Conducted experiments: Reichenbach, Ros, Fernández-Varo, Casals, and Campos.

Contributed new reagents or analytic tools: Makriyannis.

Performed data analysis: Reichenbach, Ros, and Morales-Ruiz.

Wrote or contributed to the writing of the manuscript: Reichenbach, Fernández-Varo, Jiménez, Casals, and Morales-Ruiz.

References

Akhmetshina A, Dees C, Busch N, Beer J, Sarter K, Zwerina J, Zimmer A, Distler O, Schett G, and Distler JH (2009) The cannabinoid receptor CB2 exerts antifibrotic effects in experimental dermal fibrosis. *Arthritis Rheum* **60:**1129–1136.

Arthur MJ (2000) Fibrogenesis II. Metalloproteinases and their inhibitors in liver fibrosis. *Am J Physiol Gastrointest Liver Physiol* **279:**G245–G249.

Clària J and Jiménez W (1999) Renal dysfunction and ascites in carbon tetrachloride-induced cirrhosis in rats, in *The Liver and the Kidney* (Arroyo V, Schrier RW, Rodés J, and Ginès P eds) pp 379–396, Blackwell Science, Boston.

Daviaud D, Boucher J, Gesta S, Dray C, Guigne C, Quilliot D, Ayav A, Ziegler O, Carpene C, Saulnier-Blache JS, et al. (2006) TNF-α up-regulates apelin expression in human and mouse adipose tissue. *FASEB J* **20:**1528–1530.

Deveaux V, Cadoudal T, Ichigotani Y, Teixeira-Clerc F, Louvet A, Manin S, Nhieu JT, Belot MP, Zimmer A, Even P, et al. (2009) Cannabinoid CB2 receptor potentiates obesity-associated inflammation, insulin resistance and hepatic steatosis. *PLoS One* **4:**e5844.

Friedman SL (2008) Hepatic stellate cells: protean, multifunctional, and enigmatic cells of the liver. *Physiol Rev* **88:**125–172.

Friedman SL (2010) Evolving challenges in hepatic fibrosis. *Nat Rev Gastroenterol Hepatol* **7:**425–436.

Gressner OA, Weiskirchen R, and Gressner AM (2007) Evolving concepts of liver fibrogenesis provide new diagnostic and therapeutic options. *Comp Hepatol* **6:**7.

Hézode C, Zafrani ES, Roudot-Thoraval F, Costentin C, Hessami A, Bouvier-Alias M, Medkour F, Pawlostky JM, Lotersztajn S, and Mallat A (2008) Daily cannabis use: a novel risk factor of steatosis severity in patients with chronic hepatitis C. *Gastroenterology* **134:**432–439.

Horváth B, Magid L, Mukhopadhyay P, Bátkai S, Rajesh M, Park O, Tanchian G, Gao RY, Goodfellow CE, Glass M, et al. (2011) A new cannabinoid 2 receptor agonist HU-910 attenuates oxidative stress, inflammation, and cell death associated with hepatic ischemia/reperfusion injury. *Br J Pharmacol* doi:10.1111/j. 1476-5381.2011.01381.x.

Ibrahim MM, Deng H, Zvonok A, Cockayne DA, Kwan J, Mata HP, Vanderah TW, Lai J, Porreca F, Makriyannis A, et al. (2003) Activation of CB2 cannabinoid receptors by AM1241 inhibits experimental neuropathic pain: pain inhibition by receptors not present in the CNS. *Proc Natl Acad Sci USA* **100:**10529–10533.

Iredale JP (2007) Models of liver fibrosis: exploring the dynamic nature of inflammation and repair in a solid organ. *J Clin Invest* **117:**539–548.

Jeong WI, Osei-Hyiaman D, Park O, Liu J, Bátkai S, Mukhopadhyay P, Horiguchi N, Harvey-White J, Marsicano G, Lutz B, et al. (2008) Paracrine activation of hepatic CB1 receptors by stellate cell-derived endocannabinoids mediates alcoholic fatty liver. *Cell Metab* **7:**227–235.

Jimenez W, Parés A, Caballería J, Heredia D, Bruguera M, Torres M, Rojkind M, and Rodés J (1985) Measurement of fibrosis in needle liver biopsies: evaluation of a colorimetric method. *Hepatology* **5:**815–818.

Julien B, Grenard P, Teixeira-Clerc F, Van Nhieu JT, Li L, Karsak M, Zimmer A, Mallat A, and Lotersztajn S (2005) Antifibrogenic role of the cannabinoid receptor CB2 in the liver. *Gastroenterology* **128:**742–755.

Lee DK, Saldivia VR, Nguyen T, Cheng R, George SR, and O'Dowd BF (2005) Modification of the terminal residue of apelin-13 antagonizes its hypotensive action. *Endocrinology* **146:**231–236.

Liu HY, Yang Q, Duan RX, Zhang YW, and Tang WX (2008) [Effects of anandamide on the activation and proliferation of hepatic stellate cells through cannabinoid-2 receptors]. *Zhonghua Gan Zang Bing Za Zhi* **16:**430–434.

Malan TP Jr, Ibrahim MM, Deng H, Liu Q, Mata HP, Vanderah T, Porreca F, and Makriyannis A (2001) CB2 cannabinoid receptor-mediated peripheral antinociception. *Pain* **93:**239–245.

Marra F (1999) Hepatic stellate cells and the regulation of liver inflammation. *J Hepatol* **31:**1120–1130.

Masri B, Morin N, Cornu M, Knibiehler B, and Audigier Y (2004) Apelin (65–77) activates p70 S6 kinase and is mitogenic for umbilical endothelial cells. *FASEB J* **18:**1909–1911.

Melgar-Lesmes P, Casals G, Pauta M, Ros J, Reichenbach V, Bataller R, Morales-Ruiz M, and Jimenez W (2010) Apelin mediates the induction of profibrogenic genes in human hepatic stellate cells. *Endocrinology* **151:**5306–5314.

Melgar-Lesmes P, Pauta M, Reichenbach V, Casals G, Ros J, Bataller R, Morales-Ruiz M, and Jiménez W (2011) Hypoxia and proinflammatory factors upregulate apelin receptor expression in human stellate cells and hepatocytes. *Gut* **60:**1404–1411.

Morales-Ruiz M and Jiménez W (2005) Neovascularization, angiogenesis, and vascular remodelling in portal hypertension, in *Portal Hypertension: Pathobiology, Evaluation, and Treatment* (Sanyal AJ, Shah VH eds) pp 99–112, Humana Press, Totowa, NJ.

Muñoz-Luque J, Ros J, Fernández-Varo G, Tugues S, Morales-Ruiz M, Alvarez CE, Friedman SL, Arroyo V, and Jiménez W (2008) Regression of fibrosis after chronic stimulation of cannabinoid CB2 receptor in cirrhotic rats. *J Pharmacol Exp Ther* **324:**475–483.

Pacher P, Bátkai S, and Kunos G (2006) The endocannabinoid system as an emerging target of pharmacotherapy. *Pharmacol Rev* **58:**389–462.

Pinzani M, Gesualdo L, Sabbah GM, and Abboud HE (1989) Effects of platelet-derived growth factor and other polypeptide mitogens on DNA synthesis and growth of cultured rat liver fat-storing cells. *J Clin Invest* **84:**1786–1793.

Principe A, Melgar-Lesmes P, Fernández-Varo G, del Arbol LR, Ros J, Morales-Ruiz M, Bernardi M, Arroyo V, and Jiménez W (2008) The hepatic apelin system: a new therapeutic target for liver disease. *Hepatology* **48:**1193–1201.

Reichenbach V, Ros J, and Jiménez W (2010) Endogenous cannabinoids in liver disease: many darts for a single target. *Gastroenterol Hepatol* **33:**323–329.

Ros J, Fernández-Varo G, Muñoz-Luque J, Arroyo V, Rodés J, Gunnet JW, Demarest KT, and Jiménez W (2005) Sustained aquaretic effect of the V2-AVP receptor antagonist, RWJ-351647, in cirrhotic rats with ascites and water retention. *Br J Pharmacol* **146:**654–661.

Tam J, Liu J, Mukhopadhyay B, Cinar R, Godlewski G, and Kunos G (2011) Endocannabinoids in liver disease. *Hepatology* **53:**346–355.

Teixeira-Clerc F, Julien B, Grenard P, Tran Van Nhieu J, Deveaux V, Li L, Serriere-Lanneau V, Ledent C, Mallat A, and Lotersztajn S (2006) CB1 cannabinoid receptor antagonism: a new strategy for the treatment of liver fibrosis. *Nat Med* **12:**671–676.

Tugues S, Fernandez-Varo G, Muñoz-Luque J, Ros J, Arroyo V, Rodés J, Friedman SL, Carmeliet P, Jiménez W, and Morales-Ruiz M (2007) Antiangiogenic treatment with sunitinib ameliorates inflammatory infiltrate, fibrosis, and portal pressure in cirrhotic rats. *Hepatology* **46:**1919–1926.

Yao BB, Mukherjee S, Fan Y, Garrison TR, Daza AV, Grayson GK, Hooker BA, Dart MJ, Sullivan JP, and Meyer MD (2006) *In vitro* pharmacological characterization of AM1241: a protean agonist at the cannabinoid CB2 receptor? *Br J Pharmacol* **149:**145–154.

Address correspondence to: Dr. Wladimiro Jiménez, Servicio de Bioquímica y Genética Molecular, Hospital Clínic Universitari, Villarroel 170, Barcelona 08036, Spain. E-mail: wjimenez@clinic.ub.es

3rd Article: Adenoviral dominant negative soluble sPDGFRβ improves hepatic collagen, systemic hemodynamics and portal pressure in fibrotic rats.

This third study has two main parts. First, we studied the relationship between the activation of PDGFRβ, the hemodynamic dysfunction (MAP and PP) and the progression of fibrosis in a group of CCl_4-treated rats for different periods of time that developed variable degrees of fibrosis. Second, we investigated the effect of the impairment of PDGF system signaling by the in vivo administration of an adenovirus encoding for a soluble form of PDGFRβ.

1. Hepatic collagen accumulation is progressive during the evolution of the liver disease

CCl_4-treated animals were classified into two different groups according to the histological analysis of fibrosis represented by the % of fibrosis area compared to total area of the biopsy. An additional control group was also added (<1% of fibrosis area), the second group included fibrotic animals (1- 10% of fibrotic area) and the third group comprised cirrhotic animals some with ascites formation (>10% of fibrotic area). The collagen content increased in parallel with the worsening of fibrosis, reaching maximum values in cirrhotic animals. Figure 1A shows representative images of each group. While the control animals had no alterations in the liver parenchyma, the fibrotic animals showed initial formation of thin fibrotic septa, and cirrhotic rats presented tick fibrotic septa and well formed regenerative nodules.

2. Hemodynamic deterioration and mRNA expression of PDGFRβ directly correlate with the hepatic collagen content

Progressive hepatic architecture disruption was associated with the worsening of systemic and portal hemodynamics. Cirrhotic rats had a significant lower MAP and increased PP compared to fibrotic and control rats. Moreover, both parameters correlated with the hepatic collagen content (Figure 1B). On the other hand, PDGFRβ mRNA expression was also assessed in the three experimental groups. As expected, PDGFRβ mRNA expression increased progressively and was also significantly correlated with the collagen accumulated in the hepatic tissue.

3. *In vitro* adenoviral transduction in HepG2 cells and circulating sPDGFRβ in fibrotic rats after adenoviral transduction

HepG2 cells (a human hepatocyte cell line) were transduced with the adenoviral construct encoding for both sPDGFRβ and β-gal (used as a viral transduction control). Protein expression analysis showed that the extracellular domain (ECD) of PDGFRβ was present in the supernatant of those cells transduced with Ad-sPDGFRβ, but not in the cells transduced with Ad-β-gal or saline (Figure 2A). *In vivo* experiments were also carried out in CCl_4-treated fibrotic rats transduced with Ad-PDGFRβ, Ad-β-gal or saline as vehicle. Seven days after the transduction, the ECD of PDGFRβ was detected in the serum of fibrotic and control rats transduced with the adenovirus encoding for sPDGFRβ, but not in rats transduced with Ad-β-gal (Figure 2B).

4. Body weight, standard liver and renal function tests results in fibrotic rats after adenoviral transduction

Table 1 shows the results of the serum analysis of liver and renal function parameters. Fibrosis produced by the hepatotoxicity of CCl_4, induced an increase of AST and LDH, as well as an increase of serum creatinine. However, no significant changes were found in transduced rats with Ad-sPDGFRβ or β-gal.

5. Adenoviral expression of sPDGFRβ improves systemic and portal hemodynamics in fibrotic rats

As anticipated, rats treated with either saline or Ad-β-gal presented arterial hypotension, decreased peripheral resistance and portal hypertension. In contrast, the transduction of the adenovirus encoding for Ad-PDGFRβ was associated with a marked improvement of hemodynamic parameters, as reflected by the increase of MAP and decrease of PP. In addition, sPDGFRβ administration also improved total peripheral resistances (TPR) and splanchnic perfusion pressure (SPP) (Table 2).

6. Adenoviral expression of sPDGFRβ inhibits PDGFRβ signaling and α-SMA protein expression in the liver of fibrotic rats

In order to ascertain whether the transduction of the adenovirus was effective in inhibiting the PDGFRβ signaling pathway, protein expression of total ERK 1/2 and p-ERK 1/2 was assessed. Figure 3 shows a representative western blot of saline, β-gal, and PDGFRβ experimental groups. Animals that received the Ad-PDGFRβ adenovirus presented a decrease of hepatic phosphorylation of ERK 1/2 compared with β-gal or saline groups. Next, to assess if sPDGFRβ transduction had any effect on cell activation, protein expression of α-SMA was also measured. Indeed, there was a decrease of α-SMA, suggesting that the adenovirus encoding for sPDGFRβ was able to block PDGF downstream signaling, as well as reduce HSC activation.

7. Decreased hepatic collagen accumulation induced by sPDGFRβ expression in fibrotic rats

All results up to this point showed that the transduction of the adenovirus encoding for sPDGFRβ have beneficial effects regarding systemic and portal hemodynamics and cell proliferation. The benefits of this treatment were also reflected in the degree of collagen content in the hepatic tissue. Figure 4 shows a representative image of Sirius red stained liver sections of animals administered with saline, β-gal and sPDGFRβ-treated rats.

Research Article

EASL EUROPEAN ASSOCIATION FOR THE STUDY OF THE LIVER | JOURNAL OF HEPATOLOGY

Adenoviral dominant-negative soluble PDGFRβ improves hepatic collagen, systemic hemodynamics, and portal pressure in fibrotic rats

V. Reichenbach[1], G. Fernández-Varo[1,3,*], G. Casals[1], D. Oró[1], J. Ros[1], P. Melgar-Lesmes[1], R. Weiskirchen[2], M. Morales-Ruiz[1], W. Jiménez[1,3]

[1]*Biochemistry and Molecular Genetics Service, Hospital Clínic Provincial de Barcelona, IDIBAPS, Centro de Investigación Biomédica en Red de Enfermedades Hepáticas y Digestivas (CIBERehd), University of Barcelona, Barcelona, Spain;* [2]*Institute of Clinical Chemistry and Pathobiochemistry, RWTH-University Hospital, Aachen, Germany;* [3]*Department of Physiological Sciences I, University of Barcelona, Barcelona, Spain*

Background & Aims: Platelet-derived growth factor (PDGF) is the most potent stimulus for proliferation and migration of stellate cells. PDGF receptor β (PDGFRβ) expression is an important phenotypic change in myofibroblastic cells that mediates proliferation and chemotaxis. Here we analyzed the relationship between PDGFRβ expression, hemodynamic deterioration, and fibrosis in CCl_4-treated rats. Thereafter, we investigated the effects produced by an adenovirus encoding a dominant-negative soluble PDGFRβ (sPDGFRβ) on hemodynamic parameters, PDGFRβ signaling pathway, and fibrosis.

Methods: Mean arterial pressure, portal pressure, *PDGFRβ* mRNA expression, and hepatic collagen were assessed in 6 controls and 21 rats induced to hepatic fibrosis/cirrhosis. Next, 30 fibrotic rats were randomized into three groups receiving iv saline and an adenovirus encoding for sPDGFRβ or β-galactosidase. After 7 days, mean arterial pressure, portal pressure, serum sPDGFRβ, and hepatic collagen were measured.

Results: CCl_4-treated animals for 18 weeks showed a significantly higher increase in *PDGFRβ* mRNA compared to those treated for 13 weeks and control rats. In CCl_4-treated rats, the fibrous tissue area ranged from moderate to severe fibrosis. A direct relationship between the degree of fibrosis, hemodynamic changes, and PDGFRβ expression was observed. Fibrotic rats transduced with the adenovirus encoding sPDGFRβ showed increased mean arterial pressure, decreased portal pressure, lower activation of the PDGFRβ signaling pathway, and reduced hepatic collagen than fibrotic rats receiving β-galactosidase or saline.

Conclusions: PDGFRβ activation closely correlates with hemodynamic disorders and increased fibrosis in CCl_4-treated rats. Adenoviral dominant negative soluble PDGFRβ improved fibrosis. As a result, the hemodynamic abnormalities were ameliorated.

Introduction

Liver fibrosis occurs as a result of an accumulation of connective tissue in the liver due to an imbalance between production and degradation of extracellular matrix proteins. After liver damage, hepatic stellate cells (HSC) are activated and transdifferentiate into myofibroblast-like cells acquiring contractile, proliferative, and fibrogenic properties [1]. Under this scenario, increased cytokine response occurs through multiple mechanisms, including increased expression of membrane receptors and increased signaling. In this regard, tyrosine kinase receptors are widely overexpressed in liver damage and mediate many of the responses of stellate cells to cytokines [2]. Platelet-derived growth factor (PDGF) is a family of dimeric isoforms that target a broad spectrum of mesoderm-derived cells, such as fibroblasts, pericytes, smooth muscle cells, glial cells or mesangial cells [3]. PDGF is the most potent stimulus for proliferation and migration of HSC [4,5]. The PDGF isoforms bind to two distinct receptor tyrosine kinases. PDGFRα is constitutively expressed in quiescent HSCs, while PDGFRβ is acquired in cells undergoing myofibroblastic phenotypic changes. Both the PDGF ligand and its receptor type β are rapidly induced *in vivo* and in culture [6,7]. Binding of the ligand leads to autophosphorylation of the receptors on tyrosine residues and this event induces activation of several signaling molecules [8]. Downstream consequences of PDGF signaling in stellate cells include signaling by PI3 kinase, ERK, and other pathways [9–11]. Previous publications had described a significant overexpression of PDGFRβ mRNA and protein in an experimental bile duct-ligated (BDL) rat model

Keywords: Hepatic collagen; Systemic hemodynamics; Portal pressure; PDGFRβ; Ad-*sPDGFRβ* adenoviruses; Signaling pathway blockade.
Received 29 May 2012; received in revised form 4 July 2012; accepted 8 July 2012; available online 20 July 2012

* Corresponding author. Address: Centro de Investigación Biomédica en Red, de Enfermedades Hepáticas y Digestivas (CIBERehd), IDIBAPS, edificio Centre Esther Koplowitz, Rosselló 149-153, Barcelona 08036, Spain. Tel.: +34 93 2275400x4539; fax: +34 93 2275697.
E-mail address: guillermo.fernandez@ciberehd.org (G. Fernández-Varo).

Abbreviations: HSC, hepatic stellate cells; PDGF, platelet-derived growth factor; PDGFRβ, PDGF receptor β; BDL, bile duct-ligated; CCl_4, carbon tetrachloride; MAP, mean arterial pressure; PP, portal pressure; HR, heart rate; β-gal, β-galactosidase; pfu, plaque-forming units; sPDGFRβ, dominant-negative soluble PDGFRβ; CO, cardiac output; HEK, human embryonic kidney; ECD, extracellular domain; m.o.i., multiplicity of infection; HRP, horseradish peroxidase-conjugated; ALT, alanine transaminase; AST, aspartate transaminase; LDH, lactate dehydrogenase; TPR, total peripheral resistance; SPP, splanchnic perfusion pressure.

Research Article

and in HSC and myofibroblasts [12]. In addition, the expression of PDGF and its receptor subunits in liver tissue obtained from patients with chronic diseases correlates closely with the degree of necroinflammation and fibrosis [13]. This cytokine binds to PDGFRβ, activates Ras and consequently propagates the stimulatory signal through the phosphorylation pathway of Raf-1, MEK, and ERK1/2. ERK activation regulates proliferation and chemotaxis of HSC, and modulates nuclear signaling [14]. We have recently described that *PDGFRβ* mRNA is overexpressed in the liver of rats subjected to chronic inhalation of carbon tetrachloride (CCl_4) as compared to control animals. Moreover, we have reported the antifibrogenic effects of endocannabinoids and apelin, which are associated with the inhibition of PDGFRβ expression [15].

In the present study, we assessed the relationship between activation of PDGFRβ, hemodynamic deterioration, and progression in hepatic fibrosis in CCl_4-treated rats and, thereafter, analyzed the hemodynamic and antifibrotic effects produced by the adenoviral transduction of a dominant-negative soluble form of PDGFRβ (sPDGFRβ).

Materials and methods

Induction of fibrosis in rats

The study was performed in 51 male Wistar rats with fibrosis and in 12 control Wistar rats (Charles-River, Saint Aubin les Elseuf, France). Fibrosis was induced by repetitive CCl_4 inhalation [16]. Rats were fed *ad libitum* with standard chow and water containing phenobarbital (0.3 g L^{-1}) as drinking fluid. Animals were exposed to CCl_4 vapor atmosphere twice a week starting with 0.5 min per exposure. The duration of exposure was increased to 1 min after three sessions, to 2 min after three more sessions, to 3 min after three more sessions, to 4 min after three more sessions, and then to 5 min until the end of the study.

Relationship between fibrosis progression, systemic hemodynamics, portal pressure, and PDGFRβ expression in CCl_4-treated rats

To assess whether hepatic fibrosis directly correlates with PDGFRβ expression, CCl_4-treated rats were analyzed at week 13 (n = 13) and 18 (n = 8) after initiation of the fibrosis-inducing protocol. Animals were anesthetized with Inactin® (100 mg/kg bw, Sigma–Aldrich Chemie GmbH, Steinherim, Germany). A blood sample (1 ml) was obtained from each animal to perform standard liver and renal function tests. Hemodynamic parameters were allowed to equilibrate for 30 min and values of mean arterial pressure (MAP), portal pressure (PP), and heart rate (HR) were recorded. Animals were sacrificed by isofluorane overdose and liver specimens were collected to analyze liver histology, hepatic collagen content, and mRNA expression of *PDGFRβ*. Control rats (n = 6) were studied after similar periods of phenobarbital administration alone.

Effect of sPDGFRβ on fibrosis progression, systemic hemodynamics, and portal pressure in CCl_4-treated rats

To investigate the hemodynamic and antifibrogenic effect of blocking PDGFRβ activation, CCl_4-induced fibrosis rats were studied 18 weeks after initiation of the fibrosis induction protocol. Thirty fibrotic rats without ascites were administered recombinant adenoviruses or saline via the tail vein. The 30 fibrotic animals included in this protocol were randomly assigned to one of the following groups: (A) 10 animals were administered adenoviruses encoding β-galactosidase (β-gal) (5×10^{10} plaque-forming units (pfu) in 500 µl of saline), (B) 10 animals were administered adenoviruses encoding sPDGFRβ (5×10^{10} pfu in 500 µl of saline), and (C) 10 animals received saline (500 µl). Seven days after the iv administration of adenoviruses or saline, animals were anesthetized with Inactin® (100 mg/kg bw, Sigma–Aldrich). A blood sample (1 ml) was obtained from each animal to perform standard liver and renal function tests. The circulating levels of sPDGFRβ were analyzed including a fourth group of 6 control rats that received Ad-*sPDGFRβ* adenoviruses (5×10^{10} pfu in 500 µl of saline) as positive control. Hemodynamic parameters were allowed to equilibrate for 30 min, and MAP, PP, HR, and cardiac output (CO) were recorded. Animals were sacrificed by isofluorane overdose and liver specimens were collected to analyze hepatic collagen content and protein expression of sPDGFRβ, total ERK1/2, P-ERK1/2, and α-SMA.

Cell purification and culture

Human embryonic kidney (HEK) 293 cells and HepG2 cells (a human cell line of hepatocytes) were obtained from the American Type Culture Collection (ATCC; Manassas, Virginia, USA). These immortalized, stable cell lines can be repeatedly frozen, thawed, and propagated. HEK 293 cells were maintained in DMEM with 10% heat-inactivated fetal calf serum, 50 U/ml penicillin, 50 µg/ml streptomycin, and 2 mmol/L L-glutamine. HepG2 cells were cultured as previously described [17].

Adenoviral constructs

Two replication-defective recombinant adenoviral constructs were used. These constructs, under the control of the cytomegalovirus promoter, expressed a dominant-negative soluble PDGFRβ encoding for the extracellular domain (ECD) of the PDGF receptor type β, fused into the IgGFc domain of human immunoglobulin or β-gal [18,19]. All vectors were propagated in the HEK 293 cell line, and titers were determined by standard plaque assay [20].

In vitro viral transduction

HepG2 cells were infected with 100 multiplicity of infection (m.o.i) of adenovirus encoding sPDGFRβ or β-gal for 3 h. The adenoviruses were removed, and cells were left to recover for 24 h in complete medium. Next, cells were serum-starved for 18 h. Finally, supernatants and cells were harvested. Supernatants were concentrated by ultrafiltration using Amicon® Ultra-4 Centrifugal Filter Devices (Millipore, Billerica, MA) and were then subjected to Western blot analysis with a specific antibody for the ECD of PDGFRβ.

Hemodynamic studies

See Supplementary Materials and methods.

Fibrosis quantification

See Supplementary Materials and methods.

Hepatic mRNA expression of PDGFRβ

See Supplementary Materials and methods.

Western blot analysis of PDGFRβ, total ERK1/2, P-ERK1/2, and α-SMA

See Supplementary Materials and methods.

Measurements and statistical analysis

Serum sodium and potassium were determined by flame photometry (IL 943, Instrumentation Laboratory, Lexington, MA). Serum creatinine, alanine transaminase (ALT), aspartate transaminase (AST), and lactate dehydrogenase (LDH) were measured with the ADVIA 1650 Instrument (Siemens Healthcare Diagnostics, Tarrytown, NY).

Statistical analysis of the results was performed by one-way analysis of variance (ANOVA), Bonferroni's *post hoc* test, paired and unpaired Student's *t*-tests and Pearson's correlation when appropriate. Results are given as mean ± SEM and were considered significant at a p level of 0.05 or less.

The study was performed according to the criteria of the Investigation and Ethics Committee of the Hospital Clínic Universitari.

Results

Hepatic collagen accumulation is progressive during the evolution of liver disease

The individual response to the fibrosis-induction protocol varied widely from animal to animal. For the first part of the study, we staged animals into two different groups according to the

JOURNAL OF HEPATOLOGY

histological analysis by Sirius red staining based on the percentage of fibrotic area compared to the total area of biopsy: in the first group, n = 10 were considered fibrotic (1–10% of fibrotic area), and in the second group, n = 11 were histologically cirrhotic (>10% of fibrotic area). The collagen content in cirrhotic rats (14.93 + 0.90) was significantly higher in comparison to fibrotic animals (5.11 + 0.66, $p < 0.001$). It is of note that none of the rats in the first group developed ascites, while 9 out of 11 rats in the cirrhotic group had at least 5 ml of ascites. Control rats displayed no alterations in liver histology and had an almost negligible amount of fibrotic tissue (1.00 + 0.10, $p < 0.05$ in comparison to fibrotic and cirrhotic values). Most of the cirrhotic animals were characterized by the formation of regenerative nodules separated by fibrotic septa (Fig. 1A).

Hemodynamic deterioration and mRNA expression of PDGFRβ directly correlate with hepatic collagen content

Progressive hepatic tissue disruption was associated with the worsening of systemic hemodynamics and increased portal hypertension. Cirrhotic rats had a significantly lower MAP compared to fibrotic rats and controls ($p < 0.05$ *vs.* control and fibrotic animals). In the same way, PP increased steadily when comparing controls to fibrotic and cirrhotic rats ($p < 0.05$ between control and fibrotic rats, and $p < 0.05$ between fibrotic and cirrhotic animals). Moreover, both MAP and PP significantly correlated with the collagen content found in the analyzed livers ($p < 0.001$; $r = -0.77$ and $p < 0.001$; $r = 0.75$, respectively) (Fig. 1B). On the other hand, we measured the mRNA expression of *PDGFRβ* in all liver samples. The mRNA expression increased in parallel with the worsening of the liver disease, reaching a 4-fold increase in cirrhotic animals. There was also a significant correlation between *PDGFRβ* mRNA abundance and amount of collagen accumulation in the whole group of CCl_4-treated livers ($p < 0.05$; $r = 0.51$) (Fig. 1B).

In vitro adenoviral transduction in HepG2 cells

We analyzed whether the adenoviral construct encoding sPDGFRβ was transduced into hepatic cells *in vitro* and induced sPDGFRβ expression. Western blot analysis showed strong expression of the ECD of PDGFRβ in supernatants of HepG2 cells transduced with Ad-*sPDGFRβ*, but not in those transduced with Ad-*β-gal* (viral control) or saline. This result confirms *in vitro* adenoviral transduction, and secretion of the chimeric PDGFRβ-IgGFc protein by the infected cells (Fig. 2A).

Circulating sPDGFRβ in fibrotic rats after adenoviral transduction

To confirm *in vivo* adenoviral transduction and sPDGFRβ expression and secretion, we analyzed circulating levels 7 days after iv administration. Western blot analysis showed that fibrotic rats transduced with the adenovirus encoding sPDGFRβ showed increased protein levels of the ECD of PDGFRβ in the serum in comparison to fibrotic rats receiving Ad-*β-gal* or saline, and similar protein levels as compared to control rats transduced with Ad-*sPDGFRβ* (Fig. 2B).

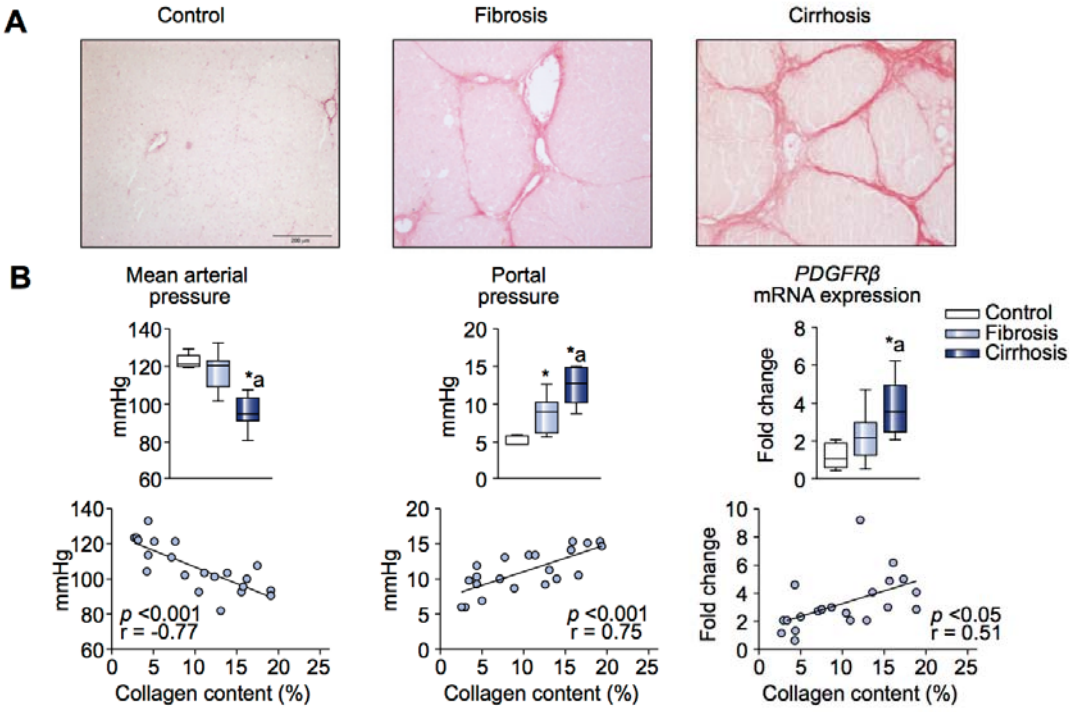

Fig. 1. Fibrosis progression, hemodynamic deterioration, and mRNA expression of *PDGFRβ*. (A) Representative liver sections from control, fibrotic and cirrhotic animals stained with Sirius red. (B) Correlation between the collagen content in all CCl_4-treated animals and systemic hemodynamics, portal pressure, and mRNA expression of *PDGFRβ*. The box contains the values between the 5th and 95th percentiles and the horizontal line is the median; whiskers show the range of the data. *$p < 0.01$ compared to control values and $^a p < 0.01$ compared to fibrotic values.

Research Article

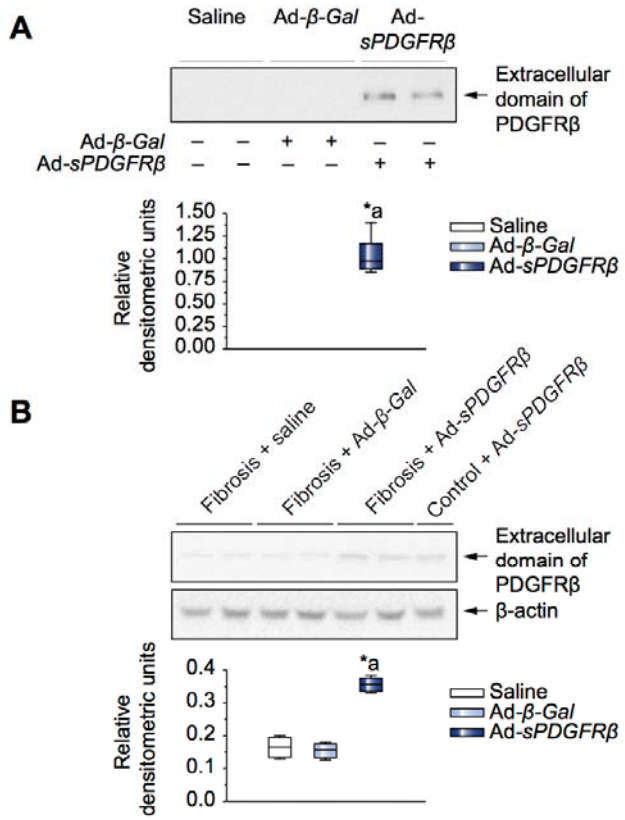

Fig. 2. *In vitro* and *in vivo* adenoviral transduction promotes sPDGFRβ expression. (A) Representative Western blot of PDGFRβ in supernatants of HepG2 cells infected (+) or not infected (−) with β-gal or sPDGFRβ. Densitometric analysis corresponds to 4 independent experiments. (B) Representative Western blot of PDGFRβ in serum of fibrotic rats administered saline, β-gal or sPDGFRβ adenoviruses. For specific details, see Fig. 1. $^{*}p$ <0.05 compared to saline values and ^{a}p <0.05 compared to β-gal values.

Body weight and standard liver and renal function test results, in fibrotic rats after adenoviral transduction

In order to determine whether adenoviral infection could induce cytopathic effects, we examined the liver and renal function by measuring related serum biochemical parameters. Table 1 shows that fibrotic rats developed marked abnormalities in liver function. As anticipated, fibrotic rats showed increased activity of AST and LDH and high levels of serum creatinine. No significant differences were found in any of these parameters among the three groups of animals. These data indicate that no additional liver damage was induced by transduction with adenoviruses.

Adenoviral expression of sPDGFRβ improves systemic and portal hemodynamics in fibrotic rats

The effects on systemic and portal hemodynamics induced by intravenous administration of Ad-*sPDGFRβ*, Ad-*β-gal*, or saline to fibrotic rats are shown in Table 2. As anticipated, fibrotic rats receiving saline showed hemodynamic deterioration characterized by arterial hypotension, decreased peripheral resistance, and increased PP. This characteristic circulatory dysfunction in fibrotic animals did not undergo any significant change after intravenous administration of Ad-*β-gal*. In contrast, transduction with the adenovirus encoding a dominant-negative soluble PDGFRβ in fibrotic rats was associated with a remarkable amelioration of the hemodynamic parameters, because these animals had significantly higher MAP and lower PP values than fibrotic rats receiving either Ad-*β-gal* or saline. In addition, administration of the Ad-*sPDGFRβ* significantly increased total peripheral resistance (TPR) and splanchnic perfusion pressure (SPP) when compared with fibrotic rats receiving saline and Ad-*β-gal*, respectively.

Adenoviral expression of sPDGFRβ inhibits PDGFRβ signaling and α-SMA protein expression in the liver of fibrotic rats

To ascertain the effectiveness of sPDGFRβ in inhibiting the PDGFRβ signaling pathway, we assessed protein expression of total ERK1/2 and P-ERK1/2 in liver samples of fibrotic rats by Western blot. As shown in Fig. 3, fibrotic animals receiving the adenoviral construct encoding the dominant-negative soluble form of PDGFRβ displayed lower hepatic ERK1/2 phosphorylation as compared to fibrotic animals receiving β-gal or saline. This result indicates that adenoviral expression of sPDGFRβ is able to block the PDGF signaling pathway in the liver of fibrotic rats by abrogation of endogenous PDGFRβ phosphorylation. Next, we analyzed the protein expression of α-SMA, a marker of fibrogenesis and cellular activation. In parallel with the results obtained analyzing the phosphorylation levels of ERK1/2, we observed that fibrotic animals receiving sPDGFRβ adenovirus showed a significant decrease of α-SMA protein expression in liver homogenates in comparison to the other groups of fibrotic animals. This result suggests that inhibition of PDGF signaling pathway by sPDGFRβ may induce a lower progression of hepatic fibrosis.

Table 1. Body weight and standard liver and renal function test results in fibrotic rats after adenoviral transduction (5×10^{10} pfu).

	Saline (n = 10)	Ad-*β-Gal* (n = 10)	Ad-*sPDGFRβ* (n = 10)
Body wt (g)	423 ± 12	427 ± 11	419 ± 6
Alanine transaminase (IU/L)	36.6 ± 6.9	67.5 ± 34.5	67.0 ± 18.5
Aspartate transaminase (IU/L)	136.6 ± 29.1	126.0 ± 42.0	153.7 ± 7.5
Lactate dehydrogenase (IU/L)	1027 ± 229	965 ± 22	1022 ± 96
Serum creatinine (mg/dl)	0.64 ± 0.07	0.68 ± 0.08	0.68 ± 0.04
Serum sodium (mEq/L)	151 ± 1.1	148 ± 0	147 ± 1.3
Serum potassium (mEq/L)	4.7 ± 0.2	4.6 ± 0.1	4.9 ± 0.3

JOURNAL OF HEPATOLOGY

Table 2. Hemodynamic effects induced by adenoviral transduction (5×10^{10} pfu).

	Saline (n = 9)	Ad-*β-Gal* (n = 10)	Ad-*sPDGFRβ* (n = 10)
Mean arterial pressure (mmHg)	113 ± 2	114 ± 3	124 ± 2*,a
Heart rate (beat.min^{-1})	442 ± 13	428 ± 9	407 ± 9
Cardiac output (ml.min^{-1})	157 ± 12	144 ± 11	127 ± 7
Total peripheral resistance (mmHg·min·ml^{-1})	0.77 ± 0.05	0.85 ± 0.06	1.02 ± 0.05*
Portal pressure (mmHg)	8.6 ± 0.4	8.7 ± 0.6	6.7 ± 0.3*,a
Splanchnic perfusion pressure (mmHg)	105 ± 3	104 ± 4	118 ± 3a

*p <0.05 compared to saline values and ap <0.05 compared to β-gal values (one-way analysis of variance and Bonferroni's *post hoc* test).

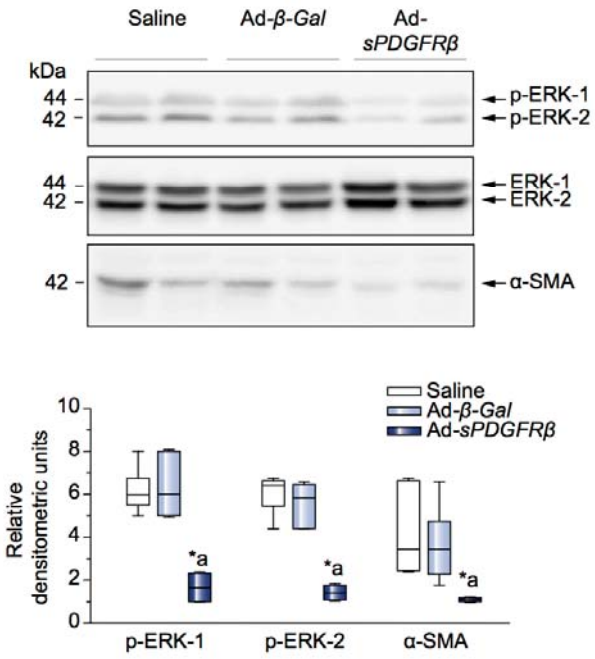

Fig. 3. Representative Western blot of total ERK1/2, P-ERK1/2, and α-SMA in liver samples of fibrotic rats. Fibrotic animals were administered saline, β-gal or sPDGFRβ adenoviruses. For specific details, see Fig. 1. *p <0.05 compared to saline values and ap <0.05 compared to β-gal values.

Decreased hepatic collagen accumulation induced by sPDGFRβ expression in fibrotic rats

As previously shown in Fig. 1A, fibrotic rats had increased intrahepatic collagen content compared to control rats. To measure the effect of sPDGFRβ on hepatic fibrosis progression, hepatic collagen deposition was assessed by Sirius red staining (Fig. 4). In concordance with hepatic α-SMA protein expression, the collagen content in fibrotic rats transduced with the dominant-negative soluble form of PDGFRβ was significantly decreased in comparison to fibrotic animals receiving the viral control Ad-*β-gal*, or saline. Therefore, this result indicates that the prevention was specific for Ad-*sPDGFRβ*.

Discussion

The PDGF family has been shown to be an important factor contributing to the perpetuation of liver fibrosis [12,13]. Early response after liver injury is characterized by rapid inductions of PDGFRβ, development of a contractile and fibrogenic phenotype, as well as growth factor modulation [1]. The *in vivo* effects of PDGFR inhibitors are more complex, based on the crosstalk with other angiogenic factors [21,22]. We have recently reported that the stimulation of CB2 receptors, as well as the blockade of the hepatic apelin system activity, is able to attenuate collagen deposition in CCl_4-treated rats through common mechanisms, such as the inhibition of PDGFRβ expression [15]. In the current study, we investigated the role of PDGFRβ in the physiopathological alterations that take place along the course of CCl_4-induced experimental liver disease. We found progressive hepatic collagen deposition during the evolution of liver disease. Indeed, CCl_4-treated rats were classified into two different groups according to the histological quantification of their liver-collagen content: fibrosis and cirrhosis. Assessment of hemodynamic parameters, together with liver biopsy examination, is a very important tool for staging and prognosis in liver disease. Furthermore, a recent study in patients with hepatitis C virus after liver transplantation has determined that a hepatic venous pressure gradient value of 6 mmHg or higher is accurate at identifying patients at risk of disease progression (area under the curve 0.96) [23]. In this study, we found a significant relationship between deterioration of the hemodynamic parameters and hepatic collagen content during fibrosis, being particularly relevant in the case of PP. CCl_4 inhalation treatment also resulted in increased hepatic expression of PDGFRβ. In this regard, this study allowed a temporal relationship to be observed between the increase in hepatic mRNA expression of *PDGFRβ* and histological fibrosis during the evolution of liver disease, and demonstrated how PDGFRβ can effectively discriminate stages of cirrhosis from fibrosis and no fibrosis. Therefore, the results obtained in the first protocol indicate that the expression of PDGFRβ significantly contributes to increased liver fibrosis and hemodynamic deterioration in CCl_4-treated rats.

Considering these results and previous investigations showing that the intravenous administration of adenoviral vectors preferentially targets the liver [24–26], in the second protocol we analyzed the therapeutic effects of intravenous administration of the adenovirus encoding a dominant-negative soluble form of PDGFRβ (sPDGFRβ). It has been described that adenoviral transduction of this soluble form of PDGFRβ blocks activation of HSCs and attenuates fibrogenesis induced by bile duct ligation in rats [18]. The *in vitro* assay showed a higher protein abundance of PDGFRβ in supernatants of HepG2 cells transduced with the adenoviral transgene sPDGFRβ. This result confirms the effectiveness of the adenoviral transduction of sPDGFRβ and its protein expression in HepG2 cells. Further, the analysis of circulating

Research Article

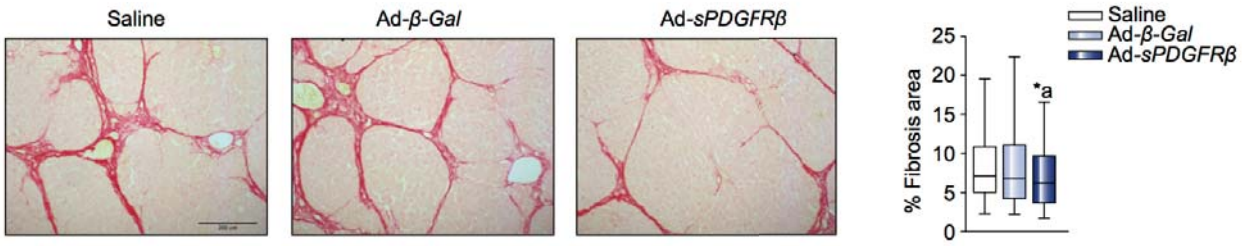

Fig. 4. Decrease of hepatic collagen content induced by sPDGFRβ. Representative liver sections from fibrotic animals administered saline, β-gal or sPDGFRβ adenoviruses stained with Sirius red. The right panel shows the corresponding quantification. For specific details, see Fig. 1. *p <0.05 compared to saline values and [a]p <0.05 compared to β-gal values.

levels of sPDGFRβ seven days after adenoviral administration showed the *in vivo* expression of this transgene. In this regard, the increased detection of the ECD of PDGFRβ in serum samples of fibrotic rats administered Ad5-*sPDGFRβ* confirms the *in vivo* expression of sPDGFRβ. The inflammatory response induced by adenoviral administration has been the subject of great concern. In this study, no significant differences were detected in serum ALT, AST, LDH, and creatinine levels among fibrotic rats receiving β-gal, sPDGFRβ adenovirus or saline. However, we cannot exclude a more significant problem in humans due to adenoviral toxicity. This important issue should be resolved in the future, probably with the use of new viral vectors or pharmacological strategies. Inhibiting phosphorylation of PDGFR with a PDGFR tyrosine kinase inhibitor has become a largely investigated therapeutic strategy in the last years. Inhibition of PDGFR activation may decrease cell proliferation and increase the rate of apoptosis. PDGF antagonists include neutralizing antibodies against ligands or receptors, inhibitors of receptor dimerization, and low molecular-weight compounds, which act through competitive binding to the active site of the receptors [27]. Although pharmacological approaches have been used to reduce PP by combined inhibition of VEGF and PDGF signaling [28,29], this study shows that specific blockade of the intrahepatic PDGFRβ pathway with adenoviral vectors was associated with a significant amelioration in the systemic and splanchnic parameters in fibrotic animals. In fact, normalization in PP induced by intravenous administration of sPDGFRβ adenovirus was accompanied by a correction of systemic hypotension. The amelioration of hemodynamic parameters is probably a consequence of the antifibrotic effect induced by sPDGFRβ. In this regard, it has been demonstrated that the PDGF antagonist exerts an antifibrotic effect in experimental-induced liver injury by BDL [18]. Using the chronic CCl_4-induced fibrosis model, we found that sPDGFRβ selectively inhibited phosphorylation of ERK1/2 in fibrotic animals, consistent with previous findings indicating that autophosphorylation of PDGFRβ is a prerequisite for PDGF downstream signaling via the Ras/ERK regulated kinase pathway [11,14]. These results indicate that the soluble receptor is effective, blocking PDGF signaling *in vivo*. We also show that adenoviral expression significantly attenuated hepatic fibrosis, as assessed by reduced α-SMA protein expression and hepatic collagen content. This is consistent with previous studies demonstrating that inhibitors of PDGF decrease α-SMA expression and the degree of fibrosis [30,31]. The reduced fibrosis observed after treatment with sPDGFRβ may be a consequence of the blockade of HSC proliferation and inhibition of chemotaxis, thereby decreasing the number of cells able to synthesize these fibrogenic markers. The results of the second protocol support the idea that less activation of the signaling pathway of PDGFRβ could further contribute to an inhibition of hepatic fibrosis.

In summary, the data presented in this paper indicate that the hepatic mRNA expression of *PDGFRβ* closely correlates with hepatic collagen content and contributes to hemodynamic deterioration in rats with CCl_4-induced fibrosis. The present investigation is the first experimental evidence documenting that blockade of the PDGFRβ signaling pathway by adenovirus transduction promotes an improvement in systemic hemodynamics and portal pressure, as well as an amelioration in the degree of fibrosis, in CCl_4-treated rats. In conclusion, these results should be interpreted as a proof-of-concept indicating that strategies addressed to block PDGF signaling pathway in the liver could be useful in the management of human liver fibrosis, providing a potential site for therapeutic intervention.

Conflict of interest

The authors who have taken part in this study declared that they do not have anything to disclose regarding funding or conflict of interest with respect to this manuscript.

Financial support

This work was supported by grants from Dirección General de Investigación Científica y Técnica (Grants SAF09-08839 to W. Jiménez and SAF2010-19025 to M. Morales-Ruiz) and from Agència de Gestió d'Ajuts Universitaris i de Recerca (SGR 2009/1496). The Centro de Investigación Biomédica en Red de Enfermedades Hepáticas y Digestivas (CIBERehd) is funded by the Instituto de Salud Carlos III.

Supplementary data

Supplementary data associated with this article can be found, in the online version, at http://dx.doi.org/10.1016/j.jhep.2012.07.012.

References

[1] Friedman SL. Mechanisms of hepatic fibrogenesis. Gastroenterology 2008;134:1655–1669.
[2] Pinzani M. PDGF and signal transduction in hepatic stellate cells. Front Biosci 2002;7:D1720–D1726.

[3] Heldin CH, Westermark B. Mechanisms of action an in vivo role of platelet-derived growth factor. Physiol Rev 1999;79:1283–1316.
[4] Marra F, Gentilini A, Pinzani M, Choudhury GG, Parola M, Herbst H, et al. Phosphatidylinositol 3-kinase is required for platelet-derived growth factor's actions on hepatic stellate cells. Gastroenterology 1997;112:1297–1306.
[5] Pinzani M, Gesualdo L, Sabbah GM, Abboud HE. Effects of platelet derived growth factor and other polypeptide mitogens on DNA synthesis and growth of cultured rat liver fat-storing. J Clin Invest 1989;84:1786–1793.
[6] Wong L, Yamasaki G, Johnson RJ, Friedman SL. Induction of beta-platelet-derived growth factor receptor in rat hepatic lipocytes during cellular activation in vivo and in culture. J Clin Invest 1994;94:1563–1569.
[7] Pinzani M, Milani S, Grappone C, Weber Jr FL, Gentilini P, Abboud HE. Expression of platelet-derived growth factor in a model of acute liver injury. Hepatology 1994;19:701–707.
[8] Magnusson PU, Looman C, Ahgren A, Wu Y, Claesson-Welsh L, Heuchel RL. Platelet-derived growth factor receptor-beta constitutive activity promotes angiogenesis in vivo and in vitro. Arterioscler Thromb Vasc Biol 2007;27:2142–2149.
[9] Pinzani M, Marra F. Cytokine receptors and signaling in hepatic stellate cells. Semin Liver Dis 2001;21:397–416.
[10] Lechuga CG, Hernandez-Nazara ZH, Hernandez E, Bustamante M, Desierto G, Cotty A, et al. PI3K is involved in PDGF-beta receptor upregulation post-PDGF-BB treatment in mouse HSC. Am J Physiol 2006;291:G1051–G1061.
[11] Rovida E, Navari N, Caligiuri A, Dello Sbarba P, Marra F. ERK5 differentially regulates PDGF-induced proliferation and migration of hepatic stellate cells. J Hepatol 2008;48:107–115.
[12] Borkham-Kamphorst E, van Roeyen CR, Ostendorf T, Floege J, Gressner AM, Weiskirchen R. Pro-fibrogenic potential of PDGF-D in liver fibrosis. J Hepatol 2007;46:1064–1074.
[13] Pinzani M, Milani S, Herbst H, DeFranco R, Grappone C, Gentilini A, et al. Expression of platelet-derived growth factor and its receptors in normal human liver and during active hepatic fibrogenesis. Am J Pathol 1996;148:785–800.
[14] Marra F, Arrighi MC, Fazi M, Caligiuri A, Pinzani M, Romanelli RG, et al. Extracellular signal-regulated kinase activation differentially regulates platelet-derived growth factor's actions in hepatic stellate cells, and is induced by in vivo liver injury in the rat. Hepatology 1999;30:951–958.
[15] Reichenbach V, Ros J, Fernández-Varo G, Casals G, Melgar-Lesmes P, Campos T, et al. Prevention of fibrosis progression in CCl_4-treated rats: role of the hepatic endocannabinoid and apelin systems. J Pharmacol Exp Ther 2012;340:629–637.
[16] Clària J, Jiménez W. Renal dysfunction and ascites in carbon tetrachloride induced cirrhosis in rats. In: Arroyo V, Ginès P, Rodés J, Schrier RW, editors. Ascites and renal dysfunction in liver disease. Pathogenesis diagnosis and treatment. Malden, MA: Blackwell Science Inc.; 1999. p. 379–396.
[17] Melgar-Lesmes P, Pauta M, Reichenbach V, Casals G, Ros J, Bataller R, et al. Hypoxia and proinflammatory factors upregulate apelin receptor expression in human stellate cells and hepatocytes. Gut 2011;60:1404–1411.
[18] Borkham-Kamphorst E, Herrmann J, Stoll D, Treptau J, Gressner AM, Weiskirchen R. Dominant-negative soluble PDGF-β receptor inhibits hepatic stellate cell activation and attenuates liver fibrosis. Lab Invest 2004;84:766–777.
[19] Fulton D, Gratton JP, McCabe TJ, Fontana J, Fujio Y, Walsh K, et al. Regulation of endothelium-derived nitric oxide production by the protein kinase Akt. Nature 1999;399:597–601.
[20] Ehrengruber MU, Lanzrein M, Xu Y, Jasek MC, Kantor DB, Schuman EM, et al. Recombinant adenovirus-mediated expression in nervous system of genes coding for ion channels and other molecules involved in synaptic function. Methods Enzymol 1998;293:483–503.
[21] Lev DC, Kim SJ, Onn A, Stone V, Nam DH, Yazici S, et al. Inhibition of platelet-derived growth factor receptor signaling restricts the growth of human breast cancer in the bone of nude mice. Clin Cancer Res 2005;11:306–314.
[22] Tsutsumi N, Yonemitsu Y, Shikada Y, Onimaru M, Tanii M, Okano S, et al. Essential role of PDGFRα-p70S6K signaling in mesenchymal cells during therapeutic and tumor angiogenesis *in vivo*: role of PDGFRalpha during angiogenesis. Circ Res 2004;94:1186–1194.
[23] Blasco A, Forns X, Carrion JA, Garcia-Pagan JC, Gilabert R, Rimola A, et al. Hepatic venous pressure gradient identifies patients at risk of severe hepatitis C recurrence after liver transplantation. Hepatology 2006;43:492–499.
[24] Fernández-Varo G, Melgar-Lesmes P, Casals G, Pauta M, Arroyo V, Morales-Ruiz M, et al. Inactivation of extrahepatic vascular Akt improves systemic hemodynamics and sodium excretion in cirrhotic rats. J Hepatol 2010;53:1041–1048.
[25] Morales-Ruiz M, Cejudo-Martín P, Fernández-Varo G, Tugues S, Ros J, Angeli P, et al. Transduction of the liver with activated Akt normalizes portal pressure in cirrhosis. Gastroenterology 2003;125:522–531.
[26] Jaffe HA, Danel C, Longenecker G, Metzger M, Setoguchi Y, Rosenfeld MA, et al. Adenovirus-mediated in vivo gene transfer and expression in normal rat liver. Nat Genet 1992;1:372–378.
[27] Östman A. PDGF receptors-mediators of autocrine tumor growth and regulators of tumor vasculature and stroma. Cytokine Growth Factor Rev 2004;15:275–286.
[28] Tugues S, Fernández-Varo G, Muñoz-Luque J, Ros J, Arroyo V, Rodés J, et al. Antiangiogenic treatment with sunitinib ameliorates inflammatory infiltrate, fibrosis, and portal pressure in cirrhotic rats. Hepatology 2007;46:1919–1926.
[29] Fernandez M, Mejias M, Garcia-Pras E, Mendez R, Garcia-Pagan JC, Bosch J. Reversal of portal hypertension and hyperdynamic splanchnic circulation by combined vascular endothelial growth factor and platelet-derived growth factor blockade in rats. Hepatology 2007;46:1208–1217.
[30] Liu Y, Wang Z, Kwong SQ, Lui EL, Friedman SL, Li FR, et al. Inhibition of PDGF, TGF-β, and Abl signaling and reduction of liver fibrosis by the small molecule Bcr-Abl tyrosine kinase antagonist Nilotinib. J Hepatol 2011;55:612–625.
[31] Gonzalo T, Beljaars L, van de Bovenkamp M, Temming K, van Loenen AM, Reker-Smit C, et al. Local inhibition of liver fibrosis by specific delivery of a platelet-derived growth factor kinase inhibitor to hepatic stellate cells. J Pharmacol Exp Ther 2007;321:856–865.

Supplementary Materials and methods

Hemodynamic studies

Rats were anesthetized with Inactin® (100 mg/kg.bw, Sigma-Aldrich) and prepared with PE-50 polyvinyl catheters in the left femoral artery. A midline abdominal incision (2 cm) was made, and the portal vein was cannulated through an ileocolic vein with a PE-50 catheter to measure PP. After verifying free blood reflux, the catheter was fixed to the mesentery with cyanoacrylate glue. The right jugular vein was also isolated and a PE-50 catheter was placed in the right atrium. A thermocouple (Columbus Instruments, Columbus, OH) was advanced to the aortic arch through a left carotid approach to monitor the intra-arterial temperature during CO measurement. The arterial catheter was connected to a highly sensitive transducer (Hewlett Packard, Avondale, PA) that was calibrated before each study. Hemodynamic parameters were recorded in a multichannel system (PowerLab®, ADInstruments, Sydney, Australia). CO was measured by thermodilution after the administration of a bolus of 200 µl of Ringer solution (20 to 23°C) into the right atrium. A spring-loaded syringe was used (Hamilton Syringe, model CR-700-200; Hamilton Co., Reno, NV) to ensure a constant injection rate and volume. Hemodynamic parameters were allowed to equilibrate for 30 minutes and MAP, PP, HR and CO values were recorded for two 30 minute time periods. Each value represents the average of 2 measurements. TPR and SPP were obtained using the following formula: TPR = MAP/CO and SPP = MAP-PP.

Fibrosis quantification

Liver sections (4 µm) were stained in 0.1% Sirius Red F3B (Sigma) in saturated picric acid (Sigma). The relative fibrosis area (expressed as a percentage of total liver area) was assessed by analyzing 32 fields of Sirius red-stained liver sections per animal. Each field was acquired at 10x magnification (Nikon Eclipse E600, Kawasaki, Kanagawa, Japan) and then analyzed using the morphometry software ImageJ v 1.37. To evaluate the relative fibrosis area, the measured collagen area was divided by the net field area and then multiplied by 100. Subtraction of vascular luminal area from the total field area yielded the final calculation of the net fibrosis area. From each animal analyzed, the amount of fibrosis was measured as a percentage and the average value presented.

Hepatic mRNA expression of PDGFRb

Liver specimens were obtained from each animal, washed in 0.1% diethyl pyrocarbonate-treated phosphate-buffered saline salt solution (140 mM NaCl, 8.5 mM Na_2HPO_4, and 1.84 mM $Na_2HPO_4 \cdot H_2O$, pH 7.4), immediately frozen in dry ice, and stored in liquid nitrogen. Liver samples from treated and untreated animals were also fixed in 10% buffered formalin for further hematoxylin and eosin and immunostaining analysis. Total RNA was extracted from the middle liver lobe of control and fibrotic rats using a commercially available kit (RNAeasy, Qiagen, Germany). RNA concentration was determined by spectrophotometric analysis (ND-100 Spectrophotometer, Nanodrop Technology). One µg of total RNA was reverse transcribed (RT) using a complementary DNA synthesis kit (High-Capacity cDNA Reverse Transcription Kit, Applied Biosystems, Foster City, CA). Specific primers and probe for PDGFRb were designed to include intron spanning using the Universal Probe Library Assay Design Center through the ProbeFinder v2.45 software (Roche Diagnostics, Indianapolis, IN). The primers included were: PDGFRb (probe#69; left: 5'-GCGGAAGCGCATCTATATCT-3', right: 5'-GCGGAAGCGCATCTATATCT-3'), and hypoxanthine-guanine phosphoribosyltransferase (HPRT) (probe#95; left: 5'-GACCGGTTCTGTCATGTCG-3', right: 5'-ACCTGGTTCATCATCACTAATCAC-3'). Primers were designed according to rat sequences (GenBank NM_031525.1 and NM_012583.2 respectively). Real time quantitative PCR was analyzed in duplicate and performed with the Light Cycler 480 (Roche Diagnostics). Ten µl total volume

reaction of diluted 1:8 cDNA, 200 nM primer dilution, 100 nM pre-validated 9-mer probe (Universal ProbeLibrary, Roche Diagnostics) and FastStart TaqMan Probe Master (Roche Diagnostics) were used in each PCR reaction. Fluorescence signal was captured during each of the 45 cycles (denaturizing 10 sec at 95ºC, annealing 20 sec at 60ºC and extension 1 sec at 72ºC). HPRT was used as a reference gene for normalization and water was used as a negative control. Relative quantification was calculated using the comparative threshold cycle (CT), which is inversely related to the abundance of mRNA transcripts in the initial sample. The mean CT of duplicate measurements was used to calculate ΔCT as the difference in CT for target and reference. The relative quantity of product was expressed as fold-induction of the target gene compared with the reference gene according to the formula $2^{-\Delta\Delta CT}$, where ΔΔCT represents ΔCT values normalized with the mean ΔCT of control samples.

Western blot analysis of PDGFRb, total ERK1/2, P-ERK1/2 and a-SMA

Hepatic tissue from treated and nontreated rats was individually homogenized as described previously [15]. To detect total ERK1/2, p-ERK1/2, a-SMA and PDGFRb, 40 µg of total denatured proteins and 80 µg of the denatured serum proteins were loaded per lane on a 10% (ERK1/2, p-ERK1/2 and a-SMA) and 7.5% (PDGFRb) SDS-polyacrylamide gel (Mini Protean III; Bio-Rad Richmond, CA). Gels were transferred for 2h to nitrocellulose membranes of 0.45 µm (Transblot Transfer Medium, Bio Rad), stained with Ponceau S red as a loading control and blocked with 5% non fat milk for in TBST buffer (50 mmol/L Tris-HCl, pH 8, containing 0.05% Tween 20 and 150 mmol/L NaCl) at room temperature for 2h. Membranes were incubated with primary antibodies rabbit polyclonal anti-PDGFRb, mouse polyclonal a-SMA (1:1000, Roche Diagnostics, Indianapolis IN) and rabbit polyclonal anti-ERK1/2 and p-ERK-1/2 (1:1000, Cell Signaling Technologies, Beverly, MA) at room temperature for 2h in TBST buffer with 5% non fat milk. PDGFRb, total ERK1/2 and p-ERK1/2 membranes were incubated with a donkey anti-rabbit horseradish peroxidase-conjugated (HRP) secondary antibody (1:2000; Amersham Biosciences, GE Healthcare, Piscataway, NJ) and the a-SMA membrane with a goat anti-mouse HRP secondary antibody (1:5000; Amersham Bioscience). The bands were visualized by chemiluminescence (Lumi-Light Western blotting substrate, Roche Diagnostics).

4th Article: Bacterial lipopolysaccharide (LPS) inhibits CB2 receptor expression in human monocytic cells. (Not published)

Cirrhotic patients with ascites are prone to bacterial infections by *E.Coli*, which can compromise seriously the condition of the patient. In order to study the role of CB2 receptors during an infection*, in vitro* experiments were carried out with U937 cells (these cells have the ability to differentiate into mature macrophages) treated with LPS to mimic the physiological situation occurring in cirrhotic patients. The obtained results are summarized next:

1. LPS stimulation downregulates CB2 mRNA and protein expression in U937 cells

CB2 mRNA expression was assessed in a time course experiment in U937 cells treated with two different doses of LPS: a pharmacological dose (1 μg/ml) and a supraphysiological dose (10 ng/ml). As shown in Figure 1A, both doses of LPS dramatically downregulated the mRNA expression of CB2 after 6 and 12 h of LPS treatment, and was significantly maintained after 24 and 30 h. Cell viability experiments confirmed that LPS did not have any adverse effect on those cells (right axis of figure 1A). The observed effect on CB2 produced by LPS was also reflected at protein level (Figure 1B). Protein expression of CB2 receptors was lower after 6 and 12 h of LPS treatment.

2. PCR array of genes related to antibacterial response pathway

To further confirm the effect on CB2 mRNA produced by LPS, we performed a commercially available PCR array of 84 genes involved in the antibacterial signaling pathway together with CB1 and CB2 genes (CNR1 and CNR2, respectively). In order to confirm that the downregulation of cannabinoid receptors and other well known genes implicated in this pathway are regulated by LPS, U937 cells were treated with Polymixin B, a potent antibiotic that prevents LPS cell binding and signaling. The results obtained were represented by a scatter dot plot graph (Figure 2), where full circles represent genes with ≥2.5 fold change. Figure 2A shows LPS-treated cells compared to non-treated cells. LPS induced the expression of 12 genes and only 5 where found downregulated included CB1 and CB2. Figure 2B shows the results after PMB

treatment. In the presence of PMB, almost all observed differences disappeared. Genes that reached statistical significance are represented on Table 1.

3. LPS decreases endocannabinoid-induced chemotactic activity in U937 cells

Chemotactic activity of U937 cells was evaluated in order to determine if the decrease in CB2 expression was correlated with functionality changes (Figure 3). Endocannabinoids, AEA and 2-AG are both well reported inducers of chemotaxis of macrophages, monocytes and also in U937 cells. Our results confirmed that both AEA and 2-AG induce the migration of U937 cells, and that pretreated cells with LPS showed a reduced chemotactic activity. To further demonstrate that these effects were mediated by CB2 receptors, the cells were exposed to AEA or 2-AG in the presence of SR144528 (1µM), a specific antagonist of CB2 receptors. As illustrated in Figure 3B, CB2 receptor blockade prevented the chemotactic-induced effect of the endocannabinoids.

4. Monocytes and macrophages of cirrhotic patients showed a marked decrease in CB1 and CB2 mRNA expression

Hepatic cirrhosis is associated with enhanced circulating levels of bacterial wall derived products, the extreme manifestation of this condition being the development of SBP. To assess if CB receptor expression was decreased in cirrhotic patients, circulating monocytes from the blood and peritoneal macrophages were isolated from the ascites of cirrhotic patients with or without SBP. Compared to healthy subjects, CB1 and CB2 expression in circulating monocytes was significantly decreased in cirrhotic patients with ascites, and the decreased was further marked in the patients with SBP. CB expression in peritoneal macrophages was lower and became almost fully suppressed in macrophages from ascites of the patients with SBP (Figure 4).

BACTERIAL LIPOPOLYSACCHARIDE (LPS) INHIBITS CB2 RECEPTOR EXPRESSION IN HUMAN MONOCYTIC CELLS

Vedrana Reichenbach[1], Javier Muñoz-Luque[1], Josefa Ros[1], Gregori Casals[1], Miguel Navasa[2,4], Guillermo Fernández-Varo[1,3,4], Manuel Morales-Ruiz[1,4], Wladimiro Jimenez[1,3,4]

[1]Service of Biochemistry and Molecular Genetics, [2] Liver Unit, Hospital Clinic, Institut d'Investigacions Biomèdiques August Pi i Sunyer (IDIBAPS), University of Barcelona, Barcelona, SPAIN. [3] Department of Physiological Sciences I, University of Barcelona, Barcelona, SPAIN, and [4] Centro de Investigación Biomédica en Red de Enfermedades Hepáticas y Digestivas (CIBERehd)

Short running title: LPS and CB2 receptor in human monocytes

Contact information:

Dr. Wladimiro Jiménez

Servicio de Bioquímica y Genética Molecular

Hospital Clinic Universitari

Villarroel 170, Barcelona 08036, SPAIN

Phone: (3493)2275400 ext 3091

Fax: (3493)2275697

E-mail: wjimenez@clinic.ub.es

Keywords: Endocannabinoids, cirrhosis, spontaneous bacterial peritonitis, cannabinoid receptor 2, monocyte migration.

ABBREVIATIONS

2-AG, 2-achachydonyl glycerol; AEA, anandamide, *BIRC3*, Baculoviral IAP repeat containing 3; BSA, bovine serum albumin; CB1, cannabinoid receptor 1; CB2, cannabinoid receptor 2; *CCL3*, Chemokine (C-C motif) ligand 3; *CCL5*, Chemokine (C-C motif) ligand 5; *CD14*, Cluster of differentiation 14; *CNR1*, Cannabinod receptor 1; *CNR2*, Cannabinoid receptor 2; *CXCL1*, Chemokine (C-X-C motif) ligand 1; *CXCL2*, Chemokine (C-X-C motif) ligand 2; *DMBT1*, Deleted in malignant brain tumors 1; FBS, fetal bovine serum, fMLP, N-formyl-methionyl-leucyl-phenylalanine; *IL1β*, Interleukin 1 beta; *IL6*, Interleukin 6; *IL8*, Interleukin 8; LPS, lipopolysaccharide; *MAPK14*, Mitogen-activated protein kinase 14; *NFKBIA,* Nuclear factor of kappa light polypeptide gene enhancer in B-cells inhibitor alpha; PMB, polymixin B; *PSTPIP1,* Proline-serine-threonine phosphatase interacting protein 1, *RIPK2*, Receptor-interacting serine-threonine kinase 2; SBP, spontaneous bacterial peritonitis; *TNF*, Tumor necrosis factor.

ABSTRACT

Objective: Endocannabinoids exert their physiological effects by interacting with CB1 and CB2 receptors, the latter being responsible for the antiinflammatory effects of endocannabinoids. Cirrhotic patients have altered host-defense response mechanisms. Here we assessed whether impaired expression of CB2 receptor in monocytic cells of cirrhotic patients could be involved in the pathogenesis of this phenomenon. **Design**: CB2 mRNA and protein expression was assessed in a differentiated human monocytic cell line (U937) stimulated with endotoxin (LPS). A PCR array of 86 different genes was assessed in U937 cells treated with LPS. A migration assay towards endocannabinoids or the CB2 antagonist, SR144528, was performed in U937 cells exposed to LPS. Finally, CB1 and CB2 mRNA expression were measured in monocytes and macrophages of cirrhotic patients with or without spontaneous bacterial peritonitis. **Results:** LPS reduced CB2 expression in human monocytes. Endocannabinoids increased the migratory activity of U937 cells, which was reverted when the experiments were performed in the presence of LPS. Transcriptional profiling showed marked upregulation of 9 genes related to proinflammatory signaling. However, only two genes encoding for CB1 and CB2 were reduced in LPS-treated cells. Circulating monocytes of cirrhotic patients showed a significantly diminished mRNA expression of CB1 and CB2. Markedly low CB1 and CB2 mRNA levels were found in peritoneal macrophages of cirrhotic patients with ascites, being almost suppressed when analyzed in patients with peritonitis. **Conclusion:** LPS reduces CB2 expression in human monocytes resulting in depressed chemotactic activity and therefore impaired host defense response of these cells.

What is already known about this subject:

- CB2 is highly expressed in the cells of the immune system, and its role modulating inflammatory responses is well known.
- Liver cirrhosis and LPS-induced sepsis have been associated with increased activity of endogenous cannabinoids.
- Cirrhotic patients have altered host-defense response mechanisms and increased susceptibility to bacterial infections.

What are the new findings:

- LPS exposure inhibits CB2 receptor messenger and protein expression in human-derived monocytic cells.
- LPS exposure decreases the migratory activity of human-derived monocytic cells.
- Down regulation of messenger expression induced by LPS in human derived monocytic cells is highly specific for CB receptors as demonstrated by array analysis of 86 different genes involved in antibacterial response.
- Circulating monocytes of cirrhotic patients show decreased expression of CB receptors. This reduction being more intense in cells obtained of patients with SBP.
- Expression of CB receptors is almost suppressed in peritoneal macrophages of patients with SBP

How might it impact on clinical practice in the foreseeable future?

These findings unveil new strategies to improve the cell armamentarium of cirrhotic patients to fight against bacterial infection.

INTRODUCTION

The peripheral cannabinoid receptor (CB2) was first identified in 1993 by Munro et al. via cloning of a novel G-protein coupled receptor expressed in a human promyelocytic leukemia HL60 human cell line.[1] Although expression levels vary among the immune cell population, the CB2 receptor has relatively high affinity for cannabinoids and is expressed by all immune cells, with the ranking order of abundance being B cells > NK cells > macrophages > polymorpho nuclear cells > T cells.[2-4] Macrophages appear to abundantly express the CB2 receptor, however, little is known about the role that this receptor plays in monocytic cell biology. Despite evidence that CB2 signaling may be involved in cell differentiation,[3] migration [5,6] and proliferation,[7-10] the mechanisms involved in these processes are poorly known. In this regard, several reports have suggested that stimulation by cytokines increases CB2 expression,[3,4,11,12] whereas LPS stimulation suppresses CB2 mRNA expression in lymphocytes.[13] Although these investigations have provided some clues on the regulation of CB2 expression, more studies are clearly needed to define the functional consequences of these changes and the role of the CB2 receptor in monocyte/macrophage cell biology.

Cirrhotic patients have altered host-defense response mechanisms and increased susceptibility to bacterial infections, which seems to be related to alterations in the intestinal barrier and/or bacterial translocation from the mucosa to the mesenteric lymph nodes and the intestinal circulation.[14,15] The extreme manifestation of this condition is spontaneous bacterial peritonitis (SBP), which occurs in patients with advanced liver disease and is defined as the infection of a previously sterile ascitic fluid with no apparent intraabdominal source of

infection.[14] In spite of the efficacy of the current antibiotic therapy in resolving peritoneal infection, the mortality rate in cirrhotic patients with SBP still remains relatively high.[16] Both liver cirrhosis and LPS-induced sepsis have been associated with increased activity of endogenous cannabinoids.[17,18] However whether any relationship exists among these phenomena is unknown.

In the present study we assessed whether LPS regulates CB2 expression in human monocytic cell lines. In addition, we assessed whether CB2 messenger expression is altered in monocyte/macrophages of cirrhotic patients. Our results indicate that LPS represses mRNA and protein expression of the CB2 receptor in human monocytes thereby affecting their functional properties. Moreover, we also observed a diminished abundance of CB2 transcripts in circulating monocytes and peritoneal macrophages of cirrhotic patients. These findings make it attractive to speculate that LPS may further alter host response mechanisms in cirrhotic patients by depressing CB2 expression in immune cells of the monocytic linage.

MATERIAL AND METHODS

Cell cultures: U937 cells, a human monoblastic leukemia cell line, were obtained from ATCC CRL-1593.2. Cells were cultured at 37°C in a 5% CO_2 atmosphere with RPMI-1640 medium (Gibco-Invitrogen, Paisley, UK) supplemented with 10% heat-inactivated fetal bovine serum and penicillin/streptomycin (50 U/ml and 50 mg/ml). To induce differentiation into adherent macrophage-like cells, U937 cells were seeded in 12-well plates (0.5×10^6 cells/ ml) and incubated for 48 h in RPMI-1640 / 10% fetal bovine serum (FBS) containing 10 ng/ml of phorbol myristic acid (PMA, Sigma Chemical Co, St. Louis, MO), a known inducer of macrophage phenotype in these cells.[19] Following PMA treatment the differentiated cells were cultured

for an additional period of 24 h in fresh medium and the different experiments were conducted as described below.

Human peritoneal macrophages, either from patients with (n=4) or without (n=3) SBP, were obtained after diagnostic paracentesis. Ascites was kept at 4°C to prevent the adhesion of the macrophages to the plastic. After centrifugation at 200 g for 10 min at 4°C, $6x10^5$ cells/well were seeded on 24-well plates (Costar, Cambridge, MA) in the ascitic fluid of the same patient from whom they were extracted. After incubation for 90 minutes at 37°C in a humidified atmosphere (95% air and 5% CO_2), the non-adherent cells were removed from the wells by three washes of 200 ml of pre-warmed Dulbecco phosphate buffered saline (DPBS), and the remaining adherent cells were incubated with phenol red-free RPMI-1640 medium supplemented with 2% heat-inactivated fetal calf serum, penicillin/streptomycin (50 U/ml and 50 mg/ml) and L-glutamine (2 mmol/l) at 37°C in a humidified atmosphere (95% air and 5% CO_2). More than 96% of the adherent cells were nonspecific esterase positive and had the morphological appearance of macrophages when examined after Giemsa staining.

Peripheral monocytes from healthy subjects (n=6) and cirrhotic patients with ascites with (n=4) or without SBP (n=6) were also isolated. Cells were obtained from fresh blood by venipuncture using acid citrate dextrose as anticoagulant. Blood was centrifuged at 800 rpm (15 min, room temperature) and leukocytes were fractionated by Ficoll-Hypaque gradient centrifugation. Then, monocytes were obtained from the mononuclear cell layer according to the method of Denholm and Wolber.[20] Briefly, mononuclear cells were resuspended in DPBS plus 0.1% bovine serum albumin (BSA), added to a percoll: 10x Hanks balanced salt solution (10:1.65 mixture) in a 10x1.5 cm round bottom

polypropylene tube and centrifuged at 1500 rpm, 25°C for 30 min. Monocytes were collected from the upper 5 mm of the gradient. Cytospin preparations of monocytes stained with Giemsa confirmed a 90-94% pure monocyte population. Cells were seeded on 24-well plates ($5x10^5$ cells/well) and incubated with RPMI-1640 medium under standard conditions of humidity and temperature.

Effect of LPS on CB2 messenger and protein expression and cell viability in U937 cells. Activated monocytic cells were washed and then incubated with RPMI-1640 supplemented with 1% heat-inactivated FBS and 10 ng/ml or 1μg/ml LPS (*E.coli* 055:B5;Sigma-Aldrich) for 6, 12, 24 and 30 h. Thereafter, mRNA and protein expression of CB2 and cell viability were determined by Real-Time PCR, Western blot and MTS assay, respectively. The specificity of the LPS effect was assessed by measuring mRNA expression of the CB2 receptor in the presence of the LPS inhibitor, Polymixin B (PMB, Sigma-Aldrich). PMB is a potent antibiotic that binds and neutralizes LPS. U937 cells were incubated with PMB (10 μg/ml) for 6, 12, 24 and 30 hours. At the end of the experiments, total RNA and proteins were extracted as described below. All experiments were reproduced at least 3 times in 3 independent assays.

Effect of LPS on endocannabinoid-induced cell migration in U937 cells. U937 differentiated cells were incubated in RPMI-1640 supplemented with 1% heat-inactivated fetal bovine serum in the absence or presence of LPS (1 μg/ml) for 6h. Directional migration was measured in the modified Boyden microchamber (NeuroProbe, Gaithersburg, USA). Cells were suspended and counted; subsequently 50 μl of cell suspension ($5×10^5$ cells/ml) was placed in the upper compartment with a polycarbonate membrane separating the two chambers. 2-arachydonylglycerol (2-AG, 1 μM), anandamide (AEA, 1 μM) or the

chemotactic tripeptide fMet-Leu-Phe (fMLP, 10 nM) were placed in the lower compartment of the chamber. When indicated, cells were also incubated in the presence of the CB2 receptor antagonist SR144528 (1 μM). After 3 h of incubation at 37°C, the cells on the upper side of the membrane were scraped off using a cotton swab and the cells that had migrated to the lower side of the filter were fixed with methanol. After staining with DiffQuick® solution (Dade Behring Inc., Newark, NJ), the cells that had migrated into the lower side were counted manually. The cells migration ability was expressed as the average cell number in four random microscopic fields (Olympus BX45, Olympus Corporation, Tokyo, Japan).

Patients. This part of the investigation was performed in circulating monocytes or peripheral macrophages isolated from 6 healthy volunteers and 16 cirrhotic patients (6 women, 10 men). The patients had a mean age of 61±12 years (range, 42-80). The etiology of cirrhosis was alcohol-induced in 5 subjects, 3 with hepatitis B surface antigen or hepatitis C–antibody associated, 3 with both alcohol-induced and viral hepatitis, 1 with chronic biliary cirrhosis and 4 of unknown etiology. The diagnosis of cirrhosis was established by liver biopsy in 12 cases and by clinical, laboratory, and ultrasonographic findings in the remaining cases. All patients had advanced liver cirrhosis and Child-Pugh score B or C. SBP was diagnosed on the basis of a polymorphonuclear cell count in ascitic fluid greater than or equal to 250 cells/mm^3 in the absence of clinical, radiologic, or laboratory data suggesting secondary peritonitis or other abdominal disorders resembling SBP (e.g., hemorrhage into ascites, pancreatitis, peritoneal tuberculosis, or carcinoma).

Cell Viability Assay. The effect of LPS treatment on U937 cell growth inhibition was studied by the MTS assay using CellTiter 96® Aqueous Assay kit (Promega, Madison, WI) following the manufacturer's instructions. Following LPS exposure, 20 μl of MTS working solution was added to each well, and the plate was incubated for 3 h at 37ºC in a CO_2 incubator. The viability was assessed on the basis of mitochondrial conversion of MTS [3-(4, 5-dimethylthiazol-2-yl)-5-(3-carboxymethoxyphenyl)-2-(4-sulfophenyl)-2H-tetrazolium, inner salt] into aqueous, soluble formazan. The quantity of formazan product is directly proportional to the number of living cells in culture and was measured by determining the A_{490nm} of the cell culture medium. The viability was calculated using the formula: % inhibition = (1 - $OD_{test}/OD_{control}$) x 100.

CB2 mRNA expression in U937 cells, human monocytes and peritoneal macrophages. See supplementary online material.

Western blot of CB2 receptor from U937 cells. See supplementary online material.

Bacterial signaling pathway PCR array. To assess the effects triggered by LPS on the transcriptome in human monocytes, activated U937 cells were incubated with LPS (10 ng/ml) for 6 h. RNA was extracted from cell lysates with TRIZOL followed by a RNA extraction column using the RNA easy kit (Qiagen, Venlo, The Netherlands). To remove residual DNA, RNA preparations were treated with RNase-Free DNAse set (Qiagen). First-strand cDNA was synthesized from 1 μg total RNA using an RT^2 first-strand kit (Qiagen) and PCR arrays were performed according to the manufacturer's

protocols (SABiosciences, Frederick, MD). Real-time PCR array for the bacterial signaling pathway was performed using human Antibacterial Response signaling pathway, RT^2 Profiler™ PCR array, (SABiosciences) according to the manufacturer's protocol. This PCR array combines the quantitative performance of SYBR Green-based real-time PCR with the multiple gene profiling capabilities of microarray to profile the expression of 84 key genes involved in innate immune response to bacteria. PCR array plates were processed in a Light Cycler 480 (Roche Diagnostics) using automated baseline and threshold cycle detection. Gene expression was normalized to internal controls to determine the fold change in gene expression between test and control samples. The relative quantity of product was expressed as fold-induction of the target gene compared with the reference gene according to the formula $2^{-\Delta\Delta CT}$. Data were interpreted using the SABiosciences' web-based PCR array data analysis tool.[21] Statistical significance is obtained after performing a Student's t-test analysis comparing to control samples.

Ethical approval. The study was performed according to the criteria of the Investigation and Ethics Committee of the Hospital Clínic Universitari.

Statistical analysis. Data are expressed as mean±SE. Statistical analysis of the results was performed by One-way analysis of variance (ANOVA) and Newman-Keuls post test or Kruskal-Wallis test with Dunns post-hoc to compare between groups or by an unpaired Student's t test or Mann-Whitney when appropriate. Differences were considered to be significant at a *p* value of 0.05 or less.

RESULTS

LPS stimulation downregulates CB2 mRNA in U937 cells. Time course expression of CB2 mRNA in LPS-treated U937 cells is shown in Figure 1. Both, pharmacological (1 μg/ml) and supraphysiological (10 ng/ml) doses of the bacterial wall product markedly inhibited transcript expression in the human monocytic cell line. This effect was observed as earlier as 6 hours following cells exposure to LPS and was significantly maintained for periods of time longer than 24 hours, regardless of using the higher or the lower dose of LPS. To ascertain whether the LPS-induced suppression of CB2 mRNA in U937 cells could be related with some effect on cell survival, monocytic cells were incubated with MTS to estimate the amount of living cells under the different experimental conditions. As shown in Figure 1A, no statistical differences in cell viability among human monocytic cells treated or not treated with LPS were observed at either, 10 ng/ml or 1 μg/ml.

Effect of LPS on CB2 protein expression. Next, Western blot experiments were conducted to further demonstrate the LPS-induced reduction of CB2 expression in human monocytes. In concordance with the RT-PCR data, following 6,12 or 24 hours exposure to LPS we observed an around 50% reduction of CB2 protein in U937 cells (Figure 1B). These results indicate that the inhibitory action of LPS on CB2 transcript expression is translated in decreased CB2 protein abundance in the human monocyte cell line.

PCR array of genes related to antibacterial response pathway. A quantitative RT-PCR (qRT-PCR) was performed to further confirm suppression of CB2 mRNA under LPS exposure in U937 cells and to compare these results with the well-established induction of LPS on other genes involved in

antibacterial response. Total RNA samples from control and LPS-treated cells were analyzed by using a commercially available PCR array that includes 84 representative genes from several biological pathways involved in antimicrobial response as well as CB receptors type 1 and 2 (*CNR1* and *CNR2*, respectively). Figure 2A displays a scatter plot report of the results obtained in the qRT-PCR array experiments indicating the position of several noteworthy genes based in their large fold differences in expression between control and LPS-exposed monocytes. Of the 86 genes assessed in this array, 17 genes demonstrated at least 2.5-fold difference between the two groups of experimental conditions. As displayed in Figure 2B, most of these differences disappeared when the experiments were performed in the presence of polymyxin B, a cationic antibiotic that prevents LPS cell binding and signaling.[22]

Table 1: Changes in expression for antibacterial response genes between untreated and LPS-treated (10 ng/ml) or LPS (10 ng/ml) + PMB (10 μg/ml) U937 cells. Genes from the experiment in figure 2 that exhibit at 2.5-fold or greater change in expression between control and LPS-treated cells are listed.

	LPS		LPS + PMB	
Genes	**Fold change**	**Significance**	**Fold change**	**Significance**
UPREGULATED GENES				
BIRC3	8.4	p<0.05	1.5	ns
CCL3	13.6	p<0.01	1.1	ns
CCL5	3.2	Ns	1.2	ns
CD14	3.0	Ns	1.2	ns
CXCL1	48.9	p<0.01	1.7	ns
CXCL2	92.4	p<0.01	3.5	ns
IL1β	15.1	p<0.01	1.8	ns
IL6	620.2	p<0.05	7.3	ns
IL8	14.1	p<0.01	1.8	p<0.05
NFKBIA	3.0	Ns	1.3	ns
RIPK2	2.7	p<0.01	1.0	ns
TNF	16.5	p<0.05	1.4	ns
DOWNREGULATED GENES				
DMBT1	2.5	Ns	1.0	ns
MAPK14	2.5	Ns	0.9	ns
PSTPIP1	2.9	Ns	0.9	ns
CNR1	8.7	p<0.001	0.5	p<0.05
CNR2	16.5	p<0.05	1.2	ns

As shown in Table 1, 12 genes were up-regulated by >2.5 fold change while 5 appeared to be down regulated in the LPS-treated samples. However, statistical differences were only reached in 9 upregulated and 2 downregulated genes, respectively. Interestingly, significant gene expression inhibitory effect of LPS was only seen in CB receptors 1 and 2.

LPS decreases endocannabinoid-induced chemotactic activity in U937 cells. Whether LPS-induced down-regulation of CB2 mRNA expression correlates with functionally significant changes was assessed by evaluating chemotactic activity in U937 cells. In fact, endocannabinoids have been shown to be powerful inducers of chemotaxis in macrophages and monocytes, including U937 cells.[23-27] In our hands, both 2-AG and AEA increased *in vitro* cell migration through the Boyden chamber in comparison to vehicle-treated cells. Moreover, cells pretreated with LPS showed a significantly attenuated endocannabinoid-induced chemotactic activity (Figure 3A). To further assess whether these effects are directly mediated by CB2 receptors, cells were exposed to AEA or 2-AG in the presence of SR144528 (1 μM), a specific antagonist of CB2 receptors. As illustrated in Figure 3B, CB2 receptor blockade fully prevented the chemotactic-induced effect of the endocannabinoid. These results indicate that LPS-induced down expression of CB2 receptors results into significant functional effects in human monocytic cells.

Monocytes and macrophages of cirrhotic patients showed a marked decrease in CB1 and CB2 mRNA expression. Hepatic cirrhosis is associated with enhanced circulating levels of bacterial wall derived products, the extreme manifestation of this condition being the development of SBP. Next, therefore,

we evaluated whether monocytic cells from cirrhotic patients without or with SBP present decreased expression of CB receptors. Circulating monocytes were isolated from blood of healthy subjects and cirrhotic patients, whereas peritoneal macrophages were obtained from ascites of cirrhotic patients without or with SBP. As compared to cells obtained from healthy subjects, circulating monocytes of cirrhotic patients showed an abrupt decrease in CB2 mRNA expression. This diminution was further accentuated at assessing the expression of this transcript in monocytes of patients with SBP, reaching values around 80% lower than monocytes of control subjects. Very low CB2 messenger expression was also observed in peritoneal macrophages of cirrhotic patients and become almost fully suppressed when macrophages were collected from ascites of patients with SBP (Figure 4). In agreement with the results obtained in the array analysis, a very similar pattern expression was found at assessing CB1 mRNA abundance in the same cells. Actually, Figure 4 also shows that CB1 receptor abundance was strongly reduced in circulating monocytes of cirrhotic patients and markedly reduced in peritoneal macrophages of patients with SBP.

DISCUSSION

The results of this investigation indicate that bacterial LPS reduces CB2 receptor expression in human monocytes resulting in depressed chemotactic activity and therefore impaired host defense response of these cells. In fact, CB2 mRNA expression is decreased in circulating monocytes and peritoneal macrophages of cirrhotic patients, a clinical condition characterized by enhanced LPS levels and increased susceptibility to bacterial infections, with

the down expression of the CB2 receptor being more accentuated when patients develop SBP.

There are compelling evidence indicating that the endogenous cannabinoid system is of major relevance in the regulation of the immune and host-defense mechanisms, most of these effects being mediated by interaction with central and peripheral CB2 receptors.[28] Actually, stimulation of these receptors attenuates the activation and release of proinflammatory mediators in neurodegenerative inflammatory disorders [29-31] and other inflammatory processes associated with liver [32,33] and cardiac [34] reperfusion injury, atherosclerosis,[36] inflammatory bowel disease [36,37] and rheumatoid arthritis.[38] Further indications on the fluid cross-talk between endocannabinoids and immunoresponse have been documented by several investigations demonstrating that the cytokine storm induced by exposing resident macrophages to LPS is markedly attenuated when these cells are stimulated with AEA [39] or selective CB2 receptor agonists such as HU-910.[33] In this scenario, our results showing that LPS markedly suppresses CB2 receptor expression may help to understand the mechanisms governing host defense depletion in pathological conditions characterized by sustained levels of endotoxin. This finding coincides with previous investigations indicating that LPS suppresses CB2 mRNA in murine B cells [13] due to the ability of LPS to modify the transcriptional start site of CB2 messenger in murine splenocytes.[40]

Pattern recognition receptors are the gate by which cells of the immune system, including lymphocytes and macrophages recognize bacterial-derived products, triggering cytokine and chemokine release which, in turn, promote

leukocyte attraction to the site of infection.[41] In addition, recent studies have demonstrated that AEA and 2-AG may also induce chemotactic activity, which is mainly mediated by CB2 receptors, in these cells.[25] Since chemotaxis is a fundamental component of the leukocyte armamentarium to fight against bacterial infection we next assessed whether LPS-induced suppression of CB2 receptors may result in a significant impairment in human leukocyte motility. Our findings showed that, in the *in vitro* motility assay, the endocannabinoids AEA and 2-AG induced migration of the human lymphocyte cell line and that LPS pretreatment significantly attenuated the migratory-induced effect of the endocannabinoids. This effect was reversed by the CB2-selective antagonist SR144528, thus confirming a role for CB2 receptors. These results demonstrating chemotactic CB2-dependent activity are in line with previous studies showing 2-AG induced migration in human polymorphonuclear cells, eosinophils, neutrophils and natural killer cells,[26,27,42] an effect which was reversed by SR144528 in all these cases.[43] Taken together our results show CB2-dependent U937 cell migration in response to endocannabinoids and that pre-exposure to LPS has the capacity to inhibit migration to these stimuli. This is an important issue, since under conditions of bacterial infection, such as SBP, enhanced migration into tissues is beneficial, but its inhibition by CB2 receptor down regulation may result in impairment of host defense response mechanisms.

To gain insight into the molecular mechanisms of endotoxin-induced down expression of CB2 receptor in human monocytes we analyzed changes in U937 cell gene expression. A quantitative RT-PCR analysis was performed using a human RT-profile PCR array which contains 84 bacterial response-

related genes and two genes corresponding to CB receptors. To our knowledge this is the first study on the effect of LPS on human monocyte gene expression using high throughput technology which offers the possibility of a wide scale analysis of genes involved in these specific pathways. Transcriptional profiling revealed that the expression of 11 genes was significantly changed in LPS-treated U937 cells compared with non stimulated cells. Most of these genes are closely related to the inflammatory response and most specifically with cytokine activation (*IL1β*, *IL6*, *IL8* and *TNF*) and chemokine receptors (*CCL3*, *CCL5*, *CXCL1* and *CXCL2*). Several genes' functions involve important pathological processes including negative regulation of inflammatory signaling pathways (*BIRC3*) [44] and detection of endotoxin by Toll-like receptors (*RIPK2*).[45] However, it is important to note that the only genes significantly reduced in LPS treated cells were *CNR1* and *CNR2* which encode for CB1 and CB2 receptors, respectively. Interestingly, all these changes in gene expression were almost fully suppressed when the experiments were performed in the presence of PMB, thus demonstrating the specificity of the effect triggered by LPS. This remarkable observation indicates that endotoxin induced suppression of CB receptor is a highly specific effect for endocannabinoid signaling.

Bacterial infections are a life-threatening event frequently occurring in patients with liver disease.[46] Infections are major precipitating agents of the underlying liver disease and are associated with high mortality rates.[47] The increased susceptibility to infection in patients with cirrhosis has been attributed to alterations in the immune response, including defective chemotaxis.[48] Since our *in vitro* assay demonstrated that LPS impairs cell mobility upon endocannabinoid challenge by a CB2 receptor-dependent mechanism, we next

assessed CB2 receptor expression in macrophages of cirrhotic patients with and without SBP. In agreement with the results obtained in the *in vitro* experiments, blood and peritoneal macrophages of cirrhotic patients showed a significant downregulation of CB receptors, this reduction being much more intense when cell were isolated from patients with SBP.

Leukocytes are a major source of endocannabinoids. Under a framework of increased bacterial wall products, such as in advanced liver disease, LPS stimulation result in 2-AG and AEA secretion.[49] Since CB2 receptors are abundantly expressed in cells of the monocytic lineage the anticipated response among others would be enhanced mobility toward the site of infection. However, LPS as demonstrated in the present investigation, would also suppress CB2 receptor expression and therefore, the leukocyte ability to respond against bacterial infection becomes seriously compromised. This, in turn, will provide a further explanation for the impaired defense response mechanisms in cirrhotic patients with liver disease.

REFERENCES

1. Munro S, Thomas KL, Abu-Shaar M. Molecular characterization of a peripheral receptor for cannabinoids. *Nature* 1993;**365**:61-65.
2. Galiègue S, Mary S, Marchand J, et al. Expression of central and peripheral cannabinoid receptors in human immune tissues and leukocyte subpopulations. *Eur J Biochem* 1995:**232**,54-61.
3. Carayon P, Marchand J, Dussossoy D, et al. Modulation and functional involvement of CB2 peripheral cannabinoid receptors during B-cell differentiation. *Blood* 1998;**92**:3605-15.
4. Lee SF, Newton C, Widen R, et al. Differential expression of cannabinoid CB(2) receptor mRNA in mouse immune cell subpopulations and following B cell stimulation. *Eur J Pharmacol* 2001;**423**:235-41.
5. Jordà MA, Verbakel SE, Valk PJ, et al. Hematopoietic cells expressing the peripheral cannabinoid receptor migrate in response to the endocannabinoid 2-arachidonoylglycerol. *Blood* 2002;**99**:2786-93.
6. Rayman N, Lam KH, Laman JD, et al. Distinct expression profiles of the peripheral cannabinoid receptor in lymphoid tissues depending on receptor activation status. *J Immunol* 2004;**172:**2111-17.
7. Massi P, Sacerdote P, Ponti W, et al. Immune function alterations in mice tolerant to delta9-tetrahydrocannabinol: functional and biochemical parameters. *J Neuroimmunol* 1998;**92**:60-66.
8. Marchand J, Bord A, Pénarier G, et al. Quantitative method to determine mRNA levels by reverse transcriptase-polymerase chain reaction from leukocyte subsets purified by fluorescence-activated cell sorting: application to peripheral cannabinoid receptors. *Cytometry* 1999;**35**:227-34.
9. Jordà MA, Lowenberg B, Delwel R. The peripheral cannabinoid receptor CB2, a novel oncoprotein, induces a reversible block in neutrophilic differentiation. *Blood* 2003;**101**:1336-43.
10. Tanikawa T, Kurohane K, Imai Y. Induction of preferential chemotaxis of unstimulated B-lymphocytes by 2-arachidonoylglycerol in immunized mice. *Microbiol Immunol* 2007;**51**:1013-19.
11. Schroder AJ, Pavlidis P, Arimura A, et al. Cutting edge: STAT6 serves as a positive and negative regulator of gene expression in IL-4-stimulated B lymphocytes. J *Immunol* 2002;**168**:996-1000.

12. Agudelo M, Newton C, Widen R, et al. Cannabinoid receptor 2 (CB2) mediates immunoglobulin class switching from IgM to IgE in cultures of murine-purified B lymphocytes. *J Neuroimmune Pharmacol* 2008;**3:**35-42.
13. Lee SF, Newton C, Widen R, et al. Downregulation of cannabinoid receptor 2 (CB2) messenger RNA expression during in vitro stimulation of murine splenocytes with lipopolysaccharide. *Adv Exp Med Biol* 2001;**493:**223-228.
14. Rimola A, Navasa M. Infections in liver disease. In: Bircher J, Benhamou JP, McIntyre N, Rizzetto M, Rodés J, eds. Oxford Textbook of Clinical Hepatology. New York: Oxford University Press 1999:1862-1874.
15. Guarner C, Soriano G. Spontaneous bacterial peritonitis. *Semin Liver Dis* 1997;**17**:203-17.
16. Navasa M, Follo A, Filella X, et al. Tumor necrosis factor and interleukin-6 in spontaneous bacterial peritonitis in cirrhosis: relationship with the development of renal impairment and mortality. *Hepatology* 1998;**27**:1227-32.
17. Wagner JA, Varga K, Ellis EF, et al. Activation of peripheral CB1 receptors in hemorrhagic shock. *Nature* 1997*;***390**:518-521.
18. Ros J, Clària J, To-Figueras J, et al. Endogenous cannabinoids: a new system involved in the homeostasis of arterial pressure in experimental cirrhosis in the rat. *Gastroenterology* 2002;**122**:85-93.
19. Tanabe SI, Grenier D. Macrophage tolerance response to *Aggregatibacter actinomycetemcomitans* lipopolysaccharide induces differential regulation of tumor necrosis factor-α, interleukin-1β and matrix metalloproteinase 9 secretion. *J Peridont Res* 2008;**43**:372-377.
20. Denholm EM, Wolber FM. A simple method for the purification of human peripheral blood monocytes. A substitute for sepracell-MN. *J Immunol Methods* 1991;**144**:247-251.
21. RT^2 Profiler PCR array data analysis version 3.5. SABiosciences (Qiagen) http://pcrdataanalysis.sabiosciences.com/pcr/arrayanalysis.php (accessed 28 Aug 2012).
22. Ros J, Leivas A, Jiménez W, et al. Effect of bacterial lipopolysaccharide on endothelin-1 production in human vascular endothelial cells. *J Hepatology* 1997;**26**:81-87.
23. Kishimoto S, Gokoh M, Oka S, et al. 2-arachidonoylglycerol induces the migration of HL-60 cells differentiated into macrophage-like cells and human peripheral blood monocytes through the cannabinoid CB2 receptor-dependent mechanism. *J Biol Chem* 2003;**278:**24469-75.

24. Maestroni GJ. The endogenous cannabinoid 2-arachidonoyl glycerol as in vivo chemoattractant for dendritic cells and adjuvant for Th1 response to a soluble protein. *FASEB J* 2004;**18**:1914-16.
25. Walter L, Franklin A, Witting A, et al. Nonpsychotropic cannabinoid receptors regulate microglial cell migration. *J Neurosci* 2003;**23:**1398-1405.
26. Oka S, Ikeda S, Kishimoto S, et al. 2-arachidonoylglycerol, an endogenous cannabinoid receptor ligand, induces the migration of EoL-1 human eosinophilic leukemia cells and human peripheral blood eosinophils. *J Leukoc Biol* 2004;**76:**1002-9.
27. Kurihara R, Tohyama Y, Matsusaka S, et al. Effects of peripheral cannabinoid receptor ligands on motility and polarization in neutrophil-like HL60 cells and human neutrophils. *J Biol Chem* 2006;**281:**12908-18.
28. Klein TW. Cannabinoid-based drugs as anti-inflammatory therapeutics. *Nat Rev Immunol* 2005;**5:**400-11.
29. Correa F, Hernangómez M, Mestre L, et al. Anandamide enhances IL-10 production in activated microglia by targeting CB(2) receptors: roles of ERK1/2, JNK, and NF-kappaB. *Glia* 2010;**58:**135-47.
30. Chung ES, Bok E, Chung YC, et al. Cannabinoids prevent lipopolysaccharide-induced neurodegeneration in the rat substantia nigra in vivo through inhibition of microglial activation and NADPH oxidase. *Brain Res* 2012;**1451:**110-16.
31. Romero-Sandoval EA, Horvath R, Landry RP, et al. Cannabinoid receptor type 2 activation induces a microglial anti-inflammatory phenotype and reduces migration via MKP induction and ERK dephosphorylation. *Mol Pain* 2009:**5:**25.
32. Bátkai S, Mukhopadhyay P, Horváth B, et al. Δ8-Tetrahydrocannabivarin prevents hepatic ischaemia/reperfusion injury by decreasing oxidative stress and inflammatory responses through cannabinoid CB2 receptors. *Br J Pharmacol* 2012;**165:**2450-61.
33. Horváth B, Magid L, Mukhopadhyay P, et al. A new cannabinoid CB2 receptor agonist HU-910 attenuates oxidative stress, inflammation and cell death associated with hepatic ischaemia/reperfusion injury. *Br J Pharmacol* 2012;**165**:2462-78.
34. Wang PF, Jiang LS, Bu J, et al. Cannabinoid-2 receptor activation protects against infarct and ischemia-reperfusion heart injury. *J Cardiovasc Pharmacol* 2012;**59**:301-07.
35. Zhao Y, Liu Y, Zhang W, et al. WIN55212-2 ameliorates atherosclerosis associated with suppression of pro-inflammatory responses in ApoE-knockout mice. *Eur J Pharmacol* 2010;**649:**285-92.

36. Wright KL, Duncan M, Sharkey KA. Cannabinoid CB2 receptors in the gastrointestinal tract: a regulatory system in states of inflammation. *Br J Pharmacol* 2008;**153:**263-70.
37. Alhouayek M, Lambert DM, Delzenne NM, et al. Increasing endogenous 2-arachidonoylglycerol levels counteracts colitis and related systemic inflammation. *FASEB J* 2011;**25:**2711-21.
38. Sumariwalla PF, Gallily R, Tchilibon S, et al. A novel synthetic, nonpsychoactive cannabinoid acid (HU-320) with anti-inflammatory properties in murine collagen-induced arthritis. *Arthritis Rheum* 2004;**5:**985-98.
39. Puffenbarger RA, Boothe C, Cabral GA. Cannabinoids inhibit LPS-inducible cytokine mRNA expression in rat microglial cells. *Glia* 2000;**29:**58-69.
40. Sherwood TA, Nong L, Agudelo M, et al. Identification of transcription start sites and preferential expression of select CB2 transcripts in mouse and human B lymphocytes. *J Neuroimmune Pharmacol* 2009;**4:**476-88.
41. Akira S, Uematsu S, Takeuchi O. Pathogen recognition and innate immunity. *Cell* 2006;**124**:783-801.
42. Kishimoto S, Muramatsu M, Gokoh M, et al. Endogenous cannabinoid receptor ligand induces the migration of human natural killer cells. *J Biochem* 2005;**137:**217-23.
43. Basu S, Dittel BN. Unraveling the complexities of cannabinoid receptor 2 (CB2) immune regulation in health and disease. *Immunol Res* 2011;**51:**26-38.
44. Rossi D, Fangazio M, Rasi S, et al. Disruption of BIRC3 associates with fludarabine chemorefractoriness in TP53 wild-type chronic lymphocytic leukemia. Blood 2012;**119:**2854-62.
45. Chin AI, Dempsey PW, Bruhn K, et al. Involvement of receptor-interacting protein 2 in innate and adaptative immune responses. *Nature* 2002;**416:**190-94.
46. Fernández J, Gustot T. Management of bacterial infections in cirrhosis. *J Hepatol* 2012;**56**:S1-12.
47. Thulstrup AM, Sørensen HT, Schønheyder HC, et al. Population-based study of the risk and short-term prognosis for bacteremia in patients with liver cirrhosis. *Clin Infect Dis* 2000;**31:**1357-61.
48. Geerts AM, Cheung KJ, Van Vlierberghe H, et al. Decreased leukocyte recruitment in the mesenteric microcirculation of rats with cirrhosis is partially restored by treatment with peginterferon: an in vivo study. *J Hepatol* 2007;**46:**804-15.
49. Di Marzo V, Bisogno T, De Petrocellis L, et al. Biosynthesis and inactivation of the endocannabinoid 2-arachidonoylglycerol in circulating and tumoral macrophages. *Eur J Biochem* 1999;**264:**258-67.

FIGURE LEGENDS

Figure 1. CB2 mRNA, protein expression, cell viability in the U937 human monocyte cell line. (A) mRNA expression of U937 cells was assessed in resting conditions and following exposure to LPS for different time incubation periods by quantitative RT-PCR as described in the material and methods section. Full circles represent the results of the cell viability assay obtained under the different experimental conditions. **(B)** Representative Western blot of CB2 protein expression levels in U937 cells treated with medium alone (M) or LPS (10 ng/ml) at 6, 12 and 24 h. Eighty micrograms of protein lysate from U937 cells was loaded per lane. The lower panel shows the densitometric analysis of all the experiments normalized to β-actin. The results were confirmed by 3 independent experiments. Results are given as means ± SE; * $p<0.05$, ** $p<0.01$ and *** $p<0.001$ vs. medium. Statistical analysis was calculated by an unpaired Student's t-test.

Figure 2. Antibacterial response genes PCR array. Relative expression comparison for 86 antibacterial response-related genes between non-treated, LPS (10 ng/ml)-treated and LPS (10 ng/ml) + PMB (10 µg/ml)-treated U937 cells. This figure represents a log transformation plot of the relative expression level of each gene ($2^{-\Delta Ct}$) between non treated U937 cells (x axis) and LPS or LPS+PMB treated U937 cells (y axis). The dashed lines and full circles indicate ≥ 2.5-fold change in the gene expression threshold. The results were confirmed by 3 independent experiments.

Figure 3. Migration assay in the U937 monocyte cell line towards 2-AG and AEA. (A) Migration assay of U937 cells towards 2-AG and AEA incubated with LPS (1 μg/ml), saline as vehicle and fMLP (10 nM) as positive control. The results are given as migrated cells/field. **(B)** Right panels show migration towards AEA and 2-AG plus a selective CB2 antagonist SR144528 (1 μM). The results were confirmed by at least 3 independent experiments. Results are given as mean±SE; * $p<0.05$, ** $p<0.01$ vs. untreated cells, *** $p<0.001$ vs. vehicle, $^{\#}$ $p<0.001$ vs. 2-AG-vehicle, † $p<0.001$ vs. AEA-vehicle, ^{c} $p<0.001$ vs. 2-AG and ^{b} $p<0.01$ vs. AEA. Statistical analysis was calculated by One-way ANOVA with Newman-Keuls post-hoc test and Kruskal-Wallis test with Dunns post-hoc test when appropriate.

Figure 4. CB1 and CB2 mRNA expression in human circulating monocytes and peritoneal macrophages of healthy subjects and cirrhotic patients. mRNA expression of both CB1 and CB2 receptors were analyzed by Real Time PCR. Circulating monocytes and peritoneal macrophages were extracted from cirrhotic patients with ascites with or without SBP. Circulating monocytes from healthy subjects were used as control. The results were confirmed by at least 3 independent experiments. Results are given as means ± SE; * $p<0.05$; ** $p<0.01$ and *** $p<0.001$ vs. control monocytes; ^{a} $p<0.05$ vs. cirrhotic macrophages. Statistical analysis was calculated by unpaired Student's t-test or One-way ANOVA when appropriated.

Fig 1.

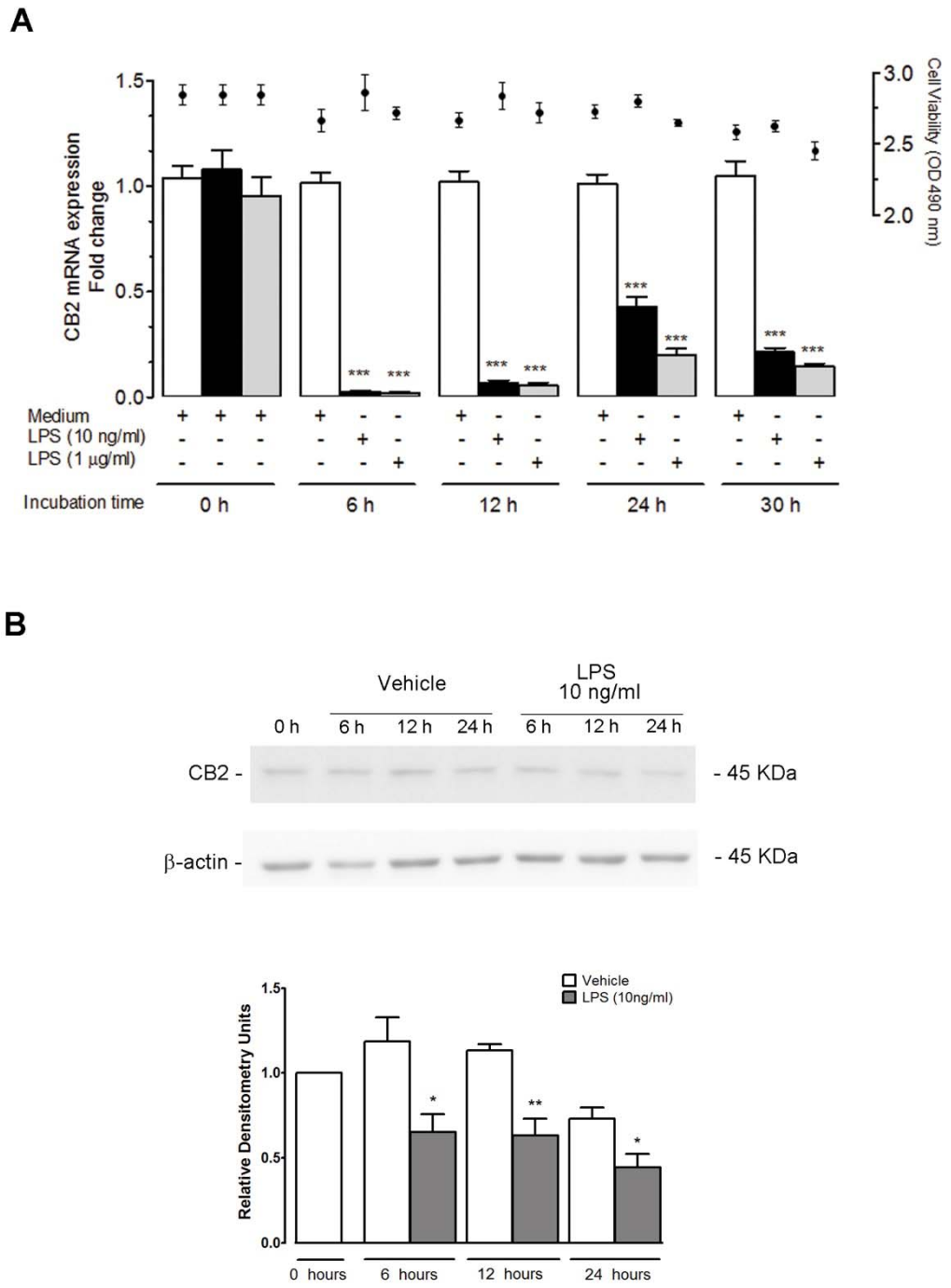
A
CB2 mRNA expression
Fold change
Cell Viability (OD 490 nm)
1.5
1.0
0.5
0.0
3.0
2.5
2.0
***
Medium
LPS (10 ng/ml)
LPS (1 µg/ml)
Incubation time
0 h
6 h
12 h
24 h
30 h
B
Vehicle
LPS
10 ng/ml
0 h
6 h
12 h
24 h
6 h
12 h
24 h
CB2 -
- 45 KDa
β-actin -
- 45 KDa
Relative Densitometry Units
Vehicle
LPS (10ng/ml)
1.5
1.0
0.5
0.0
*
**
0 hours
6 hours
12 hours
24 hours

Fig. 2

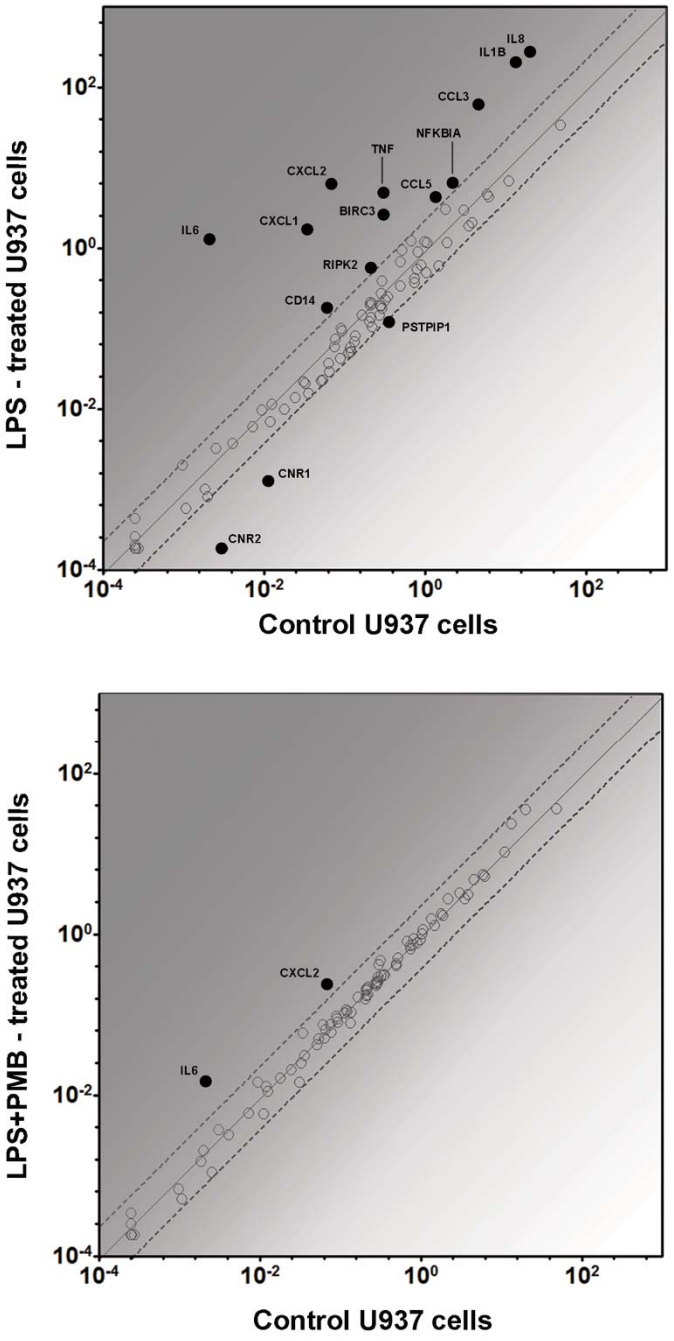
IL8
IL1B
CCL3
NFKBIA
TNF
CXCL2
CCL5
BIRC3
CXCL1
IL6
RIPK2
CD14
PSTPIP1
CNR1
CNR2
LPS - treated U937 cells
Control U937 cells
CXCL2
IL6
LPS+PMB - treated U937 cells
Control U937 cells

Fig. 3

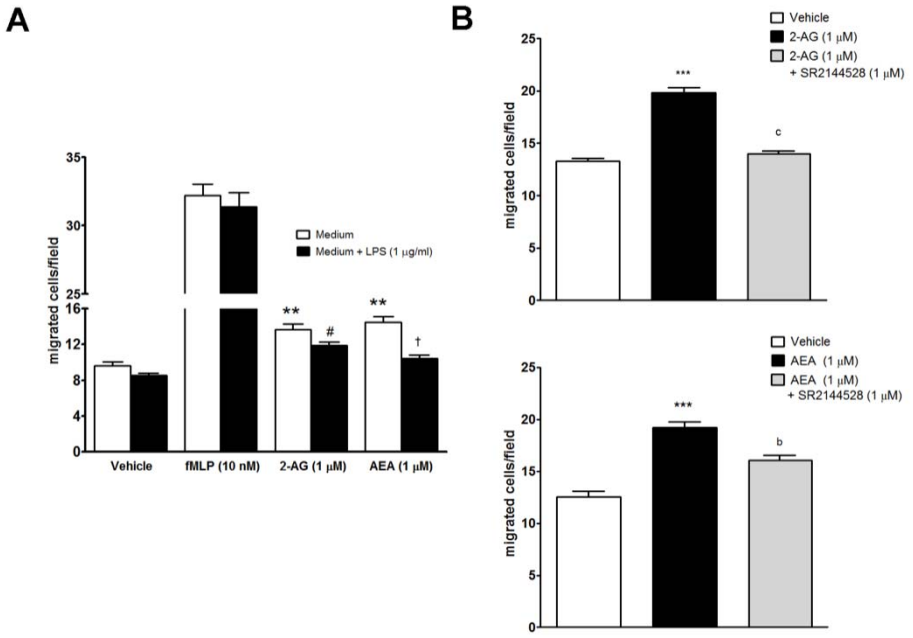
A
migrated cells/field
Medium
Medium + LPS (1 μg/ml)
Vehicle
fMLP (10 nM)
2-AG (1 μM)
AEA (1 μM)
B
Vehicle
2-AG (1 μM)
2-AG (1 μM)
+ SR2144528 (1 μM)
migrated cells/field
Vehicle
AEA (1 μM)
AEA (1 μM)
+ SR2144528 (1 μM)
migrated cells/field

Fig. 4

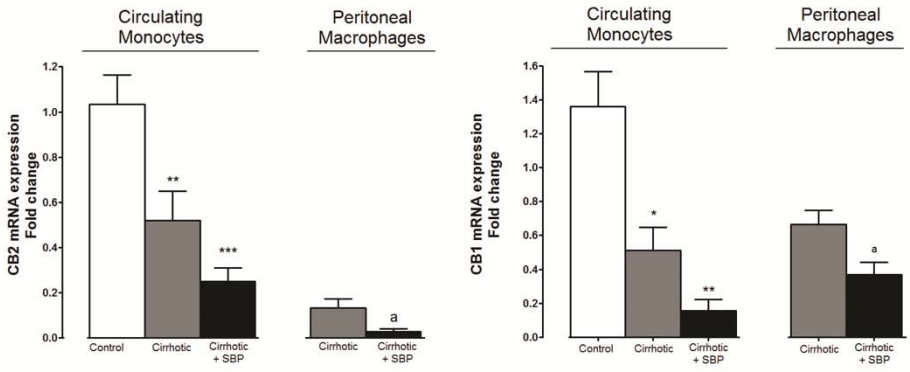
Circulating Monocytes
Peritoneal Macrophages
CB2 mRNA expression Fold change
Control
Cirrhotic
Cirrhotic + SBP
Circulating Monocytes
Peritoneal Macrophages
CB1 mRNA expression Fold change
Control
Cirrhotic
Cirrhotic + SBP

SUPLEMENTARY MATERIAL

MATERIAL AND METHODS

CB2 mRNA expression in U937 cells, human monocytes and peritoneal macrophages. Total RNA from cultured cells was extracted using a commercially available kit (TRIZOL, Gibco-Invitrogen). RNA concentration was determined by spectrophotometric analysis (ND-100 Spectrophotometer, Nanodrop Technology, Thermo Fisher Scientific, Waltham, MA). One μg of total RNA was reverse transcribed (RT) using a complementary DNA synthesis kit (High-Capacity cDNA Reverse Transcription Kit, Applied Biosystems, Foster City, CA). Real-Time PCR was performed with TaqMan probes designed with the TaqMan Gene Expression assay software from Applied Biosystems. Human CB2 receptor assay reference: Hs00275635_m1 and human HPRT assay reference: Hs01003267_m1, were designed according to the human CB2 receptor (CNR2) and HPRT gene sequence (GenBank NM_001841 and NM_000194.2), respectively. When indicated, human CB1 mRNA expression was also assessed using human CB1 receptor assay reference: Hs00275634_m1 according to the human CB1 (CNR1) gene sequence. Real time quantitative PCR was analyzed in duplicate and performed with the Light Cycler 480 (Roche Diagnostics, Indianapolis, IN). Ten μl total volume reaction of diluted 1:8 cDNA, TaqMan Universal PCR Master Mix and TaqMan Gene Expression Assay Mix, were used in each PCR reaction. Fluorescence signal was captured during each of the 45 cycles (denaturizing 10 sec at 95ºC, annealing 20 sec at 60ºC and extension 1 sec at 72ºC). HPRT was used as a reference gene for normalization, and water was used as a negative control. Relative quantification was calculated using the comparative threshold cycle (CT), which is inversely related to the abundance of mRNA transcripts in the initial sample. The mean CT of duplicate measurements was used to calculate ΔCT as the difference in CT for target and reference. The relative quantity of product was expressed as fold-induction of the target gene compared with the reference gene according to the formula $2^{-\Delta\Delta CT}$,

where ΔΔCT represents ΔCT values normalized with the mean ΔCT of control samples.

Western blot of CB2 receptor from U937 cells. The cultured cells were scraped with 1ml of buffer solution with Tris–HCl 20 mM, pH 7.4, containing 1% Triton X-100, 0.1% SDS, 50 mM NaCl, 2.5 mM EDTA, 1 mM Na4P2O7 10H2O, 20 mM NaF, 1 mM Na3VO4, 2 mM Pefabloc and Complete Mini (Roche Diagnostics). CB2 was separated on a 10% SDS-polyacrylamide (Mini Protean III, Bio-Rad, Richmond, CA) and transferred for 2h at 4°C to a nitrocellulose membrane (Transblot Transfer Medium, Bio-Rad). The membranes were stained with Ponceau-S red as a control for protein loading. Thereafter, the membranes were blocked overnight at 4ºC with 5% powdered non-fat milk in TTBS buffer. Then they were incubated for 2h at room temperature with rabbit polyclonal anti-CB2 (1:750, Cayman Chemical, Ann Arbor, MI, USA) or anti-β-actin (1:1000, Cell Signaling Technology, Beverly, MA) followed by incubation with horseradish peroxidase conjugated anti-rabbit antibody (1:2000, Amersham Biosciences, Uppsala, Sweden). Bands were visualized by chemiluminescence (ECL Western blotting analysis system; Amersham Biosciences).

DISCUSSION

In the clinical practice, the assessment of liver fibrosis degree is the starting point to initiate the treatment of patients with HCV infection, but is also very important as a diagnosis tool in order to determine the stage and the progression of the disease. For many years, the most frequently used methodology has been the liver biopsy, however, as explained earlier, it is an invasive method with its consequent risks and it is not always accurate. For this reason, there was an urgent need to search for new non-invasive tools to assess the degree of fibrosis, such as serum biomarkers. Liver fibrosis is the consequence of excessive ECM accumulation produced by sustained damage to the liver. The fibrotic matrix is mainly constituted of collagen fibers type I, III and IV that slowly accumulate over time, but also, it is also degraded to a lesser extent. The release of these degradation products to the blood flow is a manifestation of the continuous ECM turnover occurring in the liver tissue during fibrosis progression. In the first study, we assessed the efficacy of a new collagen III degradation product, CO3-610 as a serum biomarker (Barascuk et al., 2010). In order to achieve these results, the animals studied were classified into four groups according to the amount of collagen content instead of the weeks of CCl_4 treatment, as we observed that the individual response to the hepatotoxic agent varies between animals. The results showed that CO3-610, quantified by serum ELISA, was able to discriminate between mild/moderate, advanced fibrosis and cirrhosis stages, but not between controls and mild/moderate fibrosis. This suggests that CO3-610 might be more effective to assess advanced liver disease than in initial stages. CO3-610 was previously tested in a model of acute damage (Vassiliadis et al., 2011), in this study we showed that CO3-610 serum levels were significantly correlated with the liver histology after 20 weeks of CCl_4 treatment.

The most relevant finding of this study was that CO3-610 presented a strong relationship with the portal pressure. Together with the liver biopsy, the assessment of the hepatic venous pressure gradient (HVPG) is a very important tool for the diagnosis, staging and prognosis of the liver disease. Furthermore, in our study and with our animal model, CO3-610 showed a closer relationship with the collagen content than HA. This is important because HA is considered as an accurate serum marker in NAFLD and Virus C hepatitis (Guéchot et., 1996; Suzuki et al., 2005).

Interstitial collagen type I and III are the main components of fibrotic livers and the activation of the mRNA expression of collagen is considered to be a sensitive marker of active fibrogenesis. In our study, collagen 1α2 mRNA behaved as a quantitative index of fibrosis progression in contrast to collagen 3α1, which was activated in fibrotic rats, but remained at the same level in cirrhotic animals. However, when analyzing collagen type III protein accumulation by immunohistochemistry, there was an evident increase in cirrhotic tissue over fibrotic, probably due to a decrease of interstitial collagen degradation in advanced disease. The increase of MMP and TIMP expression is also a hallmark of fibrogenesis and matrix changes. In agreement with previous studies, in fibrotic animals both gelatinases (MMP2 and MMP9) and TIMP1 and 2 were upregulated. However, MMP9 mRNA levels dropped almost to control levels in cirrhotic rats, as MMP9 has been associated with early fibrosis and inflammation rather than cirrhosis.

The availability of an efficient serum biomarker able to assess accurately each stage during liver fibrosis progression would definitely improve the diagnosis and treatment of liver diseases. On the other hand, since ECM deregulation due to collagen accumulation is the main consequence of liver stiffness, deeper research on therapeutic strategies aimed at ECM modulation might be worth investigating. Another appealing strategy to treat liver diseases is through therapies focused on fibrosis progression prevention rather than reversion. In this regard, previous studies from our laboratory described that the activation of CB2 receptors by a selective agonist could induce liver fibrosis regression (Muñoz-Luque et al., 2008). Inspired by this last work, we sought to describe the role of two independent endogenous systems, the endocannabinoid and apelin systems in fibrosis progression prevention. The results indicate that the chronic administration of either AM1241 (CB2 receptor agonists) or F13A (APJ antagonist) reduce the hepatic collagen content in rats under continued CCl_4-inhalation-induced liver damage. Both long-term treatments prevented fibrosis progression through common mechanisms despite the dissimilarities between the APJ and CB2 signaling pathways, thus opening new avenues for prevention treatments in liver diseases. The improvement observed in the hepatic collagen content after AM1241 or F13A administration, was associated with a significant amelioration of the systemic and portal hemodynamics, reduced angiogenesis,

inflammatory infiltrate and apoptosis compared to vehicle-treated rats. Additionally, CB2 receptor stimulation also improved liver inflammation as indicated by AST and ALT serum decrease. Moreover, a panel of key genes involved in the fibrogenesis process was analyzed. The pharmacological stimulation of CB2 receptors and inhibition of the apelin activity reduced the messenger expression of genes related to PDGF signaling, HSC activation and ECM turnover.

The main reason for choosing this therapeutic strategy was that CB2 receptor agonism has not been related to central side effects, moreover, our group and others have already demonstrated the antifibrogenic properties of these receptors in advanced liver disease. AM1241 is one of the most selective CB2 receptor agonists currently available (Malan et al., 2001). F13A is an apelin-13 analog in which the phenylalanine C-terminus of the peptide is substituted by an alanine residue that behaves as an apelin specific antagonist. The interaction of this agonist with APJ fully abolishes the apelin downstream signaling (Lee et al., 2005). There is much experimental evidence pointing at the apelin system as an important mediator of the initiation and perpetuation of the inflammatory and fibrogenic processes occurring in the cirrhotic liver (Principe et al., 2008; Melgar-Lesmes et al., 2010, 2011).

Of note is that in contrast of what we previously found in cirrhotic rats, the administration of AM1241 and F13A to fibrotic rats inhibited apoptosis in fibrotic rats, we believe it is probably related to the different degrees of active fibrogenesis between the two groups of CCl_4-treated rats. In this study, the rats were at the initial phases of fibrosis, therefore the active fibrogenesis was higher than in rats with fully established cirrhosis (Iredale, 2007).

Stellate cell activation is characterized by the acquisition of a proliferative, proinflammatory and contractile phenotype of quiescent HSCs. The most accepted activation cell marker is α-SMA. Our results showed that both treatments reduced the expression of this mRNA, suggesting that HSC activation was repressed after CB2 agonism and APJ antagonism. In addition, our results also showed that both CB2 stimulation and APJ blockade interfere with the production of profibrogenic and tissue repair mediators produced by chronic liver injury. Both AM1241 and F13A had an inhibitory effect on PDGF signaling by decreasing the expression of PDGFRβ. Considering that PDGF is the most potent proliferation cytokine, this effect is of great

importance because the mechanism of action of both treatments involves the reduction of HSC proliferation, therefore, the progression of fibrosis is halted.

Furthermore, our results also showed that CB2 stimulation and APJ blockade also seem to interfere ECM turnover genes. The net formation of scar tissue depends on the balance between the synthesis and degradation. According to the first study, untreated rats presented and induction of Col1α2, MMP2 and both TIMP1 and 2 mRNA expression. In contrast, treated rats showed an increase of MMP/TIMP ratio in agreement with the inhibition of fibrosis progression. The altered ratio was due to TIMP1 inhibition rather than to further activation of MMP2, further supporting the concept that TIMPs are the main regulators of ECM degradation by controlling the activity of the secreted MMPs.

The second study showed that HSC activation and ECM turnover could be modulated by two different antifibrogenic agents. In connection with that, we next studied the effect of impairing PDGF signaling by interfering with PDGFRβ through the adenoviral transduction of a dominant-negative soluble form of PDGFRβ (sPDGFRβ). Following the same methodology of the first study, the rats were grouped into 3 groups (control, fibrosis and cirrhosis) according to the histological quantification of the liver collagen content. The progressive deposition of the collagen content during the evolution of the liver disease correlated with the mRNA expression of PDGFRβ demonstrating that PDGFRβ can discriminate between the different stages of fibrosis. Moreover, there was a significant relationship between the deterioration of the hemodynamic parameters and the hepatic collagen content, particularly relevant in the case of portal pressure. Taking into account the last results and the relevant role of PDGF in liver fibrosis, we evaluated the therapeutic effects of intravenous administration of sPDGFRβ. It has been described that adenoviral transduction of this soluble form blocks the activation of HSC and attenuates fibrosis induced by bile duct ligation in rats (Borkham-Kamphorst et al., 2004). *In vitro* assays showed that sPDGFRβ protein was present in HepG2 cells supernatants, confirming the effectiveness of the transduction and its protein expression in this cell type. Furthermore, the analysis *in vivo* seven days after the administration of the adenovirus confirmed the expression of sPDGFRβ in the serum of fibrotic rats. Adenoviral transduction might induce toxicity in

humans, however in our animal model, no significant differences where observed in serum parameters of liver and renal function after the transduction or either β-gal or sPDGFRβ adenovirus, therefore confirming that the adenovirus transduction did not induce an inflammatory response. The pharmacological inhibition of the phosphorylation of tyrosine kinase receptors has been largely investigated. The combined inhibition of VEGF and PDGF produced a reduction in the portal pressure of cirrhotic rats (Tugues et al., 2007; Fernández et al., 2007). Specific disruption of PDGF signaling by the adenovirus encoding for sPDGFRβ was associated with a significant amelioration in the systemic and portal hemodynamics, as reflected by an increase of MAP and a decrease of PP, compared to β-gal-treated animals.

Adenoviral transduction significantly attenuated the hepatic collagen content and protein expression of α-SMA, which is consistent with previous studies (Liu et al., 2011). Autophosphorilation of PDGFRβ is a prerequisite for PDGF downstream signaling through Ras/ERK regulated kinase pathway (Pinzani et al., 1996; Marra et al., 1999). Accordingly, we found that sPDGFRβ significantly reduced the phosphorylation of ERK1/2 in fibrotic animals, therefore confirming that the PDGF signaling pathway was compromised by the administration of the adenovirus. In addition, ERK1/2 translocate into the nucleus triggering the transcription of genes involved in cell proliferation. In this regard, here we have showed that the decrease of liver fibrosis could be associated with the effect of sPDGFRβ on HSC activation and proliferation as reflected by the disruption of PDGF signaling and reduced α-SMA.

In accordance with the second study, CB2 receptors exert antifibrogenic properties and anti-inflammatory functions in the liver. Moreover, there is compelling evidence that the endocannabinoid system is very important in the regulation of the immune and host-defense mechanisms, mediated mainly by CB2 receptors (Massi et al., 1998). Taking into account that cirrhotic patients with ascites are prone to bacterial infections, which is associated with a higher mortality rate (Fernández and Gustot, 2012), we investigated whether LPS regulates CB2 expression in human monocytic cell lines and in monocytic cells of cirrhotic patients. Several investigations have documented the existing relationship between the endocannabinoid system and immunoresponse. Cytokines released by macrophages exposed to LPS were

attenuated when the cells where treated with AEA or a selective agonist (Bátkai et al., 2012). The results of this study showed that LPS repressed CB2 receptor mRNA expression in U937 cells, resulting in a depressed chemotactic activity and therefore an impaired host-defense of those cells. LPS is able to modify the transcriptional start site of CB2 mRNA as seen in murine splenocytes (Sherwood et al., 2009) therefore, providing a possible mechanism of action of LPS on CB2 receptors. Moreover, AEA and 2-AG may also induce chemotactic activity in immune cells (Kishimoto et al., 2003, 2005) and in addition, we showed that the attenuated effect by LPS pretreatment was also observed by the blockade of CB2 receptors by a selective antagonist (SR144528), thus confirming the direct involvement of CB2 receptors. This is important, since under conditions of bacterial infection such as SBP, an enhanced migration is beneficial, but CB2 receptor inhibition may result in host-defense impairment.

The analysis of an array of antibacterial response genes reveled that the mRNA pattern expression of LPS-pretreated U937 cells compared to non-treated cells clearly differed. Most of the upregulated genes are closely correlated with cytokine activation or chemokine receptors. It is important to highlight that both CB1 and CB2 receptors where markedly downregulated and that no other genes showed these differences. Interestingly, all these changes in gene expression were almost fully suppressed when the experiments were performed in the presence of PMB, thus demonstrating the specificity of this effect triggered by LPS.

As previously mentioned, bacterial infections are life threating for cirrhotic patients with ascites. This increased susceptibility has been associated with alterations in the immune response. In agreement with the *in vitro* results obtained in U937 cells, circulating monocytes and peritoneal macrophages of cirrhotic patients presented a significant downregulation of CB receptors, being much more intense in patients with SBP. Taken together these results strengthen the fact that the endocannabinoid system has an important role in liver diseases acting as an antifibrogenic agent, but also taking part in the defense response mechanisms in cirrhotic patients.

CONCLUSIONS

From the results obtained in the four studies presented in this thesis, the conclusions are:

1) Type III collagen CO3-610 fragment closely correlates with hepatic collagen content and portal pressure in rats with fibrosis.

2) CO3-610 sequence is identical in rodents and humans, therefore, the findings suggest that this peptide could ultimately be a useful non-invasive biomarker of fibrosis in patients with liver disease.

3) The stimulation of CB2 receptors or the blockade of the apelin system is able to attenuate collagen deposition in CCl_4-treated rats through common mechanisms.

4) Both antifibrogenic strategies inhibited the mRNA expression of PDGFRβ, and altered the MMP/TIMP ratio by decreasing TIMP1 protein expression.

5) Therapies against PDGF signaling or TIMP1 activity seem to offer future therapy possibilities.

6) Hepatic mRNA expression of PDGFRβ closely correlates with the hepatic collagen content and contributes to hemodynamic deterioration in CCl_4-treated rats.

7) The specific blockade of the PDGF signaling pathway by an adenovirus transduction promotes an improvement in systemic hemodynamics and portal pressure, as well as an amelioration of the degree of fibrosis in fibrotic rats.

8) Strategies addressed to block PDGF signaling pathway in the liver could be useful in the management of human liver disease providing a potential site for therapeutic intervention.

9) LPS pretreatment markedly reduced CB2 mRNA and protein expression in a human monocytic cell line (U937) after, without affecting cell viability.

10) This CB2 expression reduction is translated into a depressed chemotactic activity, which could compromise the host-defense mechanisms of those cells.

11) Downregulation of the messenger expression induced by LPS in human derived monocytic cells is highly specific for CB receptors as demonstrated by an array analysis of 86 different genes involved in antibacterial response.

12) Circulating monocytes and peritoneal macrophages of cirrhotic patients show decreased expression of CB receptors. This reduction was more intense in cells obtained from patients with SBP and almost suppressed in peritoneal macrophages.

As a whole, after the results obtained in this thesis, it can be concluded that the assessment of liver fibrosis is an important tool for the liver disease diagnosis, and that this could be improved through the use of effective serological markers that correlate with portal hemodynamics parameters and liver fibrosis. Halting fibrosis progression could present new therapeutic options either through pharmacological intervention, or genetic impairment of key genes involved in the progression of the disease. Finally, the quality of life of cirrhotic patients with ascites affected by SBP could be substantially improved by therapies involving CB2 receptors.

REFERENCES

Andersen CU, Hilberg O, Mellemkjær S, Nielsen-Kudsk JE, Simonsen U. Apelin and pulmonary hypertension. Pulm Circ. 2011;1:334-46.

Anderson RN, Smith BL. Deaths: leading causes for 2001. Natl Vital Stat Rep. 2003;52:1-85.

Anthony PP, Ishak KG, Nayak NC, Poulsen HE, Scheuer PJ, Sobin LH. The morphology of cirrhosis: definition, nomenclature and classification. Bull World Health Organ 1977;55:521-40.

Avraham Y, Israeli E, Gabbay E, Okun A, Zolotarev O, Silberman I, Ganzburg V, Dagon Y, Magen I, Vorobia L, Pappo O, Mechoulam R, Ilan Y, Berry EM. Endocannabinoids affect neurological and cognitive function in thioacetamide-induced hepatic encephalopathy in mice. Neurobiol Dis. 2006;21:237-45.

Baker D, Pryce G, Davies WL, Hiley CR. In silico patent searching reveals a new cannabinoid receptor. Trends Pharmacol Sci. 2006;27:1-4.

Baranova A, Lal P, Birerdinc A, Younossi ZM. Non-invasive markers for hepatic fibrosis. BMC Gastroenterol 2011;11:91.

Barascuk N, Veidal SS, Larsen L, Larsen DV, Larsen MR, Wang J, Zheng Q, Xing R, Cao Y, Rasmussen LM, Karsdal MA. A novel assay for extracellular matrix remodeling associated with liver fibrosis: An enzyme-linked immunosorbent assay (ELISA) for a MMP-9 proteolytically revealed neo-epitope of type III collagen. Clin Biochem. 2010;43:899-904.

Bataller R, Brenner DA. Liver Fibrosis. J Clin Invest 2005;115:209-218.

Bátkai S, Járai Z, Wagner JA, Goparaju SK, Varga K, Liu J, Wang L, Mirshahi F, Khanolkar AD, Makriyannis A, Urbaschek R, Garcia N Jr, Sanyal AJ, Kunos G. Endocannabinoids acting at vascular CB1 receptors mediate the vasodilated state in advanced liver cirrhosis. Nat Med. 2001;7:827-32.

Bátkai S, Osei-Hyiaman D, Pan H, El-Assal O, Rajesh M, Mukhopadhyay P, Hong F, Harvey-White J, Jafri A, Haskó G, Huffman JW, Gao B, Kunos G, Pacher P. Cannabinoid-2 receptor mediates protection against hepatic ischemia/reperfusion injury. FASEB J. 2007;21:1788-800.

Bátkai S, Mukhopadhyay P, Horváth B, Rajesh M, Gao RY, Mahadevan A, Amere M, Battista N, Lichtman AH, Gauson LA, Maccarrone M, Pertwee RG, Pacher P. Δ8-Tetrahydrocannabivarin prevents hepatic ischaemia/reperfusion injury by decreasing oxidative stress and inflammatory responses through cannabinoid CB2 receptors. *Br J Pharmacol* 2012;165:2450-61.

Beaussier M, Wendum D, Schiffer E, Dumont S, Rey C, Lienhart A, Housset C. Prominent contribution of portal mesenchymal cells to liver fibrosis in ischemic and obstructive cholestatic injuries. Lab Invest. 2007;87:292-303.

Bedossa P. Intraobserver and interobserver variations in liver biopsy interpretation in patients with chronic hepatitis C. Hepatology. 1994;20:15-20.

Benyon RC, Iredale JP, Goddard S, Winwood PJ, Arthur MJ. Expression of tissue inhibitor of metalloproteinases 1 and 2 is increased in fibrotic human liver. Gastroenterology. 1996;110:821-31.

Berry MF, Pirolli TJ, Jayasankar V, Burdick J, Morine KJ, Gardner TJ, Woo YJ. Apelin has in vivo inotropic effects on normal and failing hearts. Circulation. 2004;110,II187-93.

Berzigotti A, Ashkenazi E, Reverter E, Abraldes JG, Bosch J. Non-invasive diagnostic and prognostic evaluation of liver cirrhosis and portal hypertension. Dis Markers. 2011;31(3):129-38.

Bissell DM, Wang SS, Jarnagin WR, Roll FJ. Cell-specific expression of transforming growth factor-beta in rat liver. Evidence for autocrine regulation of hepatocyte proliferation. J Clin Invest. 1995;96:447-55.

Boeker KH, Haberkorn CI, Michels D, Flemming P, Manns MP, Lichtinghagen R. Diagnostic potential of circulating TIMP-1 and MMP-2 as markers of liver fibrosis in patients with chronic hepatitis C. Clin Chim Acta. 2002;316:71-81.

Bonner JC. Regulation of PDGF and its receptors in fibrotic diseases. Cytokine Growth Factor Rev. 2004;15:255-73.

Borkham-Kamphorst E, Herrmann J, Stoll D, Treptau J, Gressner AM, Weiskirchen R. Dominant-negative soluble PDGF-beta receptor inhibits hepatic stellate cell activation and attenuates liver fibrosis. Lab Invest. 2004;84:766-77.

Borkham-Kamphorst E, van Roeyen CR, Ostendorf T, Floege J, Gressner AM, Weiskirchen R. Pro-fibrogenic potential of PDGF-D in liver fibrosis. J Hepatol. 2007;46:1064-74.

Bosch J, Pizcueta P, Feu F, Fernández M, García-Pagán JC. Pathophysiology of portal hypertension. Gastroenterol Clin North Am. 1992;21:1-14.

Bozdayi AM, Karatayli SC, Alagöz SG, Mizrak D, Sayki M, Ozkan M, Savaş B, Erden E, Cinar K, Idılman R, Yurdaydin C. Potential proteomic biomarkers in assessing liver fibrosis using SELDI-TOF MS. Turk J Gastroenterol. 2012;23:46-53.

Breitkopf K, Godoy P, Ciuclan L, Singer MV, Dooley S. TGF-beta/Smad signaling in the injured liver. Z Gastroenterol. 2006;44:57-66.

Brindle NP, Saharinen P, Alitalo K. Signaling and functions of angiopoietin-1 in vascular protection. Circ Res. 2006;98:1014-23.

Brown AJ. Novel cannabinoid receptors. Br J Pharmacol. 2007;152:567-75.

Canbay A, Friedman S, Gores GJ. Apoptosis: the nexus of liver injury and fibrosis. Hepatology. 2004;39:273-8.

Cawston TE, Mercer E. Preferential binding of collagenase to alpha 2-macroglobulin in the presence of the tissue inhibitor of metalloproteinases. FEBS Lett. 1986;209:9-12.

Celli G, LaRochelle WJ, Mackem S, Sharp R, Merlino G. Soluble dominant-negative receptor uncovers essential roles for fibroblast growth factors in multi-organ induction and patterning. EMBO J. 1998;17:1642-55.

Christensen R, Kristensen PK, Bartels EM, Bliddal H, Astrup A. Efficacy and safety of the weight-loss drug rimonabant: a meta-analysis of randomised trials. Lancet. 2007;370:1706-13.

Chun HJ, Ali ZA, Kojima Y, Kundu RK, Sheikh AY, Agrawal R, Zheng L, Leeper NJ, Pearl NE, Patterson AJ, Anderson JP, Tsao PS, Lenardo MJ, Ashley EA, Quertermous T. Apelin

signaling antagonizes Ang II effects in mouse models of atherosclerosis. J Clin Invest. 2008;118:3343-54.

Corpechot C, El Naggar A, Poujol-Robert A, Ziol M, Wendum D, Chazouillères O, de Lédinghen V, Dhumeaux D, Marcellin P, Beaugrand M, Poupon R. Assessment of biliary fibrosis by transient elastography in patients with PBC and PSC. Hepatology. 2006;43:1118-24.

Dagon Y, Avraham Y, Ilan Y, Mechoulam R, Berry EM. Cannabinoids ameliorate cerebral dysfunction following liver failure via AMP-activated protein kinase. FASEB J. 2007;21:2431-41.

Dai T, Ramirez-Correa G, Gao WD. Apelin increases contractility in failing cardiac muscle. Eur J Pharmacol. 2006;553222-8.

Daviaud D, Boucher J, Gesta S, Dray C, Guigne C, Quilliot D, Ayav A, Ziegler O, Carpene C, Saulnier-Blache JS, Valet P, Castan-Laurell I. TNFalpha up-regulates apelin expression in human and mouse adipose tissue. FASEB J. 2006;20:1528-30.

Dray C, Knauf C, Daviaud D, Waget A, Boucher J, Buléon M, Cani PD, Attané C, Guigné C, Carpéné C, Burcelin R, Castan-Laurell I, Valet P. Apelin stimulates glucose utilization in normal and obese insulin-resistant mice. Cell Metab 2008;8:437-445.

Du WD, Zhang YE, Zhai WR, Zhou XM. Dynamic changes of type I,III and IV collagen synthesis and distribution of collagen-producing cells in carbon tetrachloride-induced rat liver fibrosis. World J Gastroenterol. 1999;5:397-403.

Edinger AL, Hoffman TL, Sharron M, Lee B, Yi Y, Choe W, Kolson DL, Mitrovic B, Zhou Y, Faulds D, Collman RG, Hesselgesser J, Horuk R, Doms RW. An orphan seven-transmembrane domain receptor expressed widely in the brain functions as a coreceptor for human immunodeficiency virus type 1 and simian immunodeficiency virus. J Virol. 1998;72:7934-40.

Eyries M, Siegfried G, Ciumas M, Montagne K, Agrapart M, Lebrin F, Soubrier F. Hypoxia-induced apelin expression regulates endothelial cell proliferation and regenerative angiogenesis. Circ Res. 2008;103:432-40.

Fallowfield JA, Mizuno M, Kendall TJ, Constandinou CM, Benyon RC, Duffield JS, Iredale JP. Scar-associated macrophages are a major source of hepatic matrix metalloproteinase-13 and facilitate the resolution of murine hepatic fibrosis. J Immunol. 2007;178:5288-5295.

Farnsworth N, Fagan SP, Berger DH, Awad SS. Child-Turcotte-Pugh versus MELD score as a predictor of outcome after elective and emergent surgery in cirrhotic patients. Am J Surg 2004;188:580-583.

Fernández J, Gustot T. Management of bacterial infections in cirrhosis. *J Hepatol* 2012;56:S1-12.

Fernandez M, Mejias M, Garcia-Pras E, Mendez R, Garcia-Pagan JC, Bosch J. Reversal of portal hypertension and hyperdynamic splanchnic circulation by combined vascular endothelial growth factor and platelet-derived growth factor blockade in rats. Hepatology. 2007;46:1208-17.

Fiorucci S, Antonelli E, Distrutti E, Severino B, Fiorentina R, Baldoni M, Caliendo G, Santagada V, Morelli A, Cirino G. PAR1 antagonism protects against experimental liver fibrosis. Role of proteinase receptors in stellate cell activation. Hepatology. 2004;39:365-75.

Fischer R, Cariers A, Reinehr R, Häussinger D. Caspase 9-dependent killing of hepatic stellate cells by activated Kupffer cells. Gastroenterology. 2002;123:845-61.

Flisiak R, Pytel-Krolczuk B, Prokopowicz D. Circulating transforming growth factor beta(1) as an indicator of hepatic function impairment in liver cirrhosis. Cytokine. 2000;12:677-81.

Forns X, Ampurdanès S, Llovet JM, Aponte J, Quintó L, Martínez-Bauer E, Bruguera M, Sánchez-Tapias JM, Rodés J. Identification of chronic hepatitis C patients without hepatic fibrosis by a simple predictive model. Hepatology. 2002;36:986-92.

Frébourg T, Delpech B, Bercoff E, Senant J, Bertrand P, Deugnier Y, Bourreille J. Serum hyaluronate in liver diseases: study by enzymoimmunological assay. Hepatology. 1986;6:392-5.

Friedman SL. Evolving challenges in hepatic fibrosis. Nat Rev Gastroenterol Hepatol. 2010;7:425-36.

Friedman SL. Hepatic stellate cells: protean, multifunctional, and enigmatic cells of the liver. Physiol Rev. 2008;88:125-72.

Friedrich-Rust M, Hadji-Hosseini H, Kriener S, Herrmann E, Sircar I, Kau A, Zeuzem S, Bojunga J. Transient elastography with a new probe for obese patients for non-invasive staging of non-alcoholic steatohepatitis. Eur Radiol. 2010;20:2390-6.

Galiègue S, Mary S, Marchand J, Dussossoy D, Carrière D, Carayon P, Bouaboula M, Shire D, Le Fur G, Casellas P. Expression of central and peripheral cannabinoid receptors in human immune tissues and leukocyte subpopulations. Eur J Biochem. 1995;232:54-61.

Gaoni Y, Mechoulam R. Isolation, structure and partial synthesis of an active constituent of hashish. J Am Chem Soc. 1964;86:1646-1647.

Garcia N Jr, Járai Z, Mirshahi F, Kunos G, Sanyal AJ. Systemic and portal hemodynamic effects of anandamide. Am J Physiol Gastrointest Liver Physiol. 2001;280:G14-20.

Giannone FA, Baldassarre M, Domenicali M, Zaccherini G, Trevisani F, Bernardi M, Caraceni P. Reversal of liver fibrosis by the antagonism of endocannabinoid CB1 receptor in a rat model of CCl(4)-induced advanced cirrhosis. Lab Invest. 2012;92:384-95.

Ginès P, Cárdenas A, Arroyo V, Rodés J. Management of cirrhosis and ascites. N Engl J Med 2004;350:1646-1654.

Glaser ST, Abumrad NA, Fatade F, Kaczocha M, Studholme KM, Deutsch DG. Evidence against the presence of an anandamide transporter. Proc Natl Acad Sci U S A. 2003;100:4269-74.

Gressner AM, Bachem MG. Cellular sources of noncollagenous matrix proteins: role of fat-storing cells in fibrogenesis. Semin Liver Dis. 1990;10:30-46.

Gressner AM, Weiskirchen R, Breitkopf K, Dooley S. Roles of TGF-beta in hepatic fibrosis. Front Biosci. 2002;7:d793-807.

Gressner OA, Weiskirchen R, Gressner AM. Biomarkers of hepatic fibrosis, fibrogenesis and genetic pre-disposition pending between fiction and reality. J Cell Mol Med. 2007;11:1031-51.

Guéchot J, Laudat A, Loria A, Serfaty L, Poupon R, Giboudeau J: Diagnostic accuracy of hyaluronan and type III procollagen amino-terminal peptide serum assays as markers of liver fibrosis in chronic viral hepatitis C evaluated by ROC curve analysis. Clin Chem 1996, 42:558-563.

Guéchot J, Loria A, Serfaty L, Giral P, Guiboudeau J, Poupon R: Serum Hyaluronan as a marker of liver fibrosis in chronic viral hepatitis C: effect of alpha-interferon therapy. J Hepatol 1995, 22:22-26.

Guéchot J, Poupon RE, Poupon R. Serum hyaluronan as a marker of liver fibrosis. J Hepatol. 1995;22(2 Suppl):103-6.

Guedez L, Courtemanch L, Stetler-Stevenson M. Tissue inhibitor of metalloproteinase (TIMP)-1 induces differentiation and an antiapoptotic phenotype in germinal center B cells. Blood. 1998;92:1342-1349.

Guerrera IC, Kleiner O. Application of mass spectrometry in proteomics. Biosci Rep. 2005;25:71-93.

Habata Y, Fujii R, Hosoya M, Fukusumi S, Kawamata Y, Hinuma S, Kitada C, Nishizawa N, Murosaki S, Kurokawa T, Onda H, Tatemoto K, Fujino M. Apelin, the natural ligand of the orphan receptor APJ, is abundantly secreted in the colostrum. Biochim Biophys Acta. 1999;1452:25-35.

Hájos N, Ledent C, Freund TF. Novel cannabinoid-sensitive receptor mediates inhibition of glutamatergic synaptic transmission in the hippocampus. Neuroscience. 2001;106:1-4.

Han S, Wang G, Qi X, Englander EW, Greeley GH Jr. Involvement of a Stat3 binding site in inflammation-induced enteric apelin expression. Am J Physiol Gastrointest Liver Physiol. 2008;295:G1068-78.

Hemmann S, Graf J, Roderfeld M, Roeb E. Expression of MMPs and TIMPs in liver fibrosis - a systematic review with special emphasis on anti-fibrotic strategies. J Hepatol. 2007;46:955-75.

Henderson NC, Iredale JP. Liver fibrosis: cellular mechanisms of progression and resolution. Clin Sci (Lond). 2007;112:265-80.

Hirooka M, Koizumi Y, Hiasa Y, Abe M, Ikeda Y, Matsuura B, Onji M.Hepatic elasticity in patients with ascites: evaluation with real-time tissue elastography. AJR Am J Roentgenol. 2011;196:W766-71.

Horiuchi Y, Fujii T, Kamimura Y, Kawashima K. The endogenous, immunologically active peptide apelin inhibits lymphocytic cholinergic activity during immunological responses. J Neuroimmunol. 2003;144:46-52.

Hosoya M, Kawamata Y, Fukusumi S, Fujii R, Habata Y, Hinuma S, Kitada C, Honda S, Kurokawa T, Onda H, Nishimura O, Fujino M. Molecular and functional characteristics of APJ. Tissue distribution of mRNA and interaction with the endogenous ligand apelin. J Biol Chem. 2000;275:21061-7.

Howlett AC, Qualy JM, Khachatrian LL. Involvement of Gi in the inhibition of adenylate cyclase by cannabimimetic drugs. Mol Pharmacol. 1986;29:307-13.

Imbert-Bismut F, Ratziu V, Pieroni L, Charlotte F, Benhamou Y, Poynard T. Biochemical markers of liver fibrosis in patients with hepatitis C virus infection: a prospective study. Lancet 2001;357:1069-1075.

Inagaki Y, Okazaki I. Emerging insights into Transforming growth factor beta Smad signal in hepatic fibrogenesis. Gut. 2007;56:284-92.

Iredale JP, Benyon RC, Pickering J, McCullen M, Northrop M, Pawley S, Hovell C, Arthur MJ. Mechanisms of spontaneous resolution of rat liver fibrosis. Hepatic stellate cell apoptosis and reduced hepatic expression of metalloproteinase inhibitors. J Clin Invest. 1998;102:538-49.

Ishida J, Hashimoto T, Hashimoto Y, Nishiwaki S, Iguchi T, Harada S, Sugaya T, Matsuzaki H, Yamamoto R, Shiota N, Okunishi H, Kihara M, Umemura S, Sugiyama F, Yagami K, Kasuya Y, Mochizuki N, Fukamizu A. Regulatory roles for APJ, a seven-transmembrane receptor related to angiotensin-type 1 receptor in blood pressure in vivo. J Biol Chem. 2004;279:26274-9.

Ito T. Cytological studies on stellate cells of Kupffer and fat storing cells in the capillary wall of human liver. Acta Anat Nippon 1951;26:2.

Japp AG, Newby DE. The apelin-APJ system in heart failure: pathophysiologic relevance and therapeutic potential. Biochem Pharmacol. 2008;75:1882-92.

Jarcuska P, Janicko M, Veselíny E, Jarcuska P, Skladaný L. Circulating markers of liver fibrosis progression. Clin Chim Acta. 2010;411:1009-17.

Jiao J, Sastre D, Fiel MI, Lee UE, Ghiassi-Nejad Z, Ginhoux F, Vivier E, Friedman SL, Merad M, Aloman C. Dendritic cell regulation of carbon tetrachloride-induced murine liver fibrosis regression. Hepatology. 2012;55:244-55.

Jiménez W, Clária J, Arroyo V, Rodés J. Carbon tetrachloride induced cirrhosis in rats: a useful tool for investigating the pathogenesis of ascites in chronic liver disease. J Gastroenterol Hepatol. 1992;7:90-7.

Julien B, Grenard P, Teixeira-Clerc F, Van Nhieu JT, Li L, Karsak M, Zimmer A, Mallat A, Lotersztajn S. Antifibrogenic role of the cannabinoid receptor CB2 in the liver. Gastroenterology. 2005;128:742-55.

Kamal SM, Turner B, He Q, Rasenack J, Bianchi L, Al Tawil A, Nooman A, Massoud M, Koziel MJ, Afdhal NH. Progression of fibrosis in hepatitis C with and without schistosomiasis: correlation with serum markers of fibrosis. Hepatology. 2006;43:771-9.

Katugampola SD, Maguire JJ, Matthewson SR, Davenport AP. [(125)I]-(Pyr(1))Apelin-13 is a novel radioligand for localizing the APJ orphan receptor in human and rat tissues with evidence for a vasoconstrictor role in man. Br J Pharmacol. 2001;132:1255-60.

Kidoya H, Takakura N. Biology of the apelin-APJ axis in vascular formation. J Biochem. 2012;152:125-131.

Kishimoto S, Gokoh M, Oka S, Muramatsu M, Kajiwara T, Waku K, Sugiura T. 2-arachidonoylglycerol induces the migration of HL-60 cells differentiated into macrophage-like cells and human peripheral blood monocytes through the cannabinoid CB2 receptor-dependent mechanism. J Biol Chem 2003;278: 24469-24475.

Kishimoto S, Muramatsu M, Gokoh M, Oka S, Waku K, Sugiura T. Endogenous cannabinoid receptor ligand induces the migration of human natural killer cells. J Biochem 2005;137: 217-223.

Kisseleva T, Cong M, Paik Y, Scholten D, Jiang C, Benner C, Iwaisako K, Moore-Morris T, Scott B, Tsukamoto H, Evans SM, Dillmann W, Glass CK, Brenner DA. Myofibroblasts revert to an inactive phenotype during regression of liver fibrosis. Proc Natl Acad Sci U S A. 2012;109:9448-53.

Kisseleva T, Uchinami H, Feirt N, Quintana-Bustamante O, Segovia JC, Schwabe RF, Brenner DA. Bone marrow-derived fibrocytes participate in pathogenesis of liver fibrosis. J Hepatol. 2006;45:429-38.

Klein TW. Cannabinoid-based drugs as anti-inflammatory therapeutics. Nat Rev Immunol. 2005;5:400-11.

Knäuper V, Bailey L, Worley JR, Soloway P, Patterson ML, Murphy G. Cellular activation of proMMP-13 by MT1-MMP depends on the C-terminal domain of MMP-13. FEBS Lett. 2002;532:127-30.

Knittel T, Fellmer P, Ramadori G. Gene expression and regulation of plasminogen activator inhibitor type I in hepatic stellate cells of rat liver. Gastroenterology. 1996;111:745-54.

Knittel T, Mehde M, Grundmann A, Saile B, Scharf JG, Ramadori G. Expression of matrix metalloproteinases and their inhibitors during hepatic tissue repair in the rat. Histochem Cell Biol. 2000;113:443-53.

Knittel T, Mehde M, Kobold D, Saile B, Dinter C, Ramadori G. Expression patterns of matrix metalloproteinases and their inhibitors in parenchymal and non-parenchymal cells of rat liver: regulation by TNF-alpha and TGF-beta1. J Hepatol. 1999;30:48-60.

Knittel T, Schuppan D, Meyer zum Büschenfelde KH, Ramadori G. Differential expression of collagen types I, III, and IV by fat-storing (Ito) cells in vitro. Gastroenterology 1992;102:1724-35.

Knodell RG, Ishak KG, Black WC, Chen TS, Craig R, Kaplowitz N, Kiernan TW, Wollman J. Formulation and application of a numerical scoring system for assessing histological activity in asymptomatic chronic active hepatitis. Hepatology 1981;1:431-435.

Koguchi W, Kobayashi N, Takeshima H, Ishikawa M, Sugiyama F, Ishimitsu T. Cardioprotective effect of apelin-13 on cardiac performance and remodeling in end-stage heart failure. Circ J. 2012;76:137-44.

Krizhanovsky V, Yon M, Dickins RA, Hearn S, Simon J, Miething C, Yee H, Zender L, Lowe SW. Senescence of activated stellate cells limits liver fibrosis. Cell. 2008;134:657-67.

Lee DK, Cheng R, Nguyen T, Fan T, Kariyawasam AP, Liu Y, Osmond DH, George SR, O'Dowd BF. Characterization of apelin, the ligand for the APJ receptor. J Neurochem. 2000;74:34-41.

Lee DK, Saldivia VR, Nguyen T, Cheng R, George SR, O'Dowd BF. Modification of the terminal residue of apelin-13 antagonizes its hypotensive action. Endocrinology. 2005;146:231-6.

Leroy V, Monier F, Bottari S, Trocme C, Sturm N, Hilleret MN, Morel F, Zarski JP. Circulating matrix metalloproteinases 1, 2, 9 and their inhibitors TIMP-1 and TIMP-2 as serum markers of liver fibrosis in patients with chronic hepatitis C: comparison with PIIINP and hyaluronic acid. Am J Gastroenterol. 2004;99:271-9.

Leyland H, Gentry J, Arthur MJ, Benyon RC. The plasminogen-activating system in hepatic stellate cells. Hepatology. 1996;24:1172-8.

Lichtinghagen R, Michels D, Haberkorn CI, Arndt B, Bahr M, Flemming P, Manns MP, Boeker KH. Matrix metalloproteinase (MMP)-2, MMP-7, and tissue inhibitor of metalloproteinase-1 are closely related to the fibroproliferative process in the liver during chronic hepatitis C. J Hepatol. 2001;34:239-47.

Lim YS, Lee HC, Lee HS. Switch of cadherin expression from E- to N-type during the activation of rat hepatic stellate cells. Histochem Cell Biol. 2007;127:149-60.

Lindquist JN, Stefanovic B, Brenner DA. Regulation of collagen alpha1(I) expression in hepatic stellate cells. J Gastroenterol. 2000;35 Suppl 12:80-3.

Liu Y, Wang Z, Kwong SQ, Lui EL, Friedman SL, Li FR, Lam RW, Zhang GC, Zhang H, Ye T. Inhibition of PDGF, TGF-β, and Abl signaling and reduction of liver fibrosis by the small molecule Bcr-Abl tyrosine kinase antagonist Nilotinib. J Hepatol. 2011;55:612-25.

Lu Y, Zhu X, Liang GX, Cui RR, Liu Y, Wu SS, Liang QH, Liu GY, Jiang Y, Liao XB, Xie H, Zhou HD, Wu XP, Yuan LQ, Liao EY. Apelin-APJ induces ICAM-1, VCAM-1 and MCP-1 expression via NF-κB/JNK signal pathway in human umbilical vein endothelial cells. Amino Acids. 2012 Apr 25.

Malan TP Jr, Ibrahim MM, Deng H, Liu Q, Mata HP, Vanderah T, Porreca F, Makriyannis A. CB2 cannabinoid receptor-mediated peripheral antinociception. Pain. 2001;93:239-45.

Malyszko J, Malyszko JS, Pawlak K, Wolczynski S, Mysliwiec M. Apelin, a novel adipocytokine, in relation to endothelial function and inflammation in kidney allograft recipients.Transplant Proc. 2008;40:3466-3469.

Marra F. Hepatic stellate cells and the regulation of liver inflammation. J Hepatol. 1999;31:1120-30.

Marra F, Arrighi MC, Fazi M, Caligiuri A, Pinzani M, Romanelli RG, Efsen E, Laffi G, Gentilini P. Extracellular signal-regulated kinase activation differentially regulates platelet-derived growth factor's actions in hepatic stellate cells, and is induced by in vivo liver injury in the rat. Hepatology. 1999;30:951-8.

Massi P, Sacerdote P, Ponti W, Fuzio D, Manfredi B, Viganó D, Rubino T, Bardotti M, Parolaro D. Immune function alterations in mice tolerant to delta9-tetrahydrocannabinol: functional and biochemical parameters. J Neuroimmunol 1998;92, 60-66.

Mastroianni CM, Liuzzi GM, D'Ettorre G, Lichtner M, Forcina G, Di Campli NF, Riccio P, Vullo V. Matrix metalloproteinase-9 and tissue inhibitors of matrix metalloproteinase-1 in plasma of patients co-infected with HCV and HIV. HIV Clin Trials. 2002;3:310-315.

Matsuda LA, Lolait SJ, Brownstein MJ, Young AC, Bonner TI. Structure of a cannabinoid receptor and functional expression of the cloned cDNA. Nature. 1990;346:561-4.

Mazzucotelli A, Ribet C, Castan-Laurell I, Daviaud D, Guigné C, Langin D, Valet P. The transcriptional co-activator PGC-1alpha up regulates apelin in human and mouse adipocytes. Regul Pept. 2008;150:33-7.

Medhurst AD, Jennings CA, Robbins MJ, Davis RP, Ellis C, Winborn KY, Lawrie KW, Hervieu G, Riley G, Bolaky JE, Herrity NC, Murdock P, Darker JG. Pharmacological and immunohistochemical characterization of the APJ receptor and its endogenous ligand apelin. J Neurochem. 2003;84:1162-72.

Melgar-Lesmes P, Casals G, Pauta M, Ros J, Reichenbach V, Bataller R, Morales-Ruiz M, Jiménez W. Apelin mediates the induction of profibrogenic genes in human hepatic stellate cells. Endocrinology. 2010;151:5306-14.

Melgar-Lesmes P, Pauta M, Reichenbach V, Casals G, Ros J, Bataller R, Morales-Ruiz M, Jiménez W. Hypoxia and proinflammatory factors upregulate apelin receptor expression in human stellate cells and hepatocytes. Gut. 2011;60:1404-11.

Ministerio de Sanidad, Servicios Sociales e Igualdad. 6. Índice de General de Mortalidad. 6.14 CIrrosis hepática. *http://www.msc.es/estadEstudios/estadisticas/inforRecopilaciones/atlas/atlasDatos.htm* (accessed 28 aug 2012).

Morales-Ruiz M, Cejudo-Martín P, Fernández-Varo G, Tugues S, Ros J, Angeli P, Rivera F, Arroyo V, Rodés J, Sessa WC, Jiménez W. Transduction of the liver with activated Akt normalizes portal pressure in cirrhotic rats. Gastroenterology. 2003;125:522-31.

Moreno M, Bataller R. Cytokines and renin-angiotensin system signaling in hepatic fibrosis. Clin Liver Dis. 2008;12:825-52.

Muñoz-Luque J, Ros J, Fernández-Varo G, Tugues S, Morales-Ruiz M, Alvarez CE, Friedman SL, Arroyo V, Jiménez W. Regression of fibrosis after chronic stimulation of cannabinoid CB2 receptor in cirrhotic rats. J Pharmacol Exp Ther. 2008;324:475-83.

Munro S, Thomas KL, Abu-Shaar M. Molecular characterization of a peripheral receptor for cannabinoids. Nature. 1993;365:61-5.

Murphy FR, Issa R, Zhou X, Ratnarajah S, Nagase H, Arthur MJ, Benyon C, Iredale JP. Inhibition of apoptosis of activated hepatic stellate cells by tissue inhibitor of metalloproteinase-1 is mediated via effects on matrix metalloproteinase inhibition: implications for reversibility of liver fibrosis. J Biol Chem. 2002;277:11069-76.

Overton HA, Babbs AJ, Doel SM, Fyfe MC, Gardner LS, Griffin G, et al. Deorphanization of a G protein-coupled receptor for oleoylethanolamide and its use in the discovery of small-molecule hypophagic agents. Cell Metab 2006;3:167-175

Pacher P, Bátkai S, Kunos G. The endocannabinoid system as an emerging target of pharmacotherapy. Pharmacol Rev. 2006;58:389-462.

Paik YH, Schwabe RF, Bataller R, Russo MP, Jobin C, Brenner DA. Toll-like receptor 4 mediates inflammatory signaling by bacterial lipopolysaccharide in human hepatic stellate cells. Hepatology. 2003;37:1043-55.

Perrillo RP. The role of liver biopsy in hepatitis C. Hepatology. 1997;26(3 Suppl 1):57S-61S.

Pinzani M, Gentilini A, Caligiuri A, De Franco R, Pellegrini G, Milani S, Marra F, Gentilini P. Transforming growth factor-beta 1 regulates platelet-derived growth factor receptor beta subunit in human liver fat-storing cells. Hepatology. 1995;21:232-9.

Pinzani M, Milani S, Herbst H, DeFranco R, Grappone C, Gentilini A, Caligiuri A, Pellegrini G, Ngo DV, Romanelli RG, Gentilini P. Expression of platelet-derived growth factor and its receptors in normal human liver and during active hepatic fibrogenesis. Am J Pathol. 1996;148:785-800.

Pinzani M, Marra F. Cytokine receptors and signaling in hepatic stellate cells. Semin Liver Dis. 2001;21:397-416.

Poirier O, Ciumas M, Eyries M, Montagne K, Nadaud S, Soubrier F. Inhibition of apelin expression by bmp signaling in endothelial cells. Am J Physiol Cell Physiol. 2012 Aug 15. [Epub ahead of print]

Poynard T, Munteanu M, Deckmyn O, Ngo Y, Drane F, Castille JM, Housset C, Ratziu V, Imbert-Bismut F. Validation of liver fibrosis biomarker (FibroTest) for assessing liver fibrosis progression: Proof of concept and first application in a large population. J Hepatol. 2012 May 18. [Epub ahead of print]

Principe A, Melgar-Lesmes P, Fernández-Varo G, del Arbol LR, Ros J, Morales-Ruiz M, Bernardi M, Arroyo V, Jiménez W. The hepatic apelin system: a new therapeutic target for liver disease. Hepatology. 2008;48:1193-201.

Pungpapong S, Nunes DP, Krishna M, Nakhleh R, Chambers K, Ghabril M, Dickson RC, Hughes CB, Steers J, Nguyen JH, Keaveny AP. Serum fibrosis markers can predict rapid fibrosis progression after liver transplantation for hepatitis C. Liver Transpl. 2008;14:1294-302.

Qi Z, Atsuchi N, Ooshima A, Takeshita A, Ueno H. Blockade of type beta transforming growth factor signaling prevents liver fibrosis and dysfunction in the rat. Proc Natl Acad Sci U S A. 1999;96:2345-9.

Rajesh M, Pan H, Mukhopadhyay P, Bátkai S, Osei-Hyiaman D, Haskó G, Liaudet L, Gao B, Pacher P. Cannabinoid-2 receptor agonist HU-308 protects against hepatic ischemia/reperfusion injury by attenuating oxidative stress, inflammatory response, and apoptosis. J Leukoc Biol. 2007;821382-9.

Reichenbach V, Ros J, Jiménez W. Endogenous cannabinoids in liver disease: Many darts for a single target. Gastroenterol Hepatol. 2010;33:323-9. Epub 2009 Sep 16. [Article in Spanish]

Rinaldi-Carmona M, Barth F, Héaulme M, Shire D, Calandra B, Congy C, Martinez S, Maruani J, Néliat G, Caput D, et al. SR141716A, a potent and selective antagonist of the brain cannabinoid receptor. FEBS Lett. 1994;350:240-4.

Rinaldi-Carmona M, Barth F, Millan J, Derocq JM, Casellas P, Congy C, Oustric D, Sarran M, Bouaboula M, Calandra B, Portier M, Shire D, Brelière JC, Le Fur GL. SR 144528, the first potent and selective antagonist of the CB2 cannabinoid receptor. J Pharmacol Exp Ther. 1998;284:644-50.

Ronkainen VP, Ronkainen JJ, Hänninen SL, Leskinen H, Ruas JL, Pereira T, Poellinger L, Vuolteenaho O, Tavi P. Hypoxia inducible factor regulates the cardiac expression and secretion of apelin. FASEB J. 2007;21:1821-30.

Ros J, Clària J, To-Figueras J, Planagumà A, Cejudo-Martín P, Fernández-Varo G, Martín-Ruiz R, Arroyo V, Rivera F, Rodés J, Jiménez W. Endogenous cannabinoids: a new system involved in the homeostasis of arterial pressure in experimental cirrhosis in the rat. Gastroenterology. 2002;122:85-93.

Rosenberg WM, Voelker M, Thiel R, Becka M, Burt A, Schuppan D, Hubscher S, Roskams T, Pinzani M, Arthur MJ; European Liver Fibrosis Group. Serum markers detect the presence of liver fibrosis: a cohort study. Gastroenterology. 2004;127:1704-13.

Saario SM, Savinainen JR, Laitinen JT, Järvinen T, Niemi R. Monoglyceride lipase-like enzymatic activity is responsible for hydrolysis of 2-arachidonoylglycerol in rat cerebellar membranes. Biochem Pharmacol. 2004;67:1381-7.

Sandrin L, Fourquet B, Hasquenoph JM, Yon S, Fournier C, Mal F, Christidis C, Ziol M, Poulet B, Kazemi F, Beaugrand M, Palau R. Transient elastography: a new noninvasive method for assessment of hepatic fibrosis. Ultrasound Med Biol. 2003;29:1705-13.

Sawane M, Kidoya H, Muramatsu F, Takakura N, Kajiya K. Apelin attenuates UVB-induced edema and inflammation by promoting vessel function. Am J Pathol. 2011;179:2691-2697.

Scott IC, Masri B, D'Amico LA, Jin SW, Jungblut B, Wehman AM, Baier H, Audigier Y, Stainier DY. The g protein-coupled receptor agtrl1b regulates early development of myocardial progenitors. Dev Cell. 2007;12:403-13.

Sherwood TA, Nong L, Agudelo M, Newton C, Widen R, Klein TW. Identification of transcription start sites and preferential expression of select CB2 transcripts in mouse and human B lymphocytes. J Neuroimmune Pharmacol. 2009;4:476-88.

Sicklick JK, Choi SS, Bustamante M, McCall SJ, Pérez EH, Huang J, Li YX, Rojkind M, Diehl AM. Evidence for epithelial-mesenchymal transitions in adult liver cells. Am J Physiol Gastrointest Liver Physiol. 2006;291:575-83.

Siddiquee K, Hampton J, Khan S, Zadory D, Gleaves L, Vaughan DE, Smith LH. Apelin protects against angiotensin II-induced cardiovascular fibrosis and decreases plasminogen activator inhibitor type-1 production. J Hypertens. 2011;29:724-31.

Siegmund SV, Uchinami H, Osawa Y, Brenner DA, Schwabe RF. Anandamide induces necrosis in primary hepatic stellate cells. Hepatology. 2005;41:1085-95.

Starowicz K, Nigam S, Di Marzo V. Biochemistry and pharmacology of endovanilloids. Pharmacol Ther. 2007;114:13-33.

Sugiura T, Waku K. Cannabinoid receptors and their endogenous ligands. J Biochem. 2002;132:7-12.

Suzuki A, Angulo P, Lymp J, Li D, Satomura S, Lindor K. Hyaluronic acid, an accurate serum marker for severe hepatic fibrosis in patients with non-alcoholic fatty liver disease. Liver Int. 2005;25:779-86.

Svegliati Baroni G, D'Ambrosio L, Ferretti G, Casini A, Di Sario A, Salzano R, Ridolfi F, Saccomanno S, Jezequel AM, Benedetti A. Fibrogenic effect of oxidative stress on rat hepatic stellate cells. Hepatology. 1998;27:720-6.

Tam J, Liu J, Mukhopadhyay B, Cinar R, Godlewski G, Kunos G. Endocannabinoids in liver disease. Hepatology. 2011;53:346-55.

Tatemoto K, Hosoya M, Habata Y, Fujii R, Kakegawa T, Zou MX, Kawamata Y, Fukusumi S, Hinuma S, Kitada C, Kurokawa T, Onda H, Fujino M. Isolation and characterization of a novel endogenous peptide ligand for the human APJ receptor. Biochem Biophys Res Commun. 1998;251:471-6.

Tatemoto K, Takayama K, Zou MX, Kumaki I, Zhang W, Kumano K, Fujimiya M. The novel peptide apelin lowers blood pressure via a nitric oxide-dependent mechanism. Regul Pept. 2001;99:87-92.

Teixeira-Clerc F, Belot MP, Manin S, Deveaux V, Cadoudal T, Chobert MN, Louvet A, Zimmer A, Tordjmann T, Mallat A, Lotersztajn S. Beneficial paracrine effects of cannabinoid receptor 2 on liver injury and regeneration. Hepatology. 2010;52:1046-59.

Teixeira-Clerc F, Julien B, Grenard P, Tran Van Nhieu J, Deveaux V, Li L, Serriere-Lanneau V, Ledent C, Mallat A, Lotersztajn S. CB1 cannabinoid receptor antagonism: a new strategy for the treatment of liver fibrosis. Nat Med. 2006;12:671-6.

Tiani C, Garcia-Pras E, Mejias M, de Gottardi A, Berzigotti A, Bosch J, Fernandez M. Apelin signaling modulates splanchnic angiogenesis and portosystemic collateral vessel formation in rats with portal hypertension. J Hepatol. 2009;50:296-305.

Toniutto P, Fabris C, Bitetto D, Falleti E, Avellini C, Rossi E, Smirne C, Minisini R, Pirisi M. Role of AST to platelet ratio index in the detection of liver fibrosis in patients with recurrent hepatitis C after liver transplantation. J Gastroenterol Hepatol 2007;22:1904-8.

Tran A, Benzaken S, Saint-Paul MC, Guzman-Granier E, Hastier P, Pradier C, Barjoan EM, Demuth N, Longo F, Rampal P. Chondrex (YKL-40), a potential new serum fibrosis marker in patients with alcoholic liver disease. Eur J Gastroenterol Hepatol. 2000;12:989-93.

Tsukada S, Parsons CJ, Rippe RA. Mechanisms of liver fibrosis. Clin Chim Acta. 2006;364:33-60.

Tugues S, Fernandez-Varo G, Muñoz-Luque J, Ros J, Arroyo V, Rodés J, Friedman SL, Carmeliet P, Jiménez W, Morales-Ruiz M. Antiangiogenic treatment with sunitinib ameliorates inflammatory infiltrate, fibrosis, and portal pressure in cirrhotic rats. Hepatology. 2007;46:1919-26.

Vassiliadis E, Larsen DV, Clausen RE, Veidal SS, Barascuk N, Larsen L, Simonsen H, Silvestre TS, Hansen C, Overgaard T, Leeming DJ, Karsdal MA. Measurement of CO3-610, a potential liver biomarker derived from matrix metalloproteinase-9 degradation of collagen type iii, in a rat model of reversible carbon-tetrachloride-induced fibrosis. Biomark Insights. 2011;6:49-58.

Veidal SS, Vassiliadis E, Barascuk N, Zhang C, Segovia-Silvestre T, Klickstein L, Larsen MR, Qvist P, Christiansen C, Vainer B, Karsdal MA. Matrix metalloproteinase-9-mediated type III collagen degradation as a novel serological biochemical marker for liver fibrogenesis. Liver Int. 2010;30:1293-304.

Visse R, Nagase H. Matrix metalloproteinases and tissue inhibitors of metalloproteinases: structure, function, and biochemistry. Circ Res. 2003;92:827-39.

Wai CT, Greenson JK, Fontana RJ, Kalbfleisch JD, Marrero JA, Conjeevaram HS, Lok AS. A simple noninvasive index can predict both significant fibrosis and cirrhosis in patients with chronic hepatitis C. Hepatology 2003;38:518-526.

Wake K. "Sternzellen" in the liver: perisinusoidal cells with special reference to storage of vitamin A. Am J Anat. 1971;132:429-62.

Walsh KM, Timms P, Campbell S, MacSween RN, Morris AJ. Plasma levels of matrix metalloproteinase-2 (MMP-2) and tissue inhibitors of metalloproteinases -1 and -2 (TIMP-1 and TIMP-2) as noninvasive markers of liver disease in chronic hepatitis C: comparison using ROC analysis. Dig Dis Sci. 1999;44:624-30.

Wang Z, Juttermann R, Soloway PD. TIMP-2 is required for efficient activation of proMMP-2 in vivo. J Biol Chem. 2000;275:26411-5.

Watanabe T, Niioka M, Hozawa S, Kameyama K, Hayashi T, Arai M, Ishikawa A, Maruyama K, Okazaki I. Gene expression of interstitial collagenase in both progressive and recovery phase of rat liver fibrosis induced by carbon tetrachloride. J Hepatol 2000;33:224-235.

Wu YK, Yeh CF, Ly TW, Hung MS. A new perspective of cannabinoid 1 receptor antagonists: approaches toward peripheral CB1R blockers without crossing the blood-brain barrier. Curr Top Med Chem. 2011;11:1421-9.

Xu GF, Li PT, Wang XY, Jia X, Tian DL, Jiang LD, Yang JX. Dynamic changes in the expression of matrix metalloproteinases and their inhibitors, TIMPs, during hepatic fibrosis induced by alcohol in rats. World J Gastroenterol. 2004;10:3621-7.

Yata Y, Takahara T, Furui K, Zhang LP, Jin B, Watanabe A. Spatial distribution of tissue inhibitor of metalloproteinase-1 mRNA in chronic liver disease. J Hepatol. 1999;30:425-32.

Yoneda M, Fujita K, Inamori M, Nakajima A, Yoneda M, Tamano M, and Hiraishi H. Transient elastography in patients with non-alcoholic fatty liver disease (NAFLD). Dig Liver Dis. 2008;40:371-8.

Zhan SS, Jiang JX, Wu J, Halsted C, Friedman SL, Zern MA, Torok NJ. Phagocytosis of apoptotic bodies by hepatic stellate cells induces NADPH oxidase and is associated with liver fibrosis in vivo. Hepatology. 2006;43:435-43.

Zhang LP, Takahara T, Yata Y, Furui K, Jin B, Kawada N, Watanabe A. Increased expression of plasminogen activator and plasminogen activator inhibitor during liver fibrogenesis of rats: role of stellate cells. J Hepatol. 1999;31:703-11.

Zhou X, Hovell CJ, Pawley S, Hutchings MI, Arthur MJ, Iredale JP, Benyon RC. Expression of matrix metalloproteinase-2 and -14 persists during early resolution of experimental liver fibrosis and might contribute to fibrolysis. Liver Int. 2004;24:492-501.